



Modelling of accretion processes in magnetized binary stars

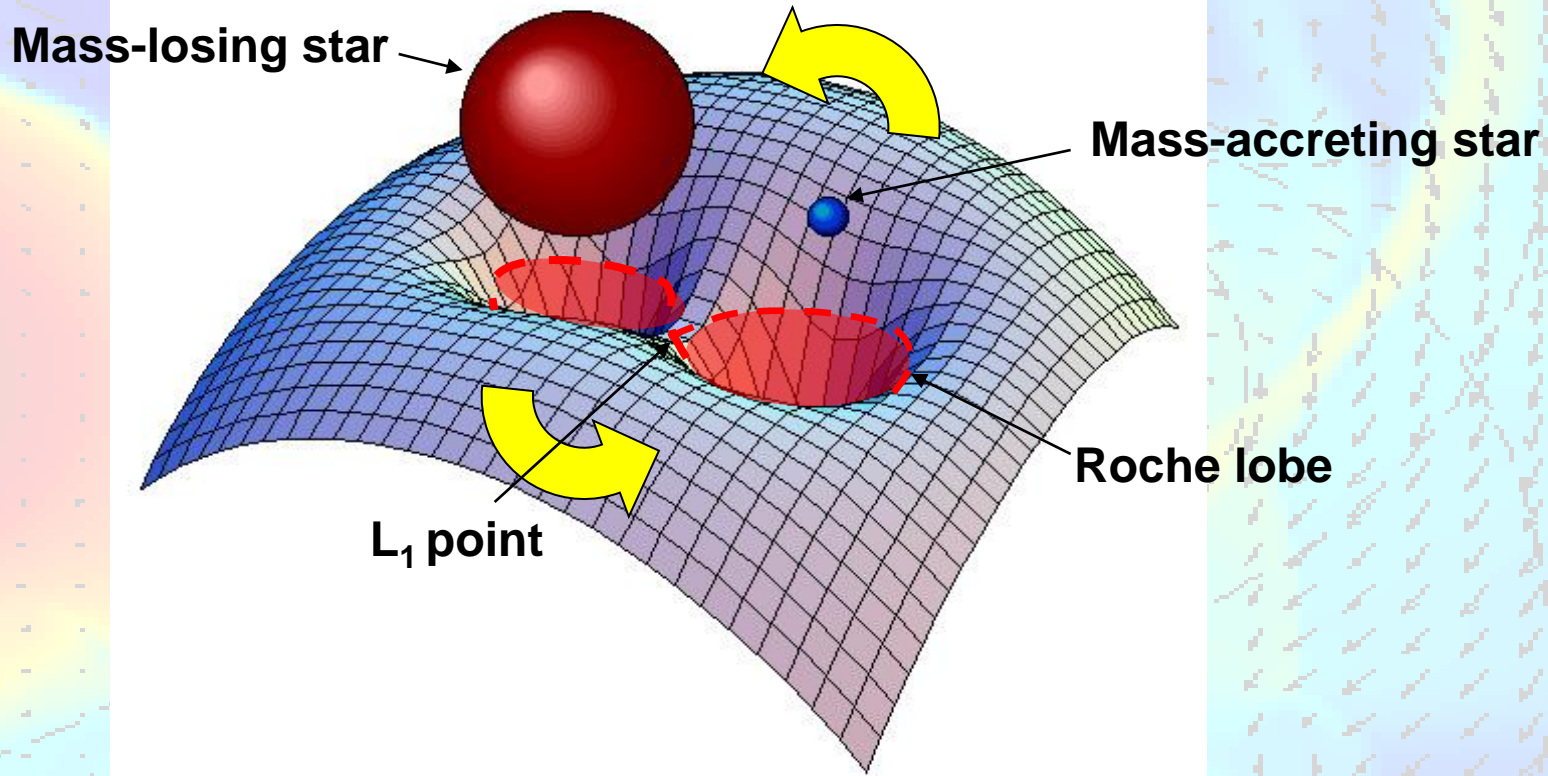
Dmitry Bisikalo

Institute of Astronomy RAS, Moscow, Russia

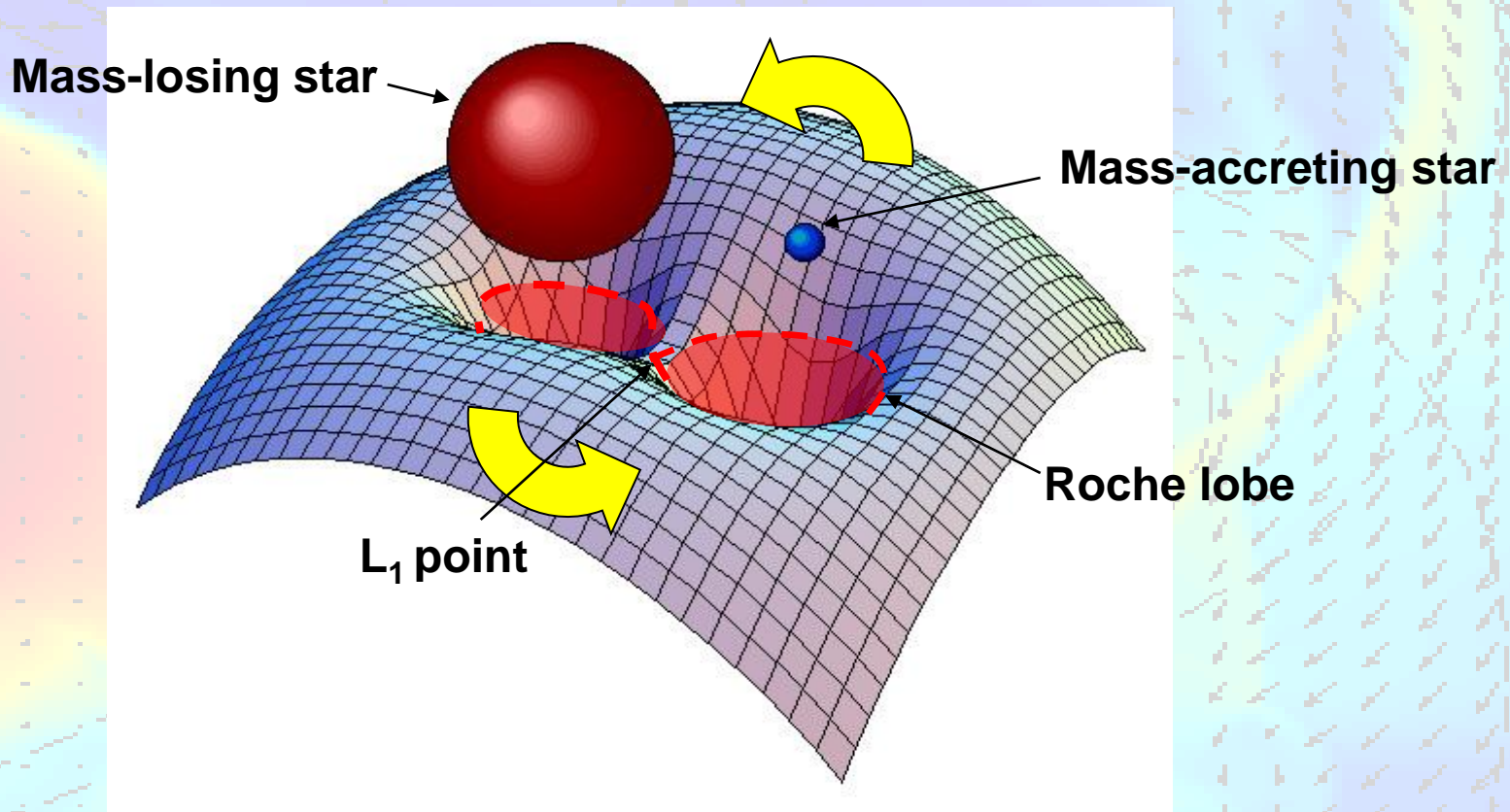
The background of the slide is a vector field plot. It features a grid of small arrows pointing outwards from a central point. The color of the plot transitions from blue on the left to yellow on the right, with a red star marking the center of the field. The text "Introductory remarks" is overlaid on this plot.

Introductory remarks

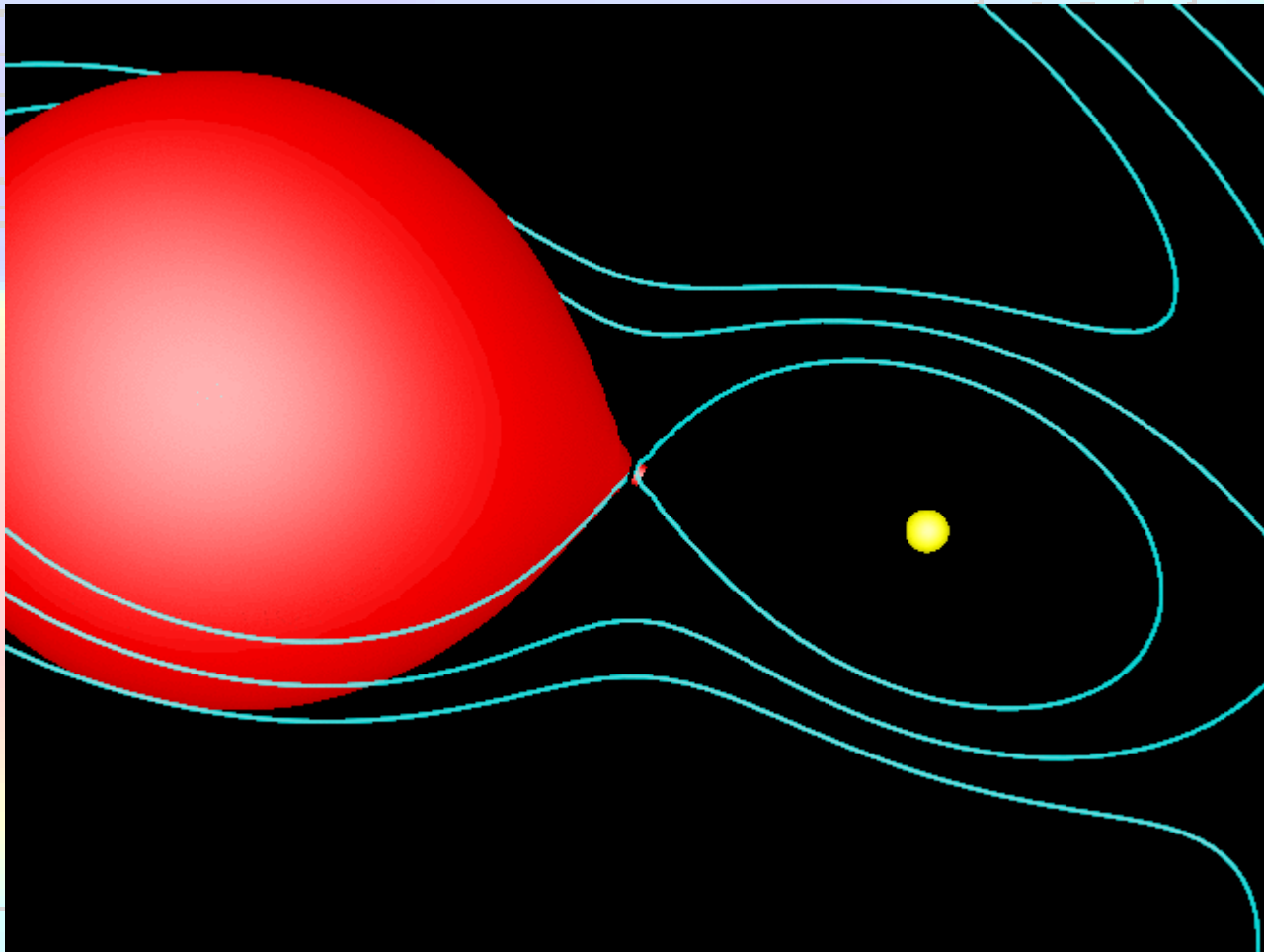
$$\Phi_R(\mathbf{r}) = -\frac{GM_1}{|\mathbf{r} - \mathbf{r}_1|} - \frac{GM_2}{|\mathbf{r} - \mathbf{r}_2|} - \frac{1}{2}(\boldsymbol{\omega} \times \mathbf{r})^2$$



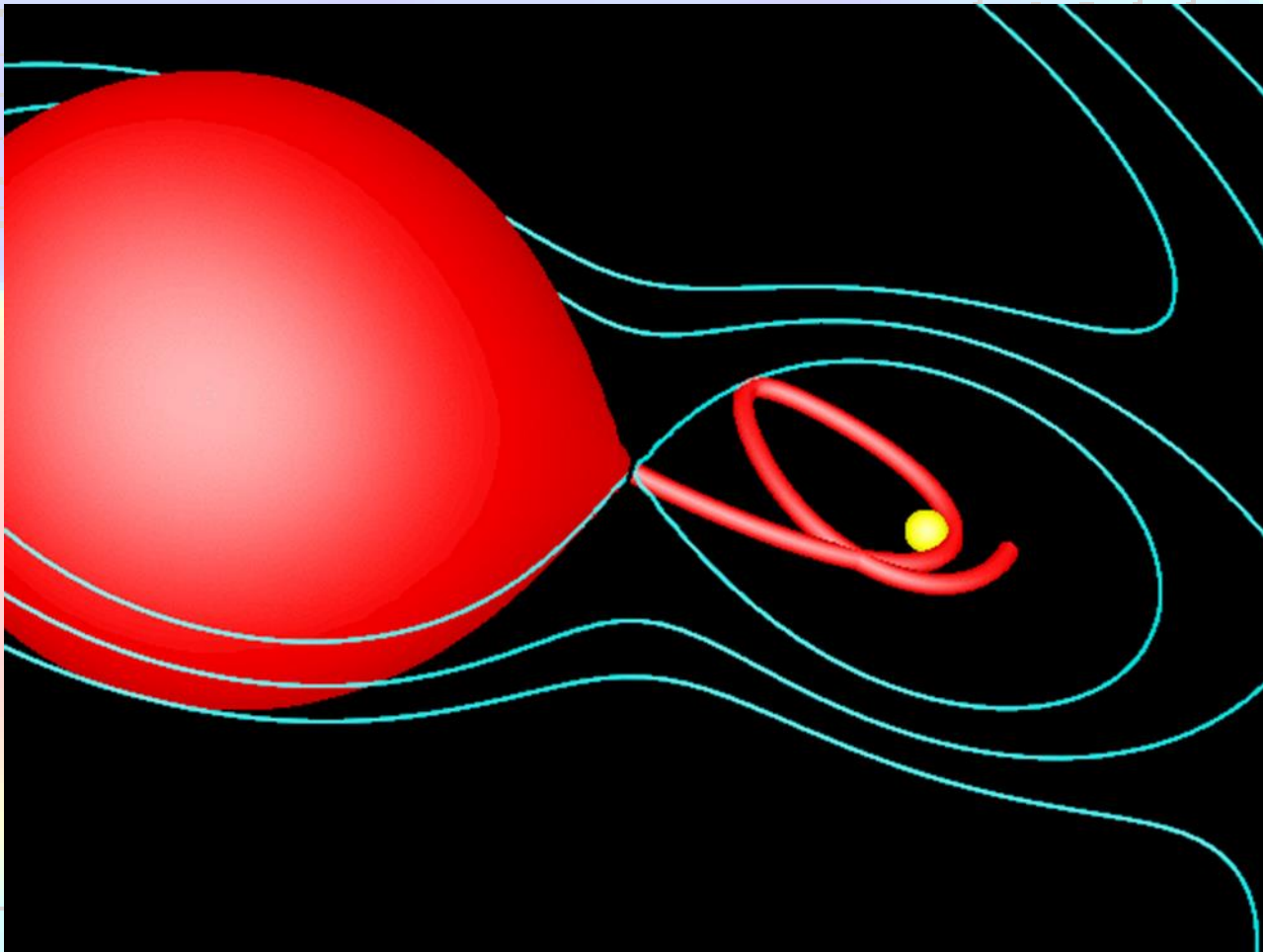
$$\Phi_R(\mathbf{r}) = -\frac{GM_1}{|\mathbf{r} - \mathbf{r}_1|} - \frac{GM_2}{|\mathbf{r} - \mathbf{r}_2|} - \frac{1}{2}(\boldsymbol{\omega} \times \mathbf{r})^2$$



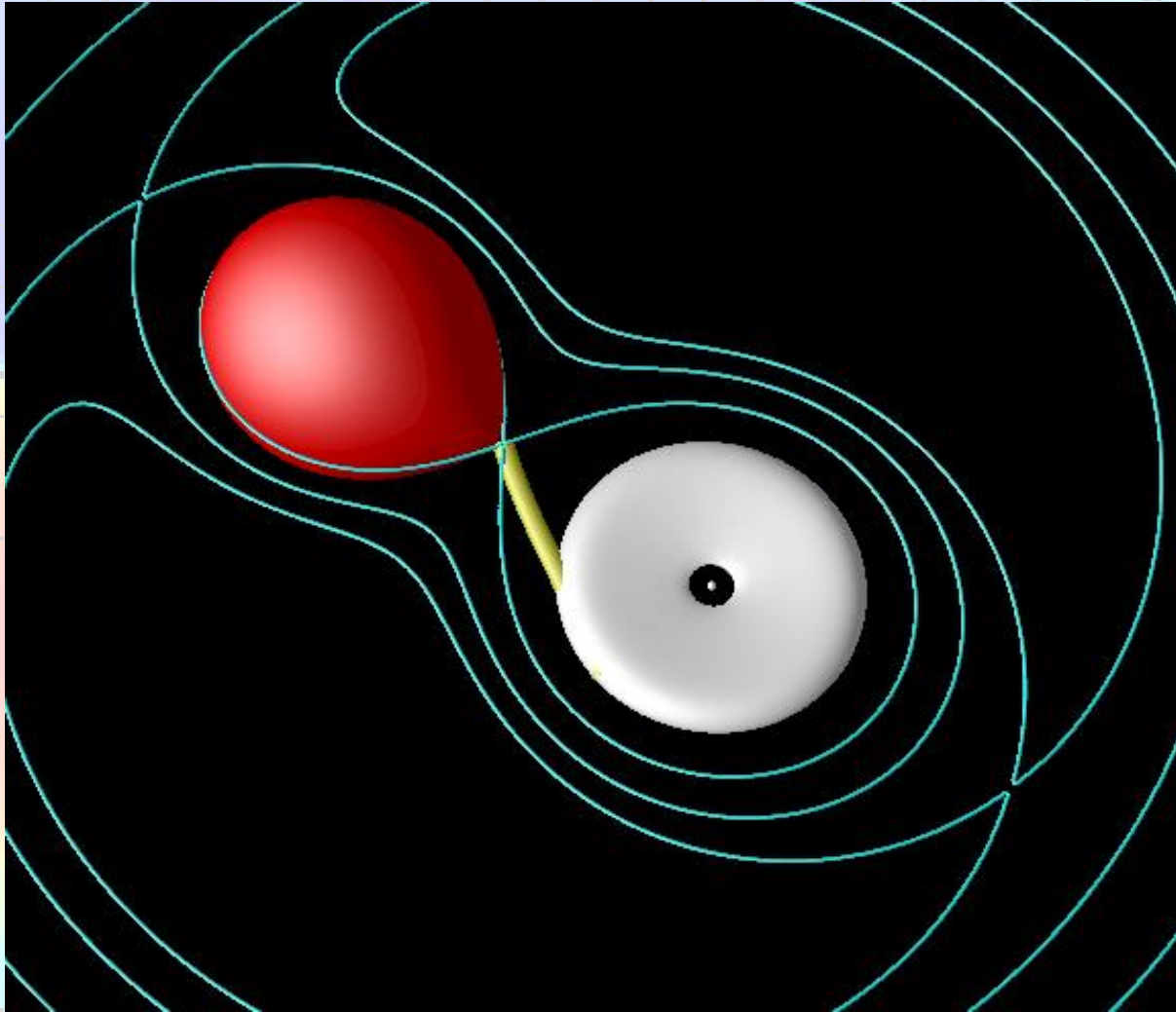
If a star during its evolution becomes large enough to fill the Roche lobe, then the mass transfer between the components of the system occurs through the vicinity of the inner Lagrangian point.



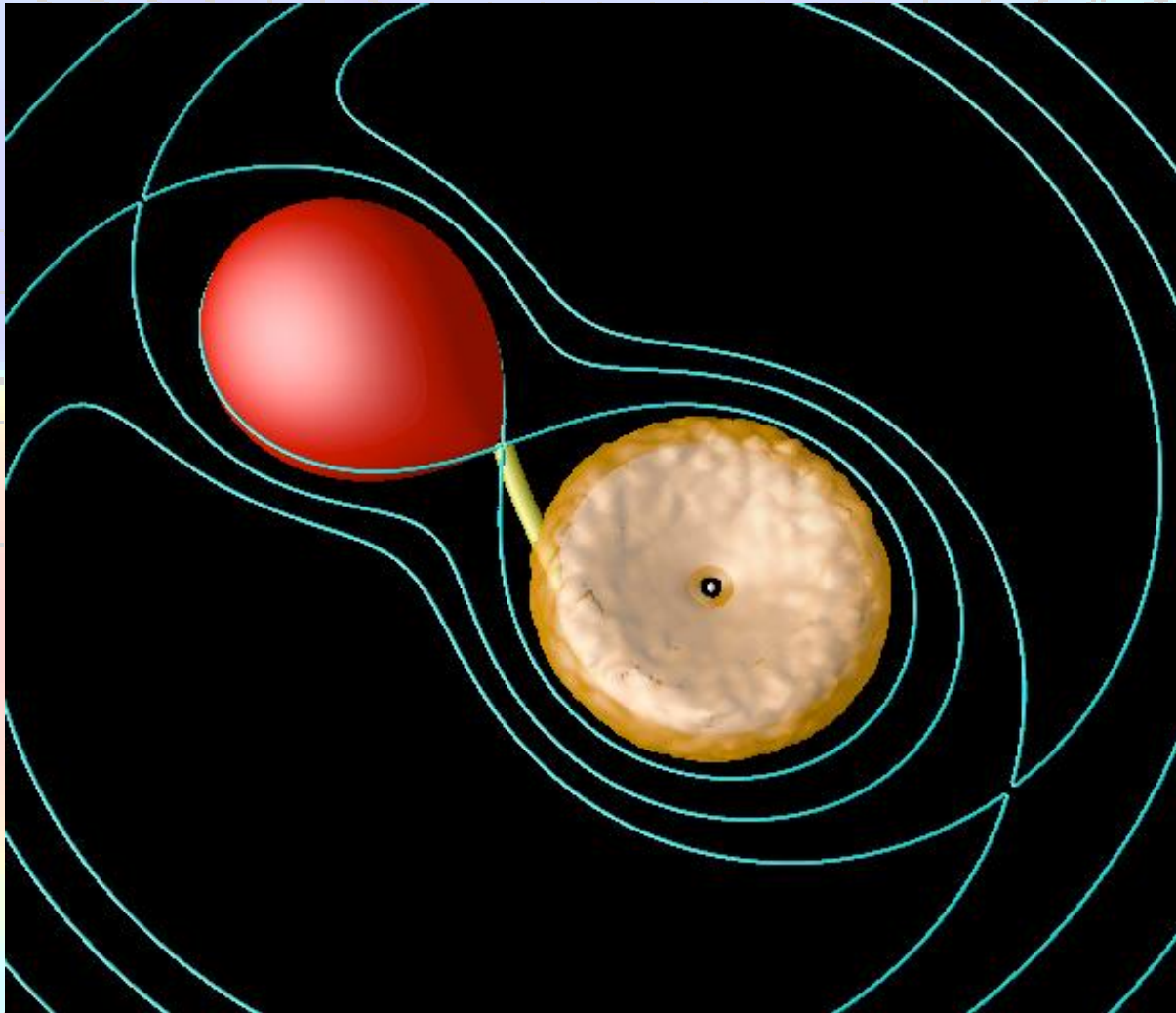
If the size of the accretor is small (**WD**) the gas of the stream will revolve around the gravitational center and form a dense ring.



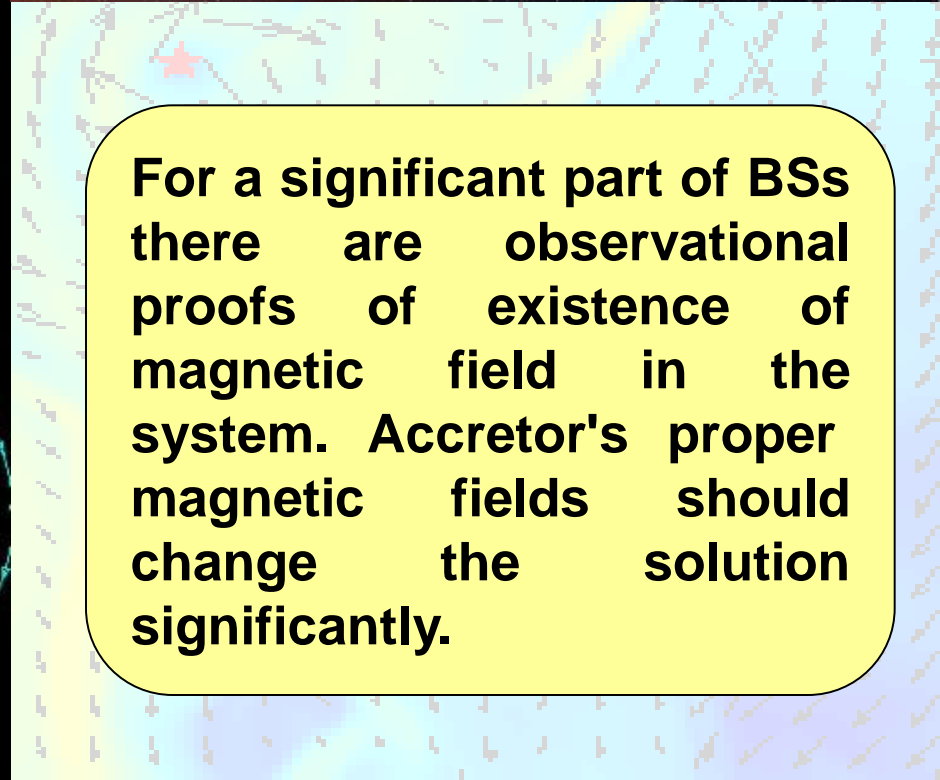
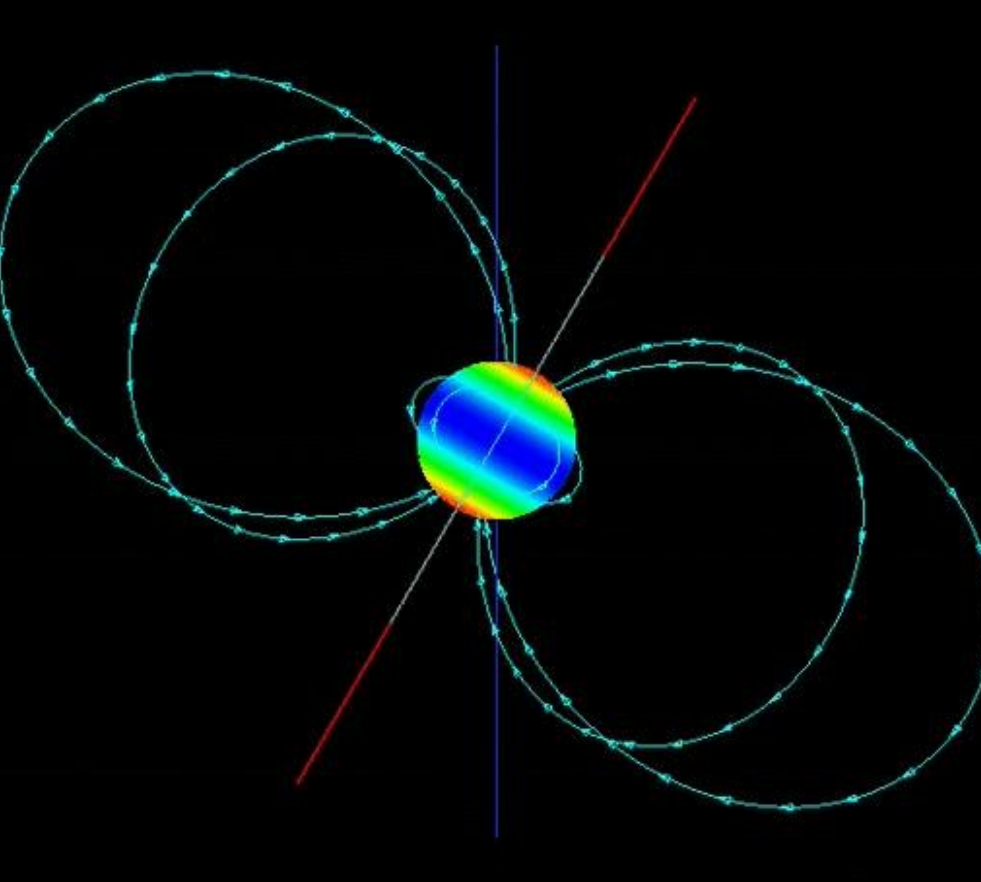
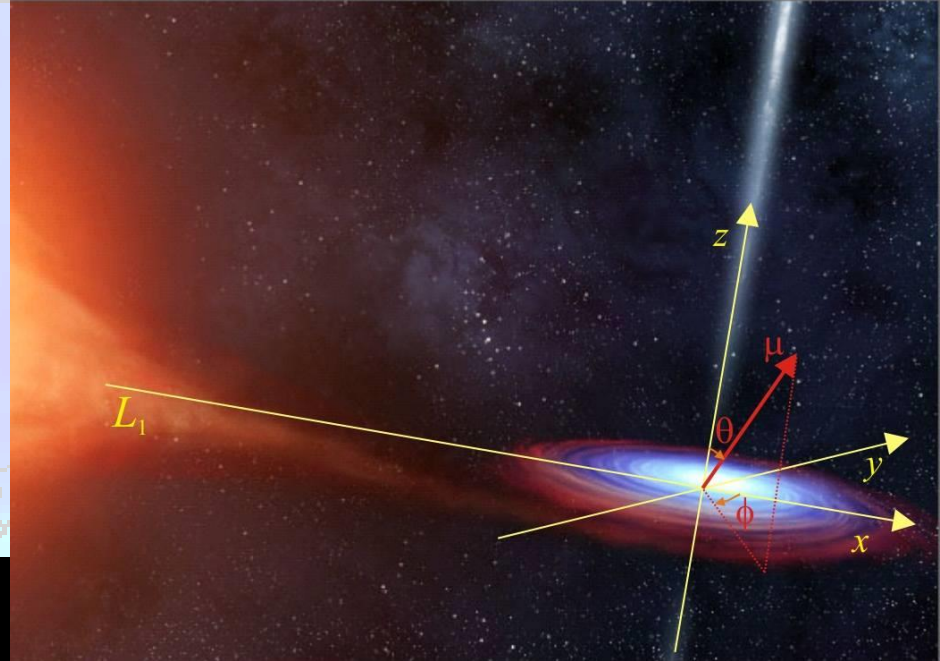
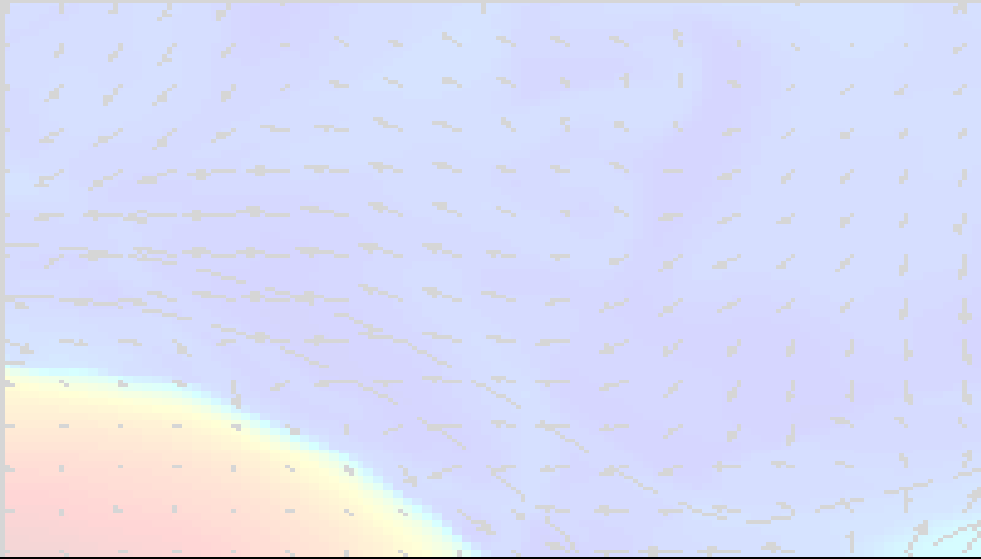
If the size of the accretor is small (**WD**) the gas of the stream will revolve around the gravitational center and form a dense ring.



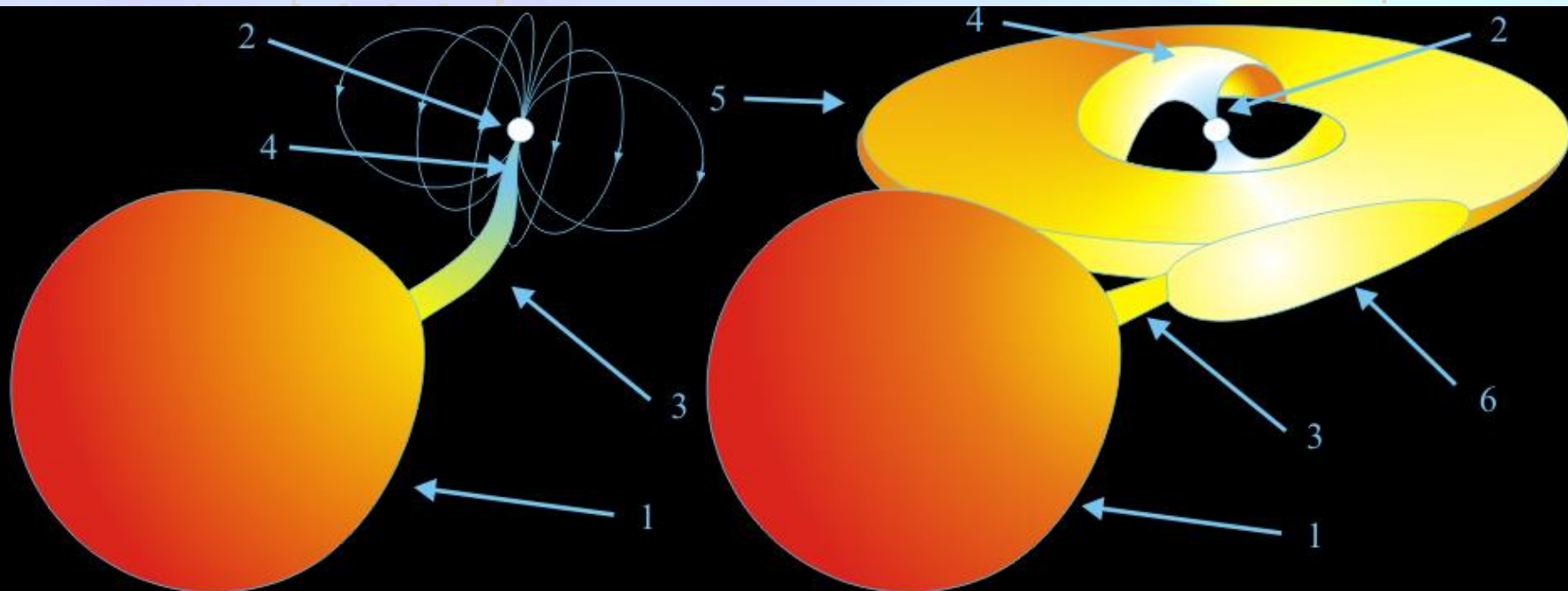
Under the action of dissipation processes the initial ring will expand and form an accretion disc.



Further redistribution of the angular momentum in the disc leads to the gas accretion and the formation of a near disc halo.



For a significant part of BSs there are observational proofs of existence of magnetic field in the system. Accretor's proper magnetic fields should change the solution significantly.



1 – donor-star, 2 – accretor, 3 – stream from L_1 , 4 – accretion column, 5 – accretion disk, 6 – hot line.

Depending on the strength of magnetic field, semi-detached binary systems, where the accretor is a magnetized white dwarf are divided into two classes: polars (or AM Her stars) and intermediate polars (or DQ Her stars). In a polar the magnetic field is so strong ($B \sim 10^7 - 10^8$ G) that matter from the donor star falls directly onto the primary star along accretion columns. In intermediate polars the magnetic field is not very strong ($B \sim 10^4 - 10^6$ G) and the accretion disc forms.



*The main details of the
flow pattern in IPs*

$$\frac{\partial \rho}{\partial t} + \nabla \cdot (\rho \vec{v}) = 0$$

$$\frac{\partial \vec{v}}{\partial t} + (\vec{v} \cdot \nabla) \vec{v} = -\frac{\nabla P}{\rho} - \frac{1}{4\pi\rho} [\vec{b} \times (\nabla \times \vec{b})] + 2(\vec{v} \times \vec{\Omega}) - \nabla \Phi - \frac{\vec{v}_{\perp}}{\tau}$$

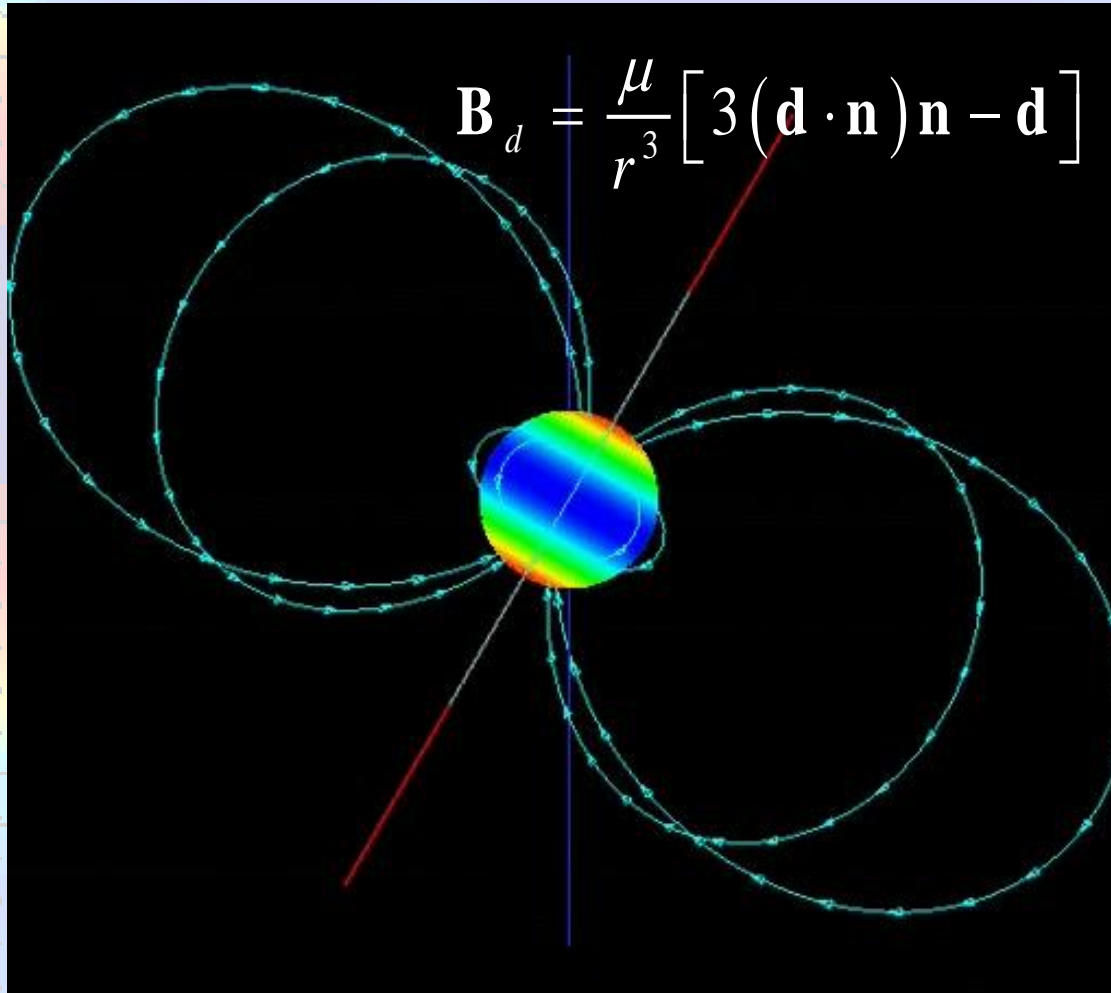
$$\frac{\partial \vec{b}}{\partial t} = \nabla \times [\vec{v} \times \vec{b} + \vec{v} \times \vec{B}_* - \eta(\nabla \times \vec{b})]$$

$$\rho T \left(\frac{\partial s}{\partial t} + (\vec{v} \cdot \nabla) s \right) = n^2 (\Gamma - \Lambda) + \frac{\eta}{4\pi} (\nabla \times \vec{b})^2$$

$$s = c_V \ln\left(\frac{P}{\rho^\gamma}\right)$$

In this model, the external magnetic field acts like a fluid that interacts efficiently with the plasma. The last term in (2) can be described as friction between the plasma and magnetic field (Zhilkin and Bisikalo, 2011).

Intermediate polar: $M_{\text{wd}}=1 M_{\text{sun}}$,
 $M_{\text{sec}}=0.5 M_{\text{sun}}$, $P=6\text{h}$, $A=2 R_{\text{sun}}$,
 $c_s=7.4 \text{ km/s}$, $M_{\text{ar}}=10^{-9} M_{\text{sun}}/\text{yr}$



The magnetic field of the accretor is considered to be a dipole type field. Here μ is the vector of the magnetic moment. We take the value $B_* = 10^5 \text{ G}$ for the magnetic induction on the surface of the compact primary star. We assume that the dipole moment is inclined to the rotation axis at the angle 30° .

Binary system in corotational frame



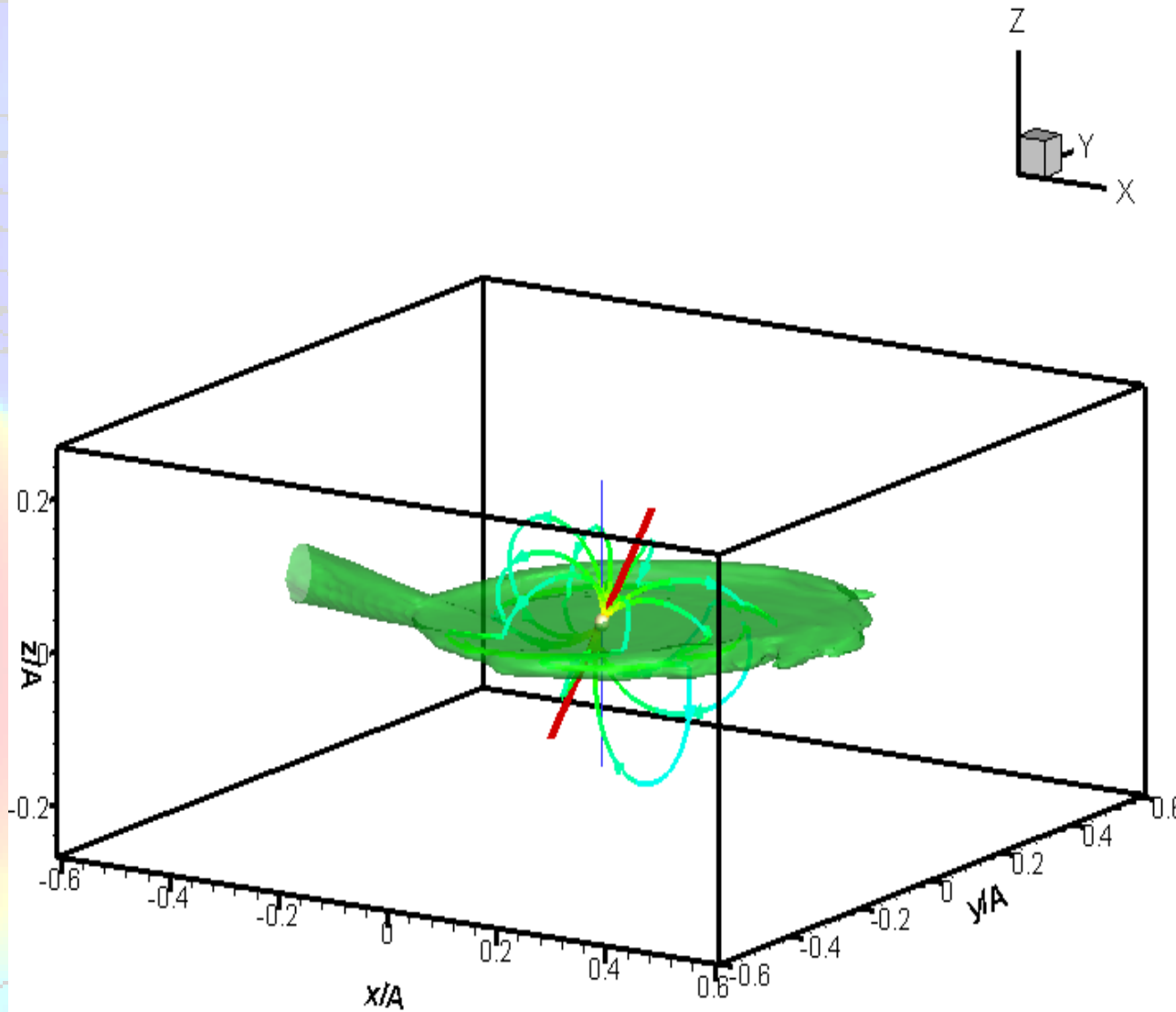
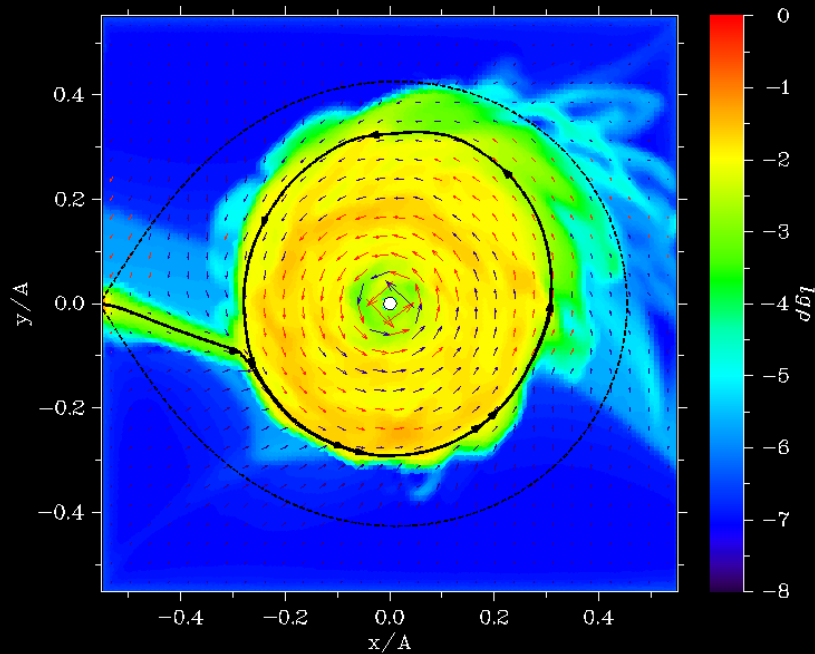


Figure shows the density isosurface. The blue line is the accretor rotation axis. The red line is the magnetic axis. The color along the magnetic field lines represents the strength of the field.

Time = $10.656 P_{orb}$ Velocity = $6.060 A\Omega$ \rightarrow

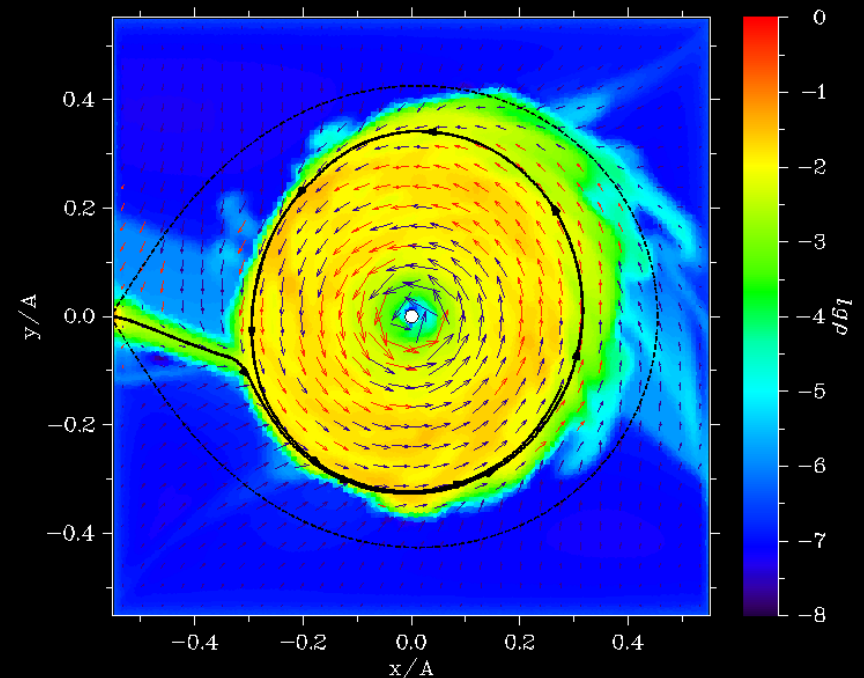


It was found out that in the MHD model the flow structure has the same qualitative features as in the pure HD solution: (i) magnetized accretion disc forms in the system;

(ii) all previously discovered waves still exist in the disc:

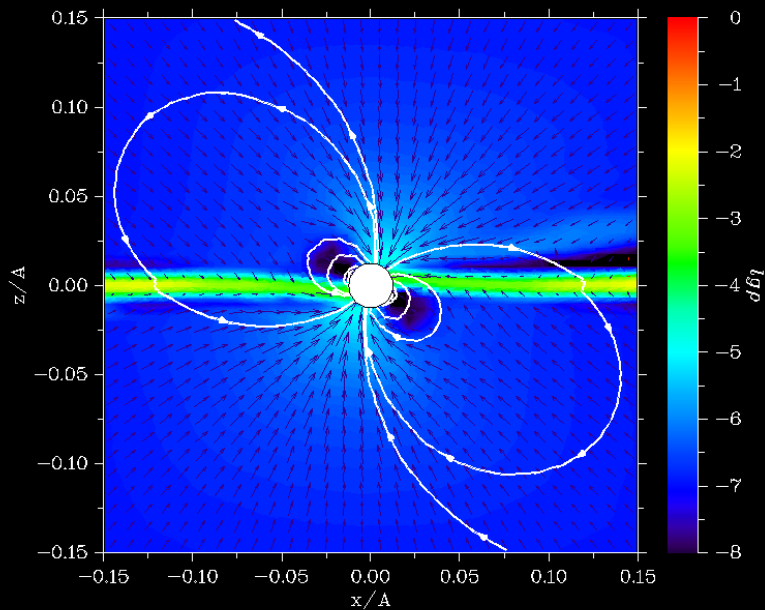
- bow shock;
- “hot line”;
- tidal shock;
- precessional wave.

Time = $13.359 P_{orb}$ Velocity = $3.000 A\Omega$ \rightarrow



Time = 12.064 P_{orb}

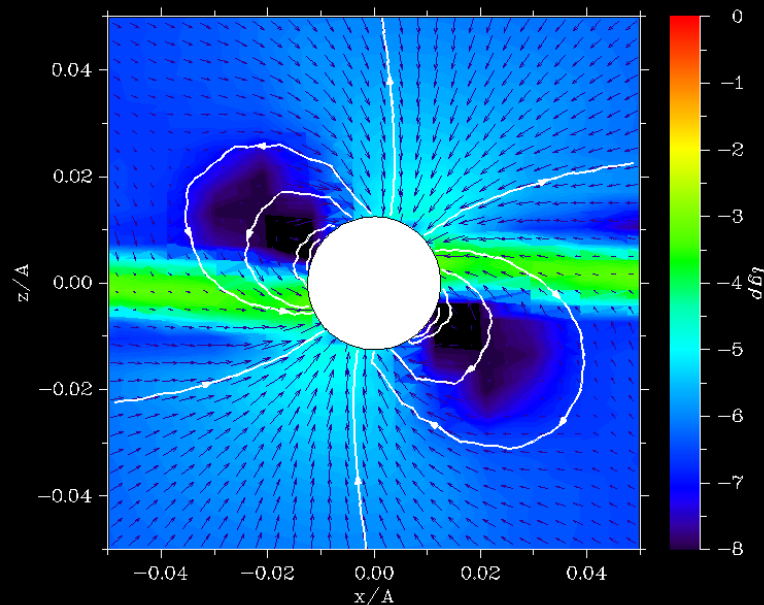
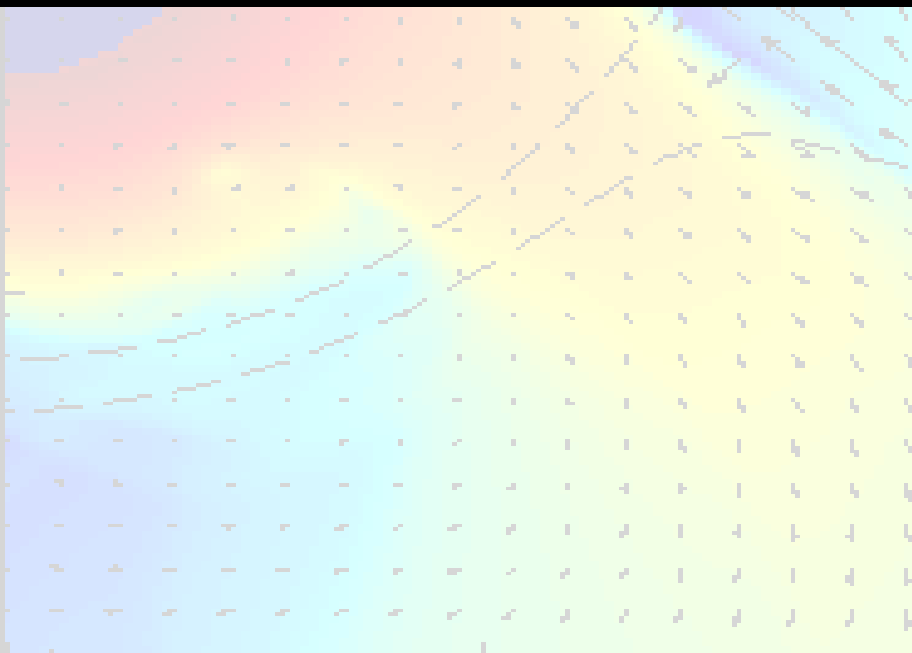
Velocity = 5.210 $A\Omega$



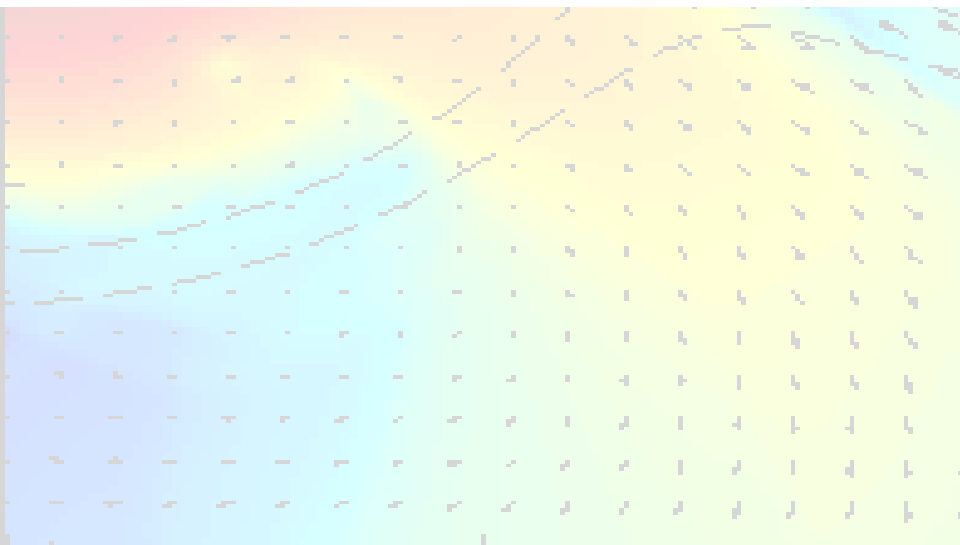
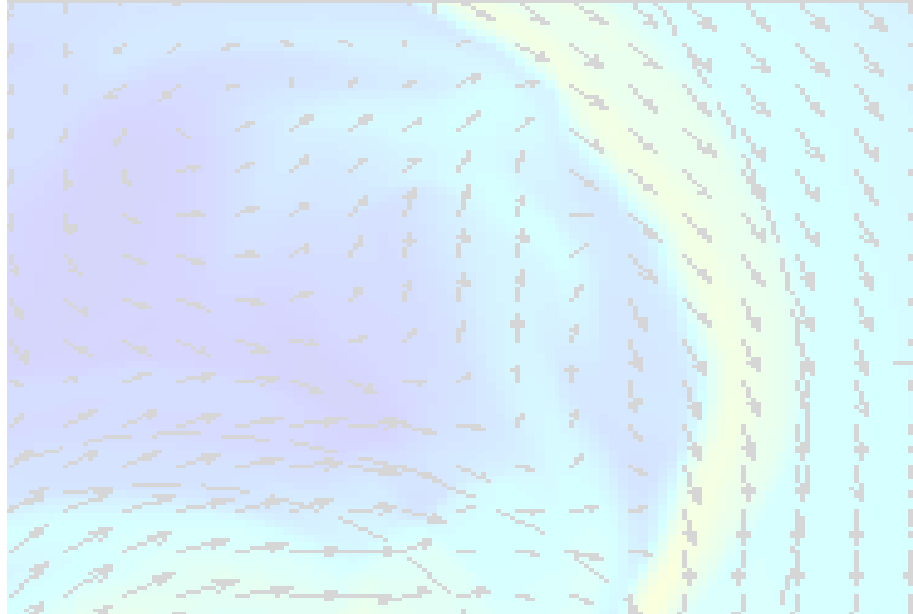
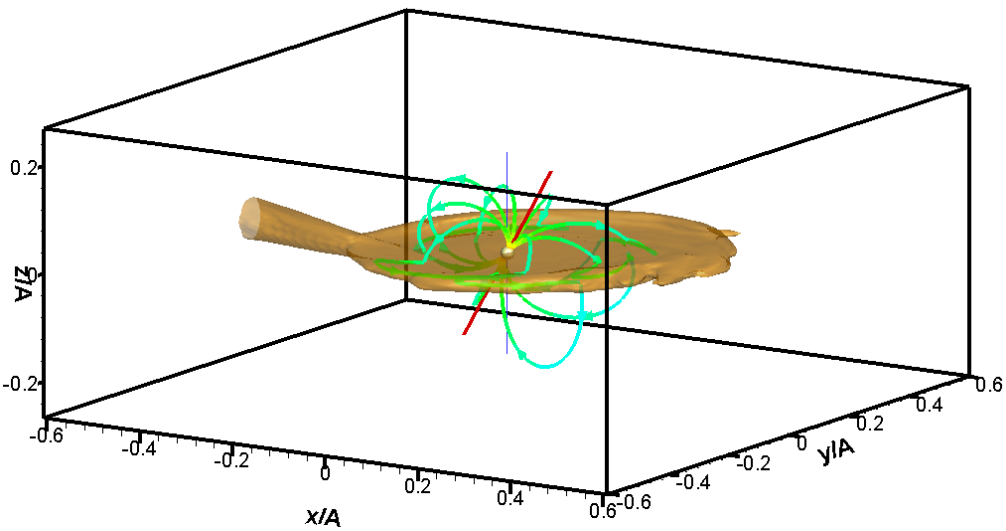
Presence of the magnetic field leads to formation of the magnetosphere and funnel flows near the magnetic poles of the primary star.

Time = 12.064 P_{orb}

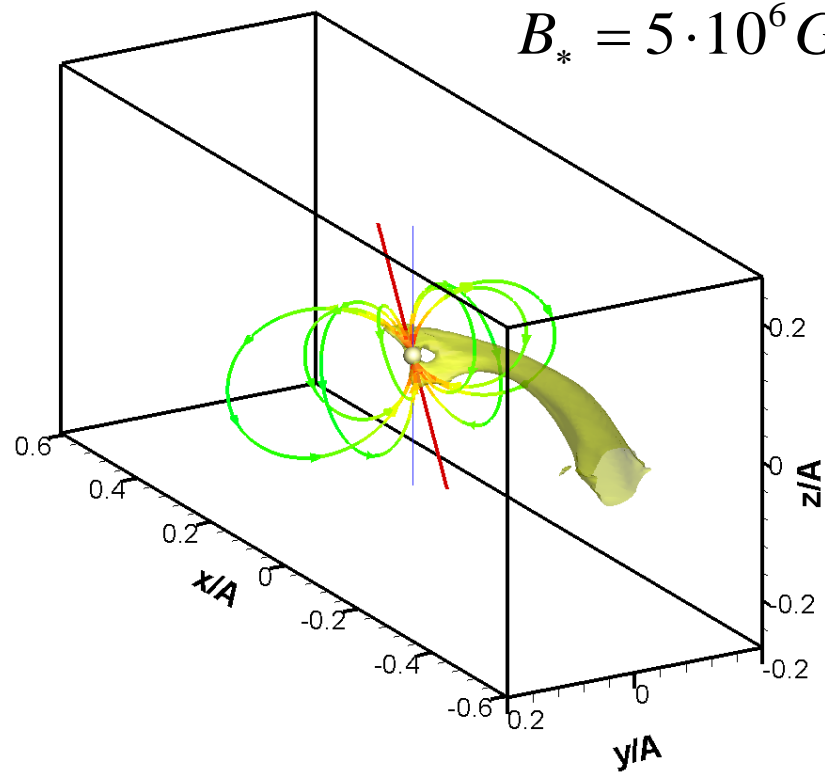
Velocity = 9.876 $A\Omega$



$$B_* = 10^5 G$$

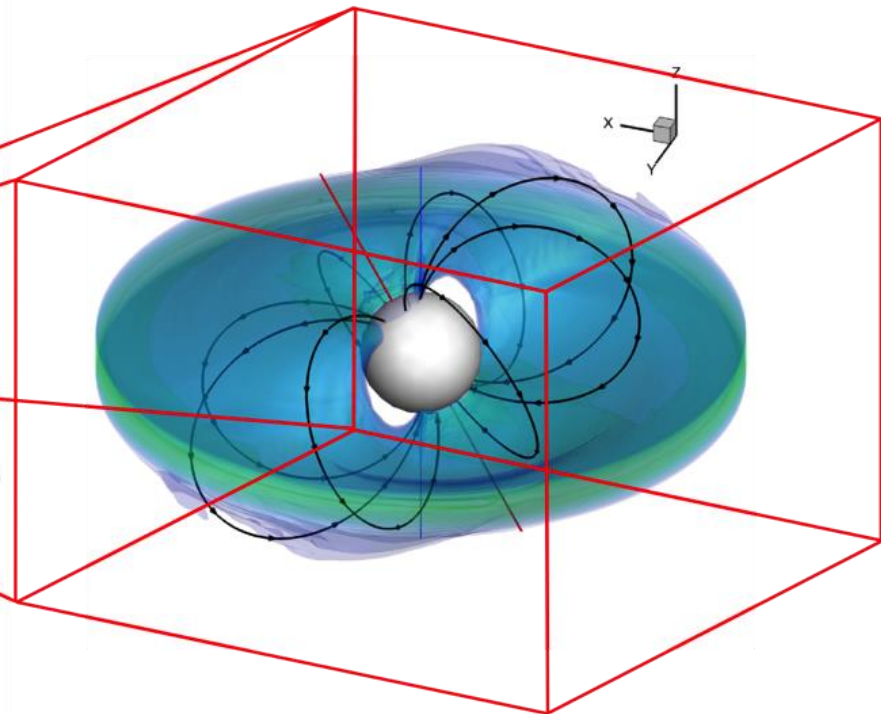
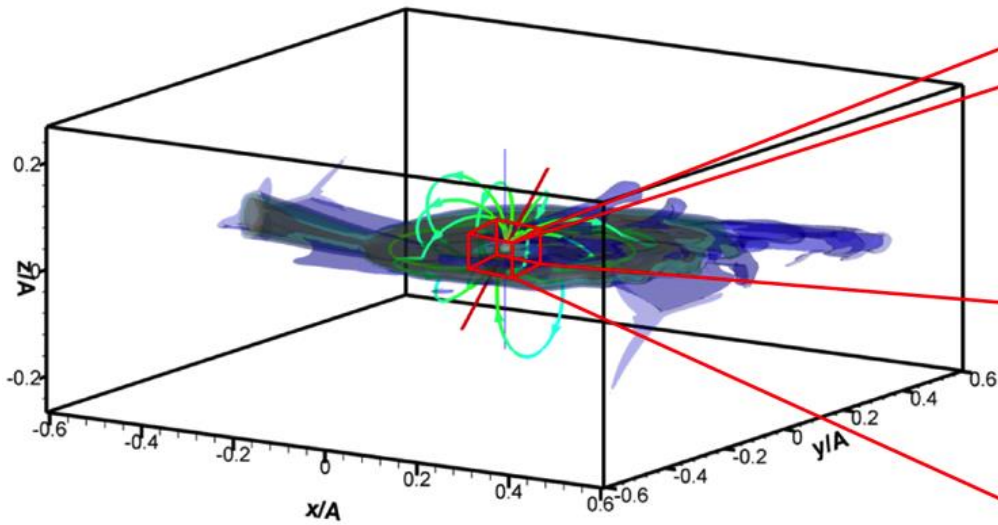


$$B_* = 5 \cdot 10^6 G$$

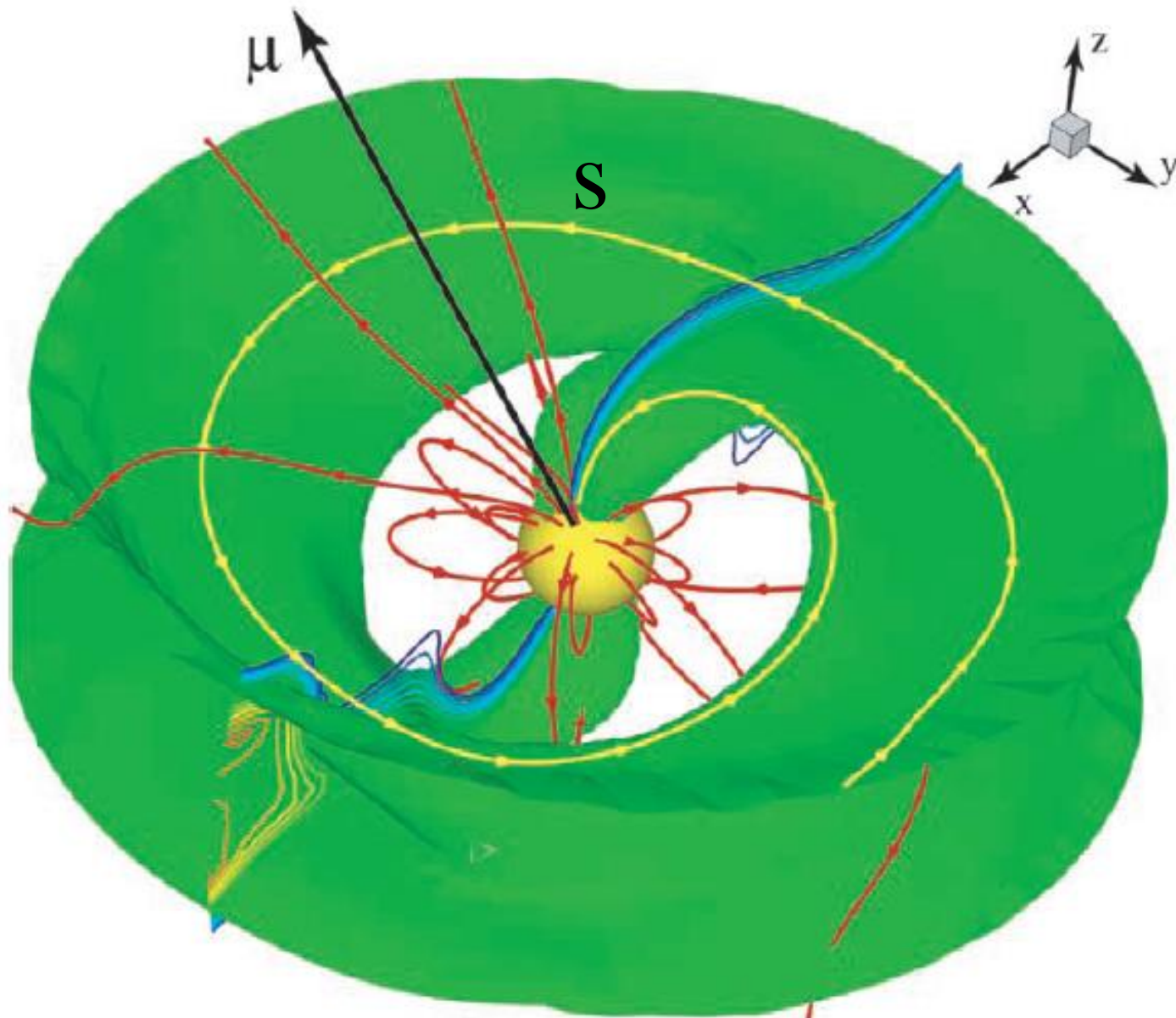




*Column accretion onto a
magnetized white dwarf
in IPs*

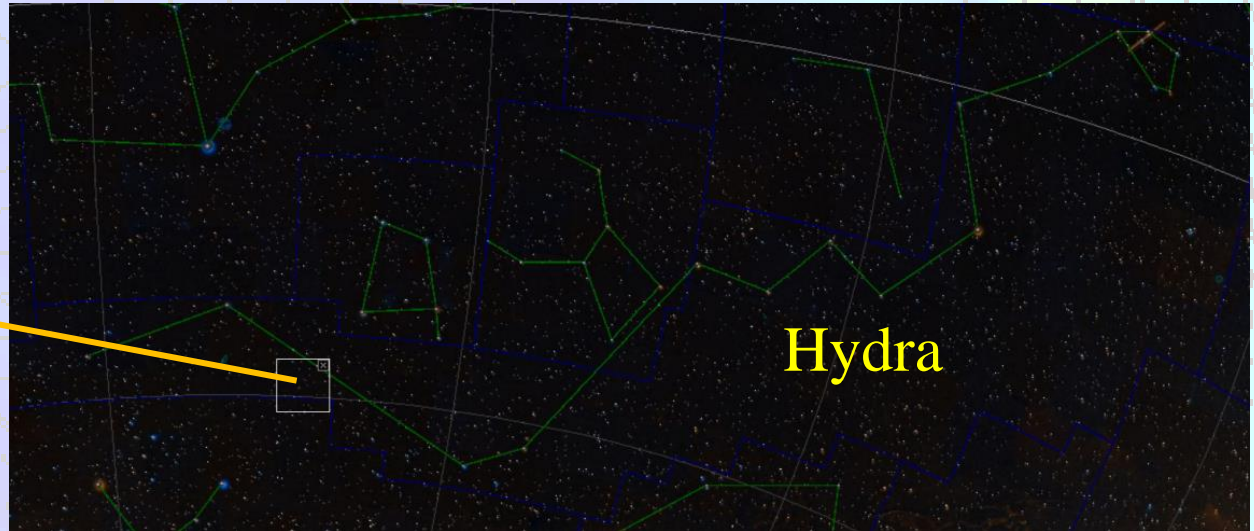
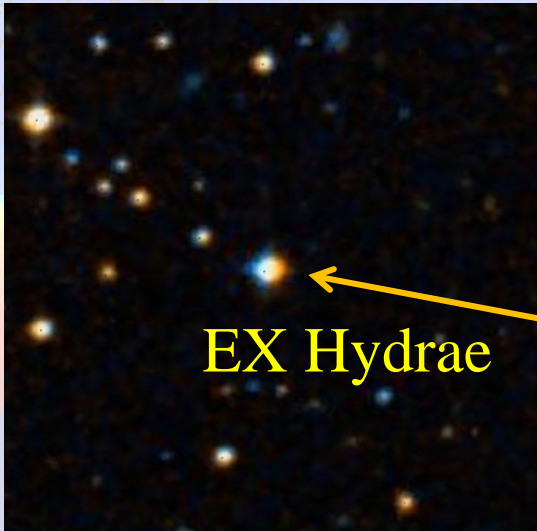


$h : 1000 \text{ km} \rightarrow 100 \text{ km}$



A.V. Koldoba, M.M. Romanova, G.V. Ustyugova, R.V.E. Lovelace, AJ 576, L53 (2002).

EX Hya

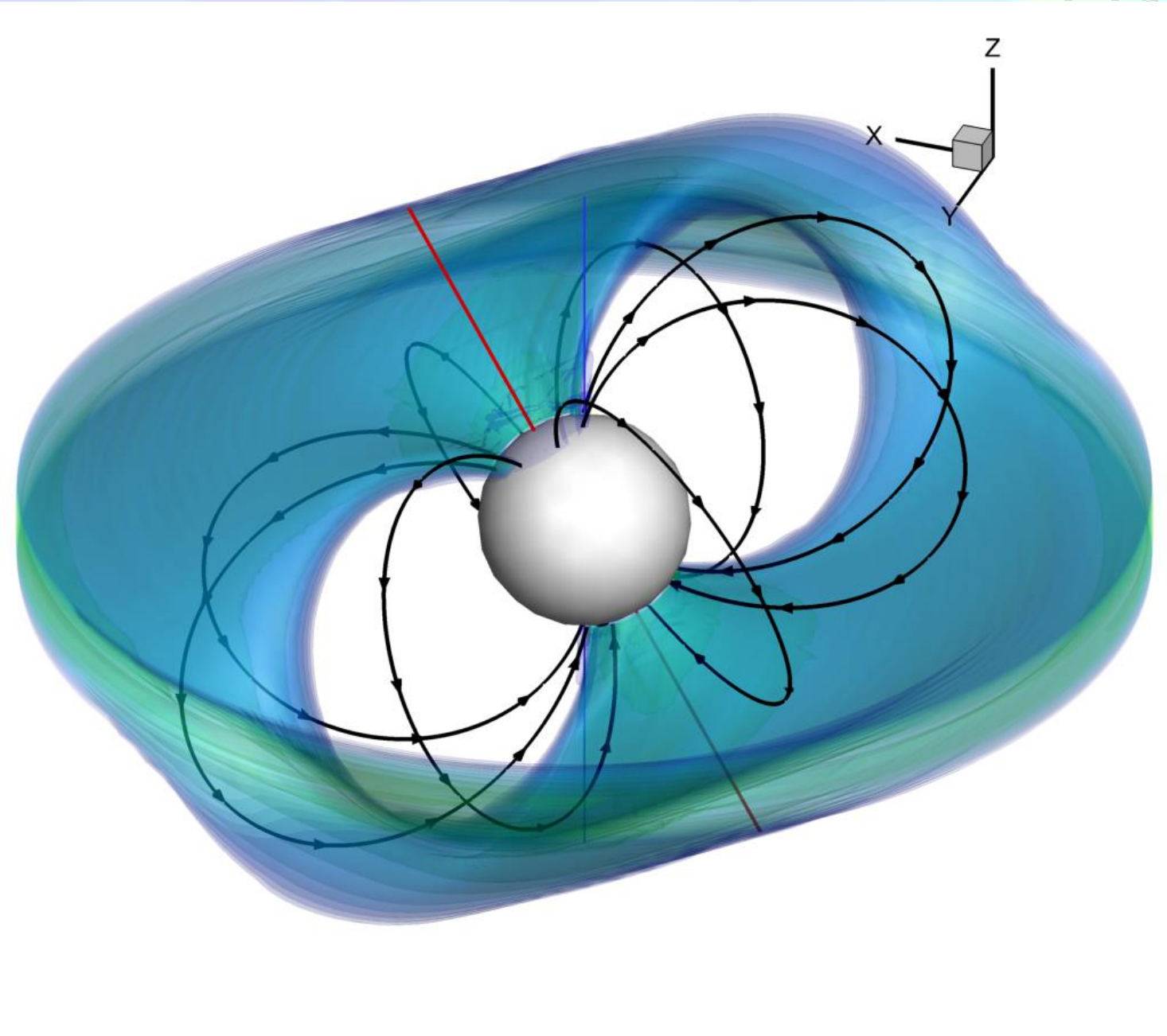


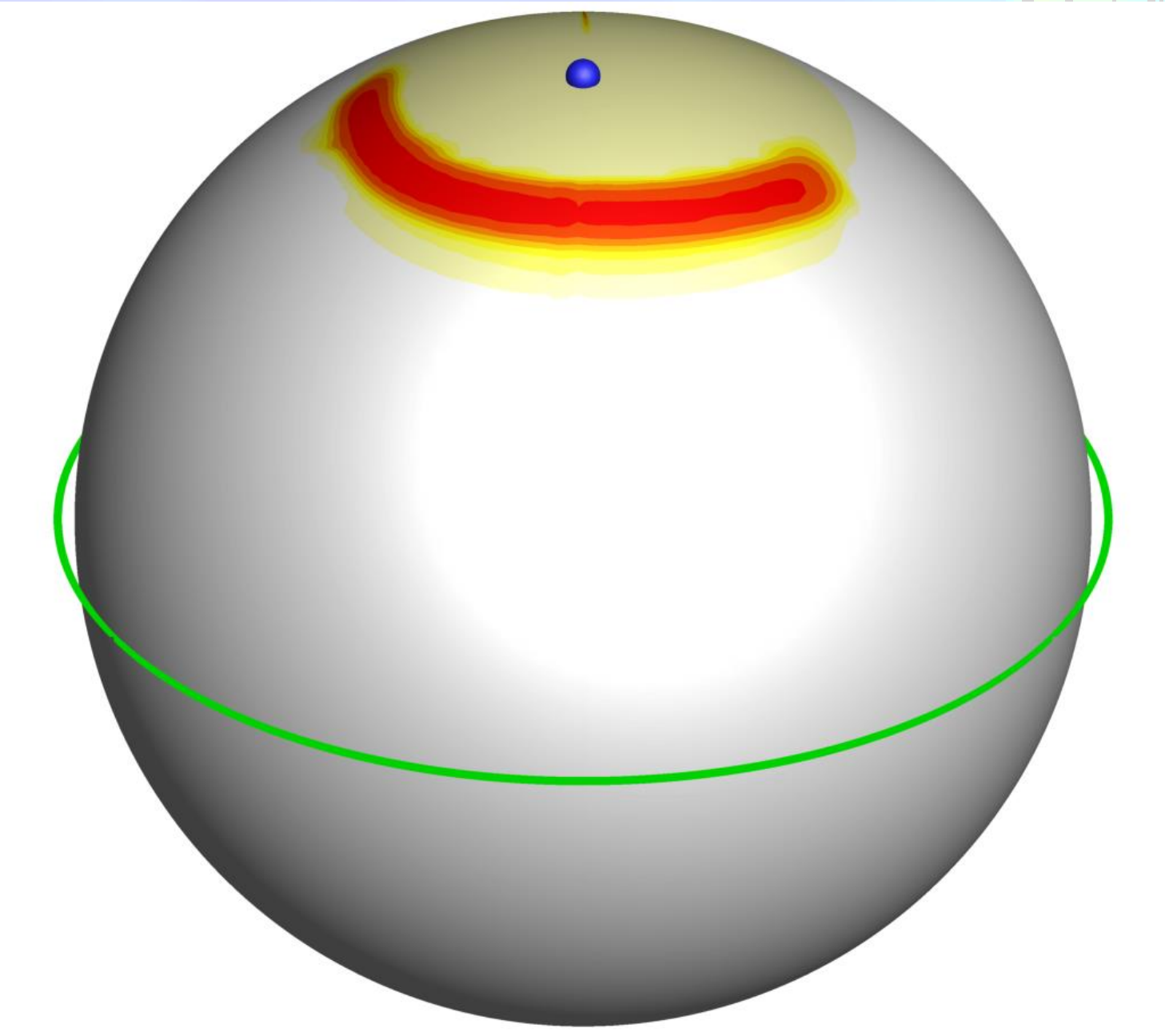
Position: $12^{\text{h}} 52^{\text{m}} 24.20^{\text{s}}$ - $29^{\circ}14' 56''$

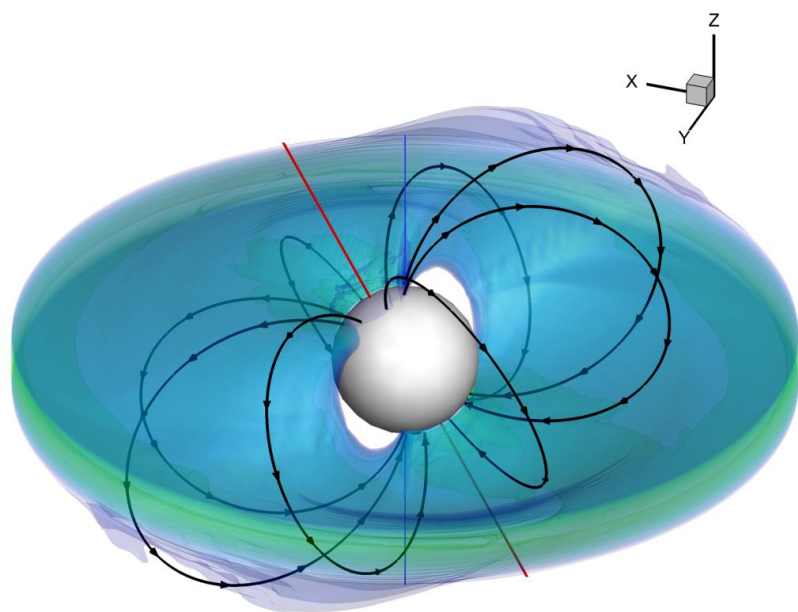
EX Hydrae (EX Hya) is one of the closest ($d \approx 65$ pc) and brightest ($9.6^{\text{m}} - 14^{\text{m}}$) cataclysmic variables. It was discovered by Kraft in 1962 and quickly recognized as an eclipsing system. EX Hya system is a typical intermediate polar.

EX Hya: parameters

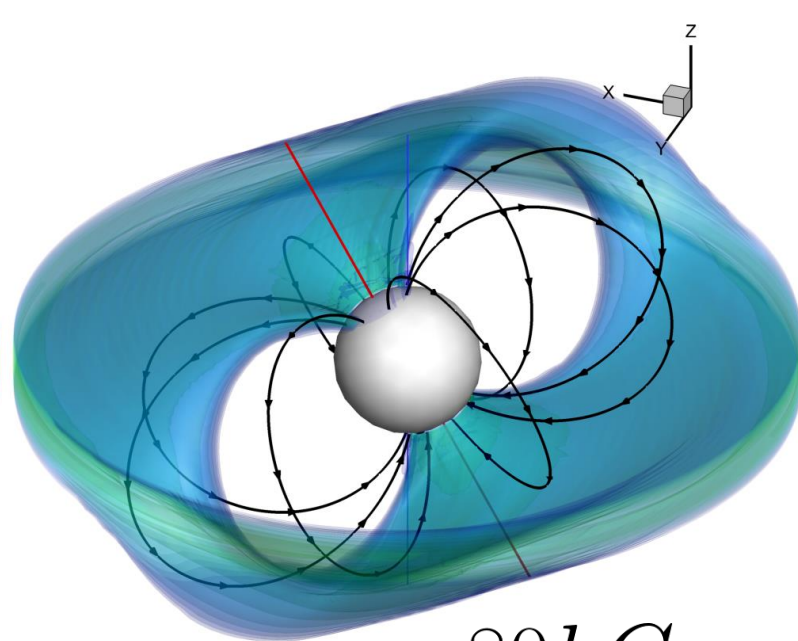
Parameter	Value
Orbital period, P_{orb}	1.63 h
Primary mass (white dwarf), M_{d}	$0.79 M_{\odot}$
Secondary mass (red dwarf), M_{a}	$0.096 M_{\odot}$
Primary radius, R_{a}	0.7×10^9 cm
Secondary radius, R_{s}	1.04×10^{10} cm
Inner disk radius, R_{d}	1.9×10^9 cm
Mass accretion rate,	3×10^{15} g/s
Binary separation, A	4.68×10^{10} cm
Binary inclination, i	77.8°
Luminosity, L	2.6×10^{32} erg/s
Primary magnetic field, B_{a}	< 1 MG (7 – 8 kG)
Primary spin period, P_{spin}	1.11 h



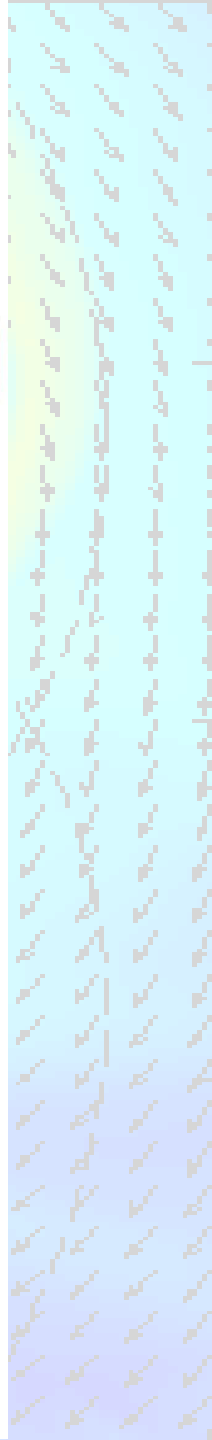
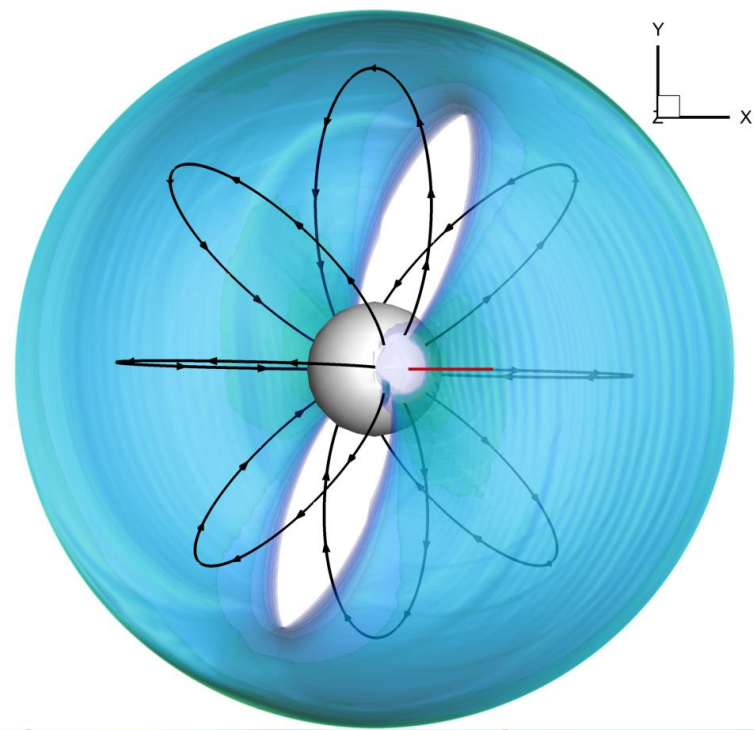
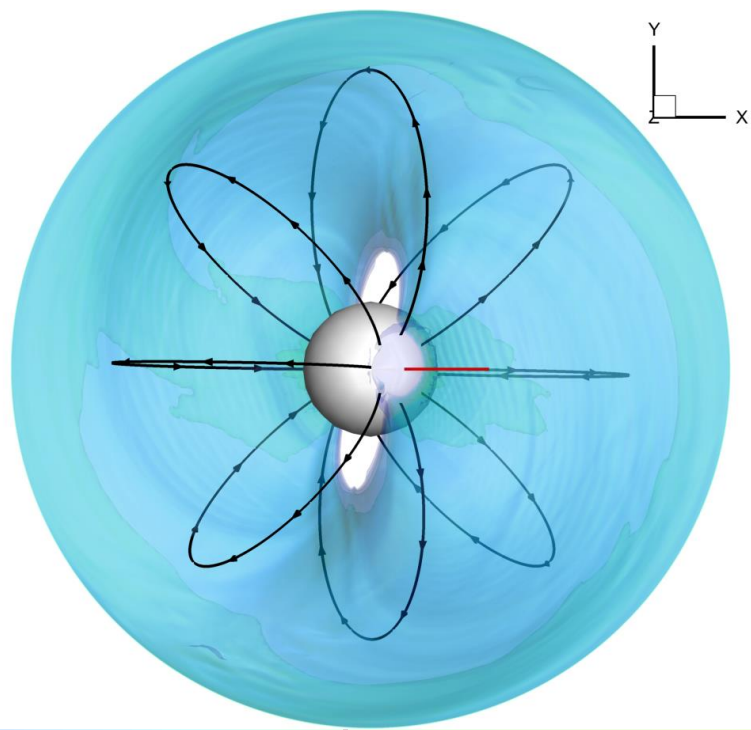


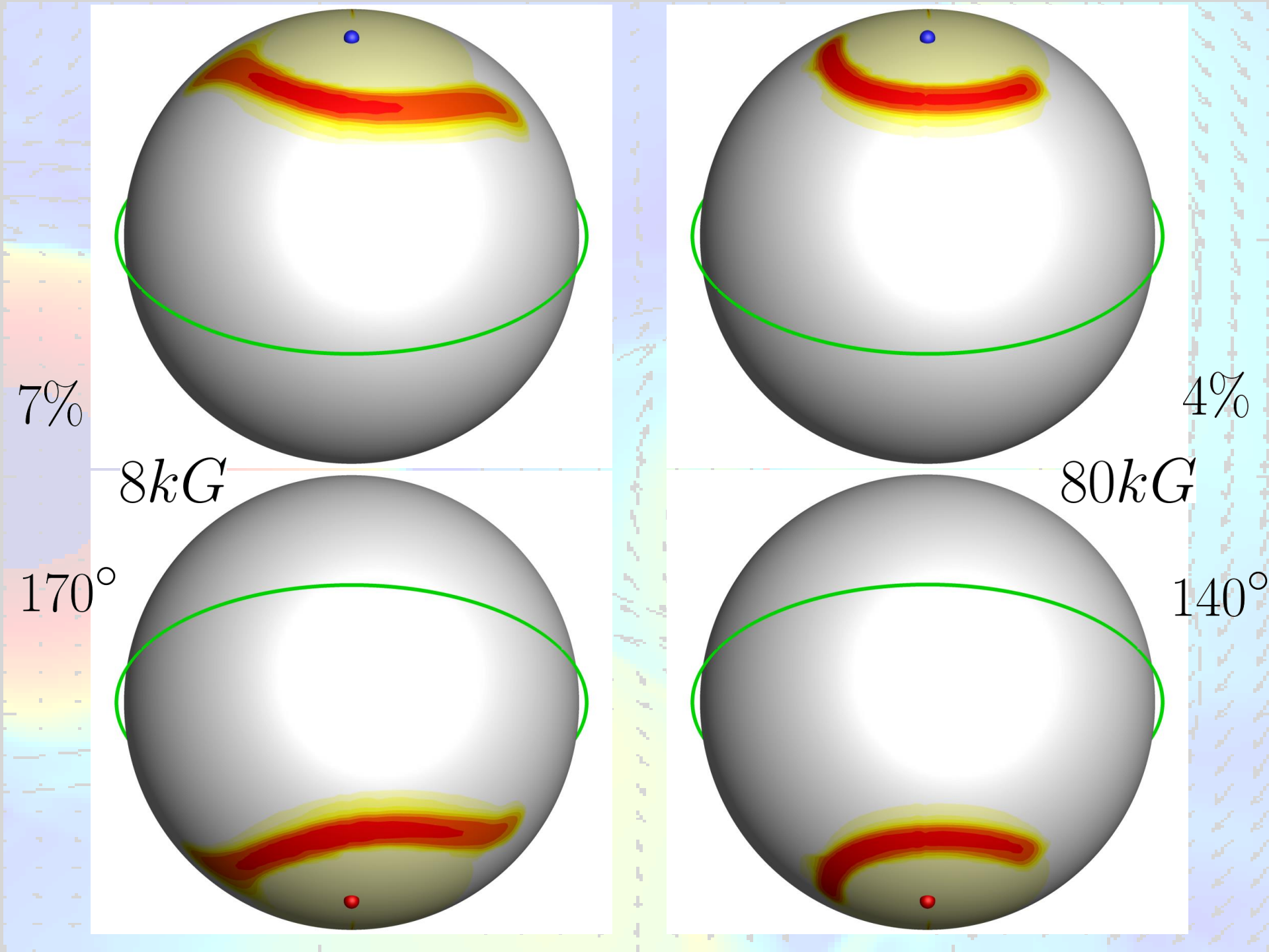


$8kG$



$80kG$





On the area of accretion curtains from fast aperiodic time variability of the intermediate polar EX Hya

Andrey N. Semena^{1*}, Mikhail G. Revnivtsev¹, David A.H. Buckley^{2,3},
Marissa M. Kotze², Ildar I. Khabibullin¹, Hannes Breytenbach^{2,4}
Amanda A. S. Gulbis², Rocco Coppejans⁵, Stephen B. Potter²

¹Space Research Institute, Russian Academy of Sciences, Profsoyuznaya 84/32, 117997 Moscow, Russia

²South African Astronomical Observatory, PO Box 9, 7935 Observatory, Cape Town, South Africa

³Southern African Large Telescope Foundation, PO Box 9, 7935 Observatory Cape Town, South Africa

⁴University of Cape Town, Private Bag X3, 7701 Rondebosch, South Africa

⁵Department of Astrophysics/IMAPP, Radboud University Nijmegen, P.O. Box 9010, 6500 GL Nijmegen, The Netherlands

ABSTRACT

We present results of a study of the fast timing variability of the magnetic cataclysmic variable (mCV) EX Hya. It was previously shown that one may expect the rapid flux variability of mCVs to be smeared out at timescales shorter than the cooling time of hot plasma in the post shock region of the accretion curtain near the WD surface. Estimates of the cooling time and the mass accretion rate, thus provide us with a tool to measure the density of the post-shock plasma and the cross-sectional area of the accretion funnel at the WD surface. We have probed the high frequencies in the aperiodic noise of one of the brightest mCV EX Hya with the help of optical telescopes, namely SALT and the SAAO 1.9m telescope. We place upper limits on the plasma cooling timescale $\tau < 0.3$ sec, on the fractional area of the accretion curtain footprint $f < 1.6 \times 10^{-4}$, and a lower limit on the specific mass accretion rate $\dot{M}/A > 3$ g sec⁻¹ cm⁻². We show that measurements of accretion column footprints via eclipse mapping highly overestimate their areas. We deduce a value of $\Delta r/r \lesssim 10^{-3}$ as an upper limit to the penetration depth of the accretion disc plasma at the boundary of the magnetosphere.

Key words: accretion, accretion discs, X-rays: binaries – stars: individual: EX Hya

1 INTRODUCTION

Confining a hot (millions K) plasma in a magnetically controlled volume is not only the goal of the thermonuclear fusion reactors in terrestrial laboratories, but also is a reality near magnetic and relativistic compact objects in binary systems. It was realised quite some time ago that the strong magnetic fields of accreting white dwarfs and neutron stars disrupt accretion flows at some distance from their surfaces to form an accretion column (or curtain) around their magnetic poles (Pringle & Rees 1972; Lamb 1974). However, very little is currently known about the geometry of these columns or curtains. It is likely that the best currently available direct measurement of the size of an accretion column footprint on a white dwarf surface, was obtained several years ago via eclipse mapping of the polar FL Cet (O'Donoghue et al. 2006).

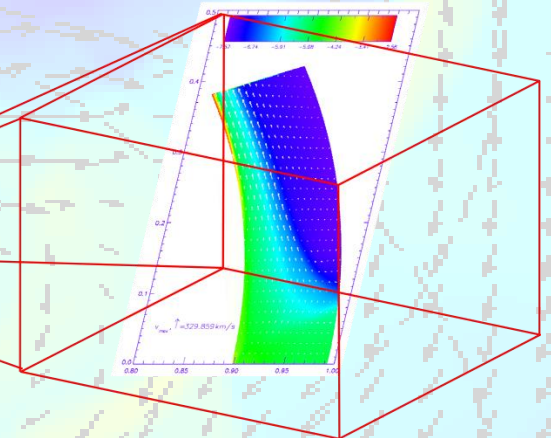
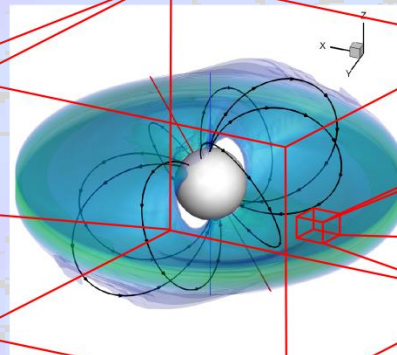
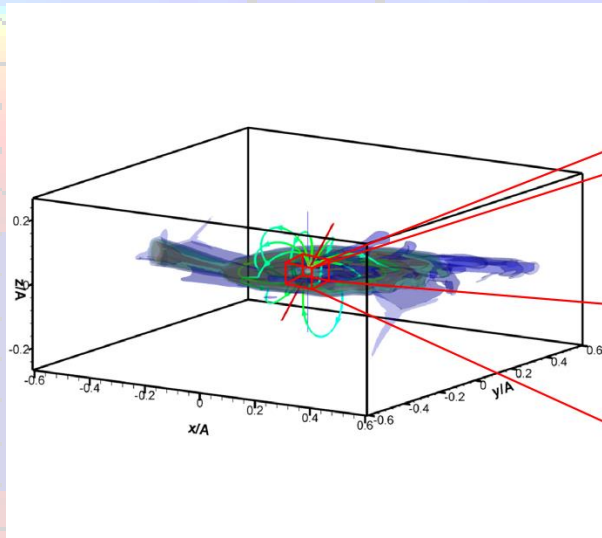
Indirectly, the geometry of the accretion col-

umn/curtain can be estimated from the density of the hot plasma which is heated by a standing shock wave near the white dwarf (WD) surface. The density determines the cooling time of the plasma, thus knowing this cooling time and the total mass accretion rate in the flow we can have a handle on the accretion column/curtain geometry. Langer, Chanmugam, & Shaviv (1981) showed that if the hot post shock region is cooling only via the bremsstrahlung emission it should be thermally unstable, generating quasi-periodic oscillations (QPOs) of the shock (see also Chevalier & Imamura 1982; Imamura et al. 1996). It was expected that such oscillations should be observable as optical brightness variations (see e.g. Larsson 1995). In later studies it was shown that there were mechanisms, like influence of cyclotron cooling, which can stabilize the post shock region (e.g. Chanmugam, Langer, & Shaviv 1985; Wu et al. 1994; Wu & Saxton 1999; Wu 2000; Saxton & Wu 2001). Another possible mechanism which might make the post-shock region oscillations invisible in lightcurves is incoherent variations of different parts of the accretion

**Semena, A.N. and
Revnivtsev, M.G.,
Astronomy Letters
40, 475 (2014)**

**Semena, A.N. et al.
MNRAS,
4426 1123 (2014)**

* E-mail: san@hea.iki.rssi.ru

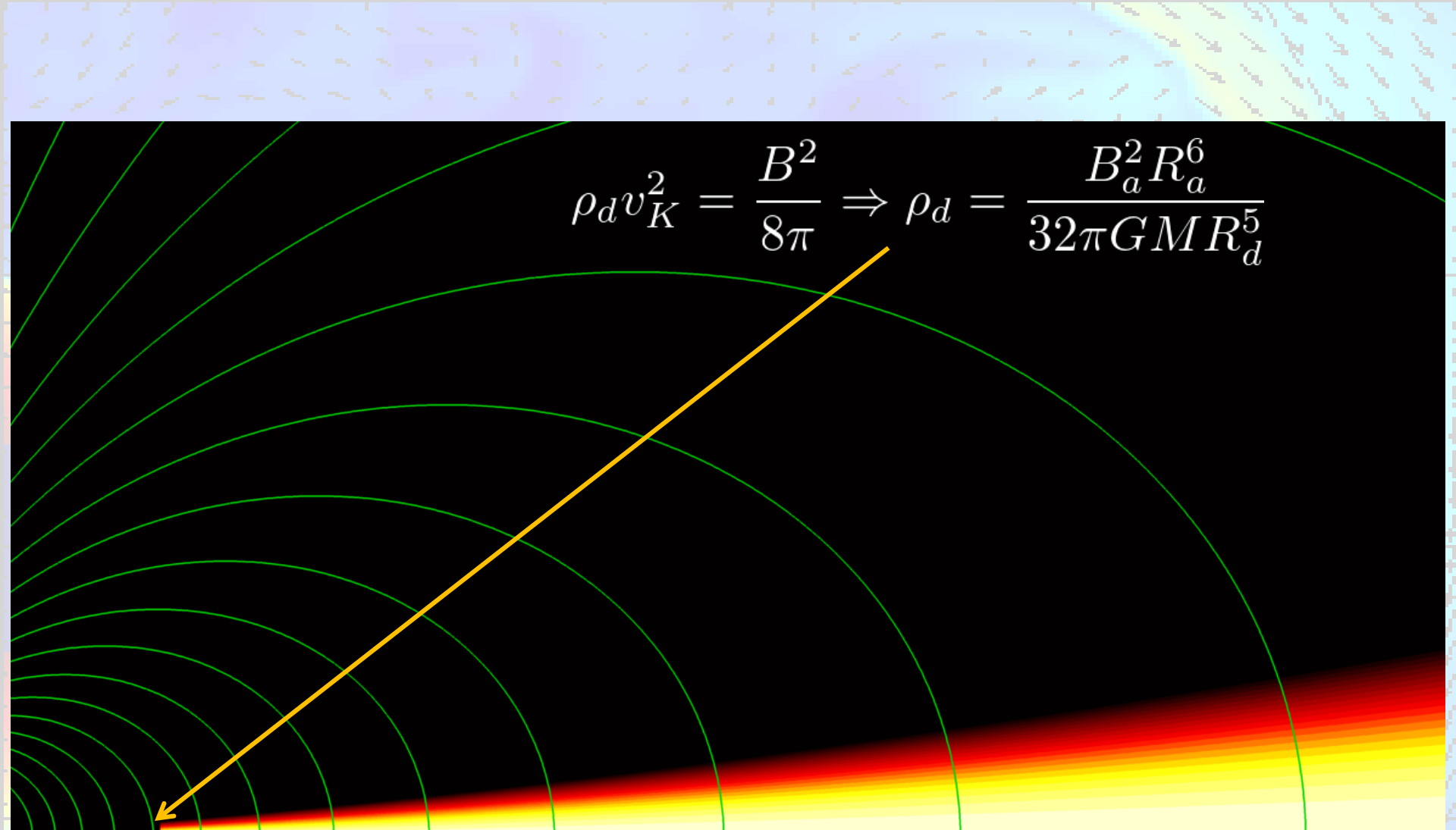


$h : 1000 \text{ km} \rightarrow 100 \text{ km} \rightarrow 10 \text{ km}$

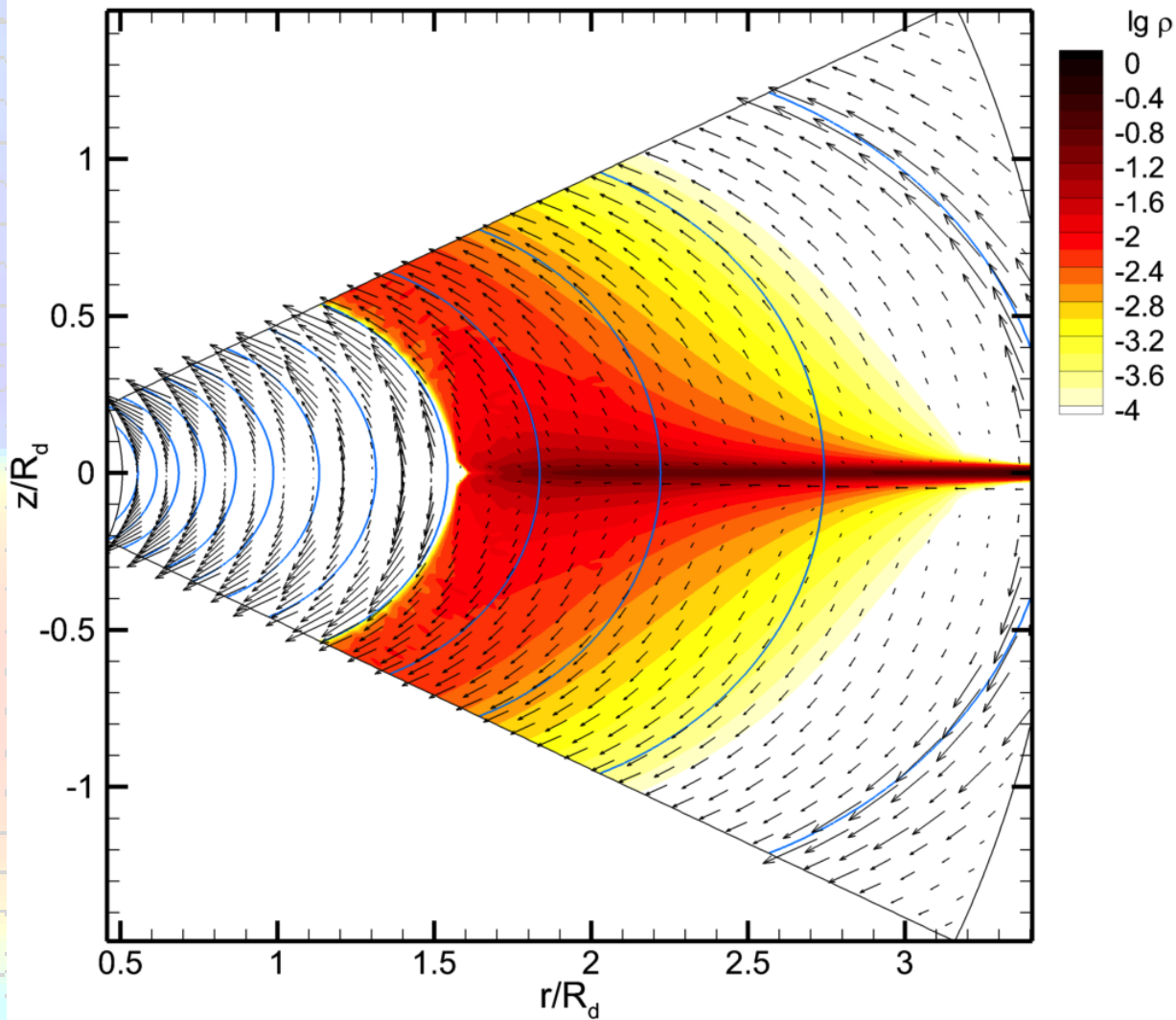
$$\rho = \rho_d e^{-z^2 / H_d^2}$$

$$H_d = \sqrt{\frac{2c_T^2 r^3}{GM}}$$

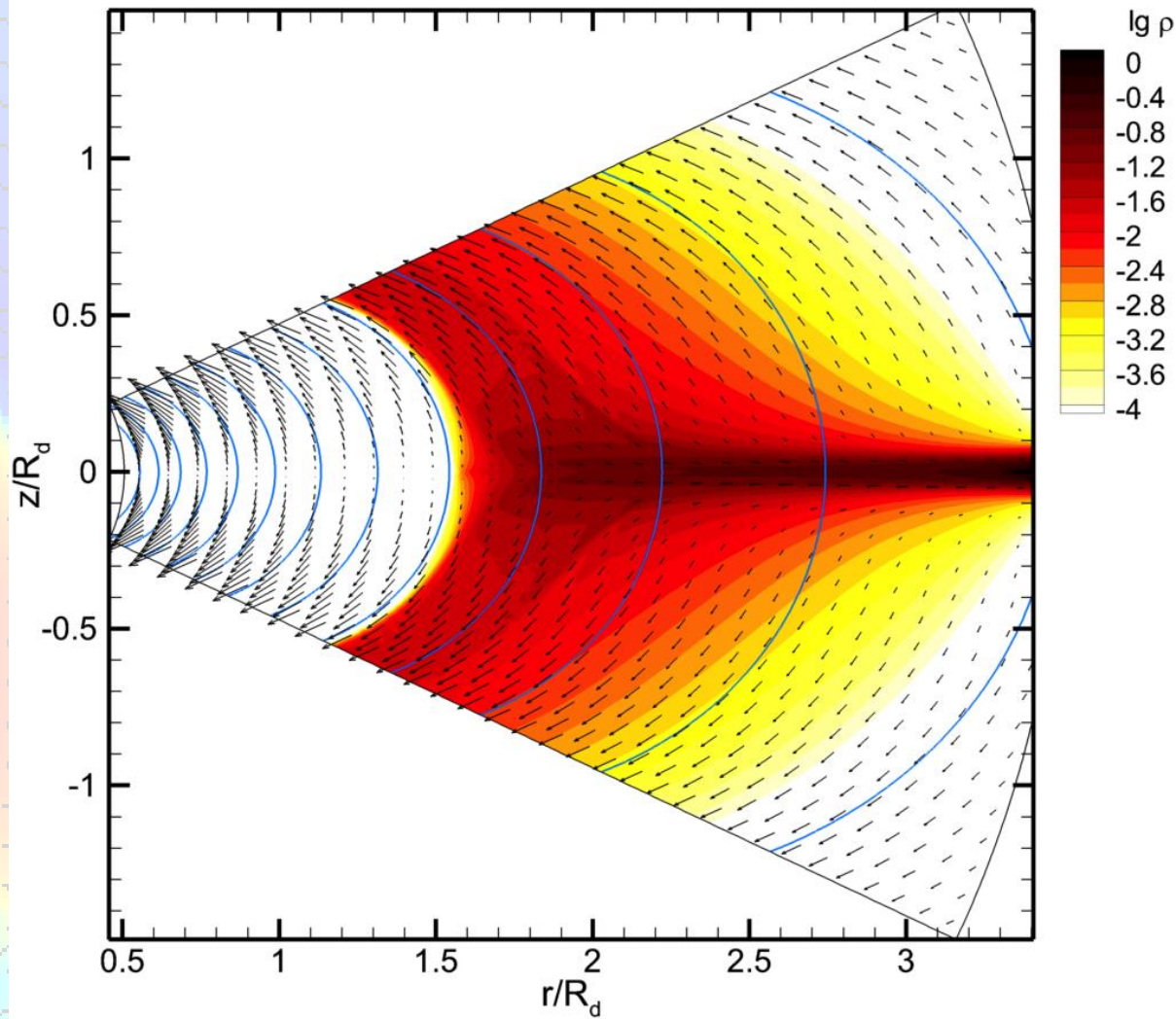
Initial distribution of density (color) and magnetic field (lines). The problem is axisymmetric and we solved it in cylindrical coordinates in the region $(0.6 R_d \leq r \leq 2.6 R_d, 0 \leq z \leq R_d)$. The initial disk was sub-keplerian and vertically hydrostatic.


$$\rho_d v_K^2 = \frac{B_a^2}{8\pi} \Rightarrow \rho_d = \frac{B_a^2 R_a^6}{32\pi G M R_d^5}$$

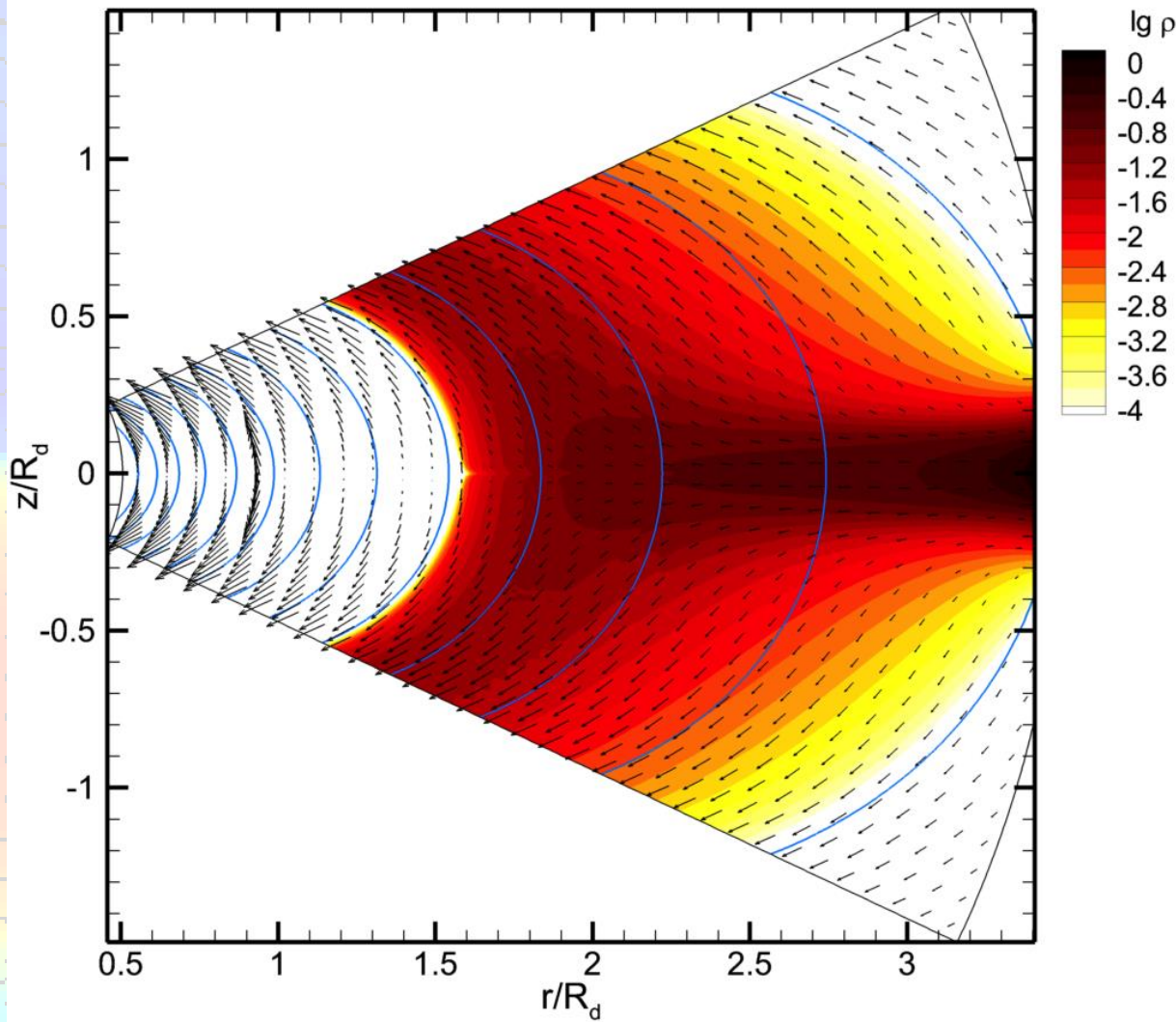
We use the inner radius of the disk R_d as a length-scale. The density in the disk can be obtained from the condition of magnetosphere equilibrium. The initial density in the corona was sufficiently low. The temperature of the disk was the model parameter.



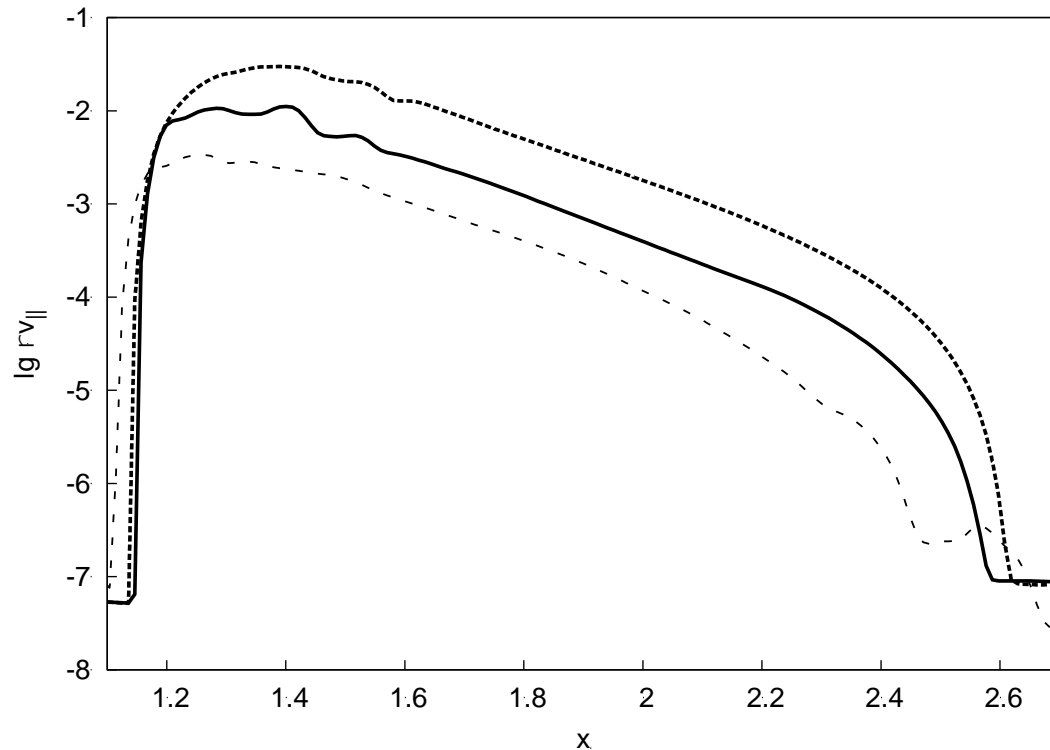
Distribution of the density (color scale) and velocity (arrows) in the meridional ($\phi = \text{const}$) plane of the Model with disk temperature $T = 10^3$ K. The curved lines correspond to the stellar magnetic-field lines.



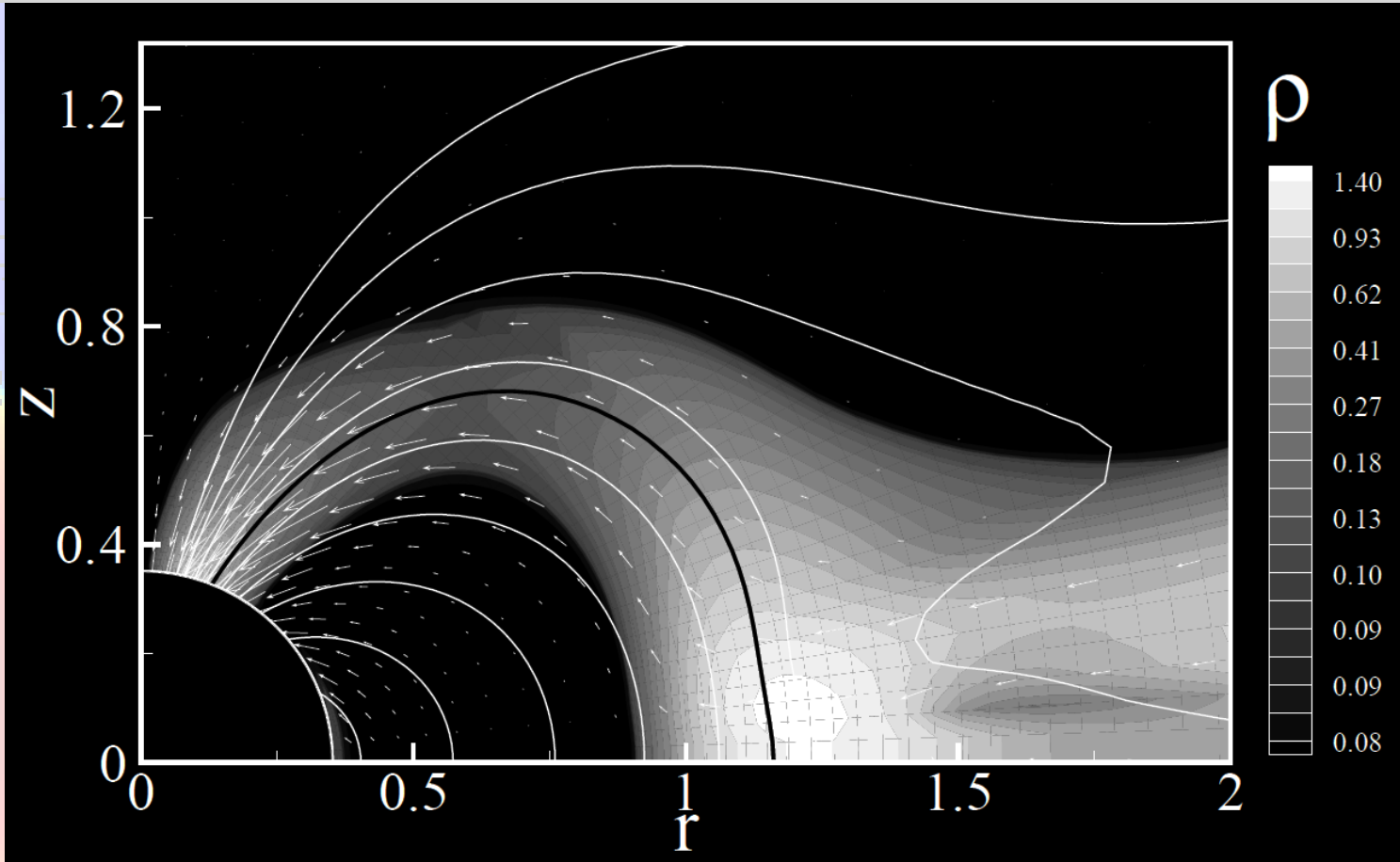
Model with disk temperature $T = 10^4$ K.



Model with disk temperature $T = 10^5$ K.



Distribution of the logarithm of the mass flux density over the cross section of the accretion flow for three accretion-disk temperature: 10^3 K (short-dashed curve), 10^4 K (solid curve), and 10^5 K (long-dashed curve).

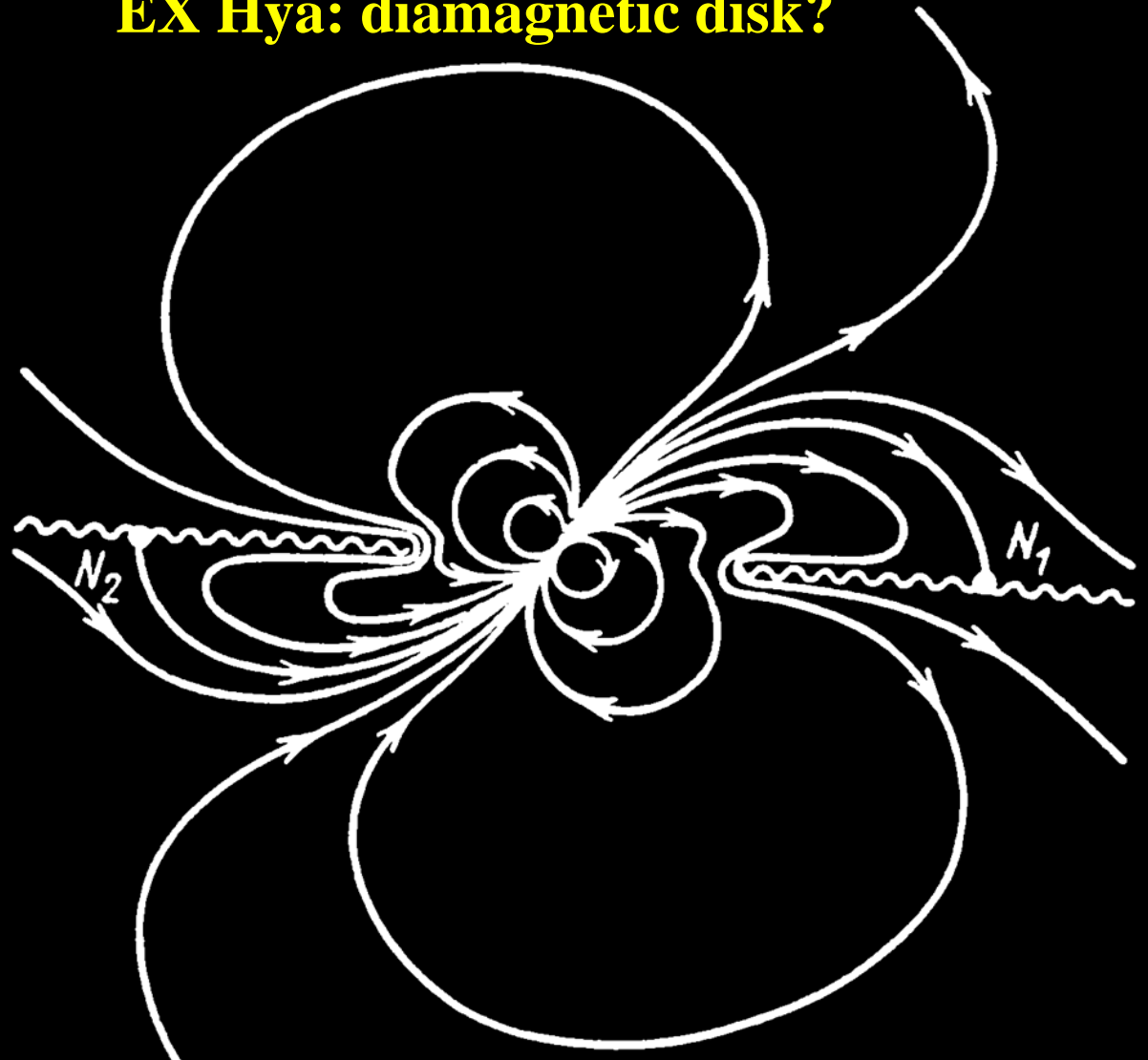


The results of the computations are in good agreement with the results obtained in other studies. However, we consider them to be **unsatisfactory** from the point of view of observations. The main conclusion following from an analysis of the results is that, in the stated formulation of the problem, the accretion curtain that is formed is too thick. Thus, in order to explain the observational data (a thin accretion curtain), we must invoke **some other ideas**.

EX Hya: diamagnetic disk?

Aly, 1980, A&A,
86, 192

Kundt, Robnik,
1980, A&A, 91,
305



Magnetic dipole with ideally conducting infinitely thin disk. The disk is purely diamagnetic and the magnetic field of the star is highly distorted.

Let us estimate the thickness of the accretion curtain in the case when the magnetic field penetrates into the plasma owing to diffusion. The thickness of the curtain will then be equal to the thickness of the diffusion layer,

$$H_m \approx \sqrt{\eta\tau},$$

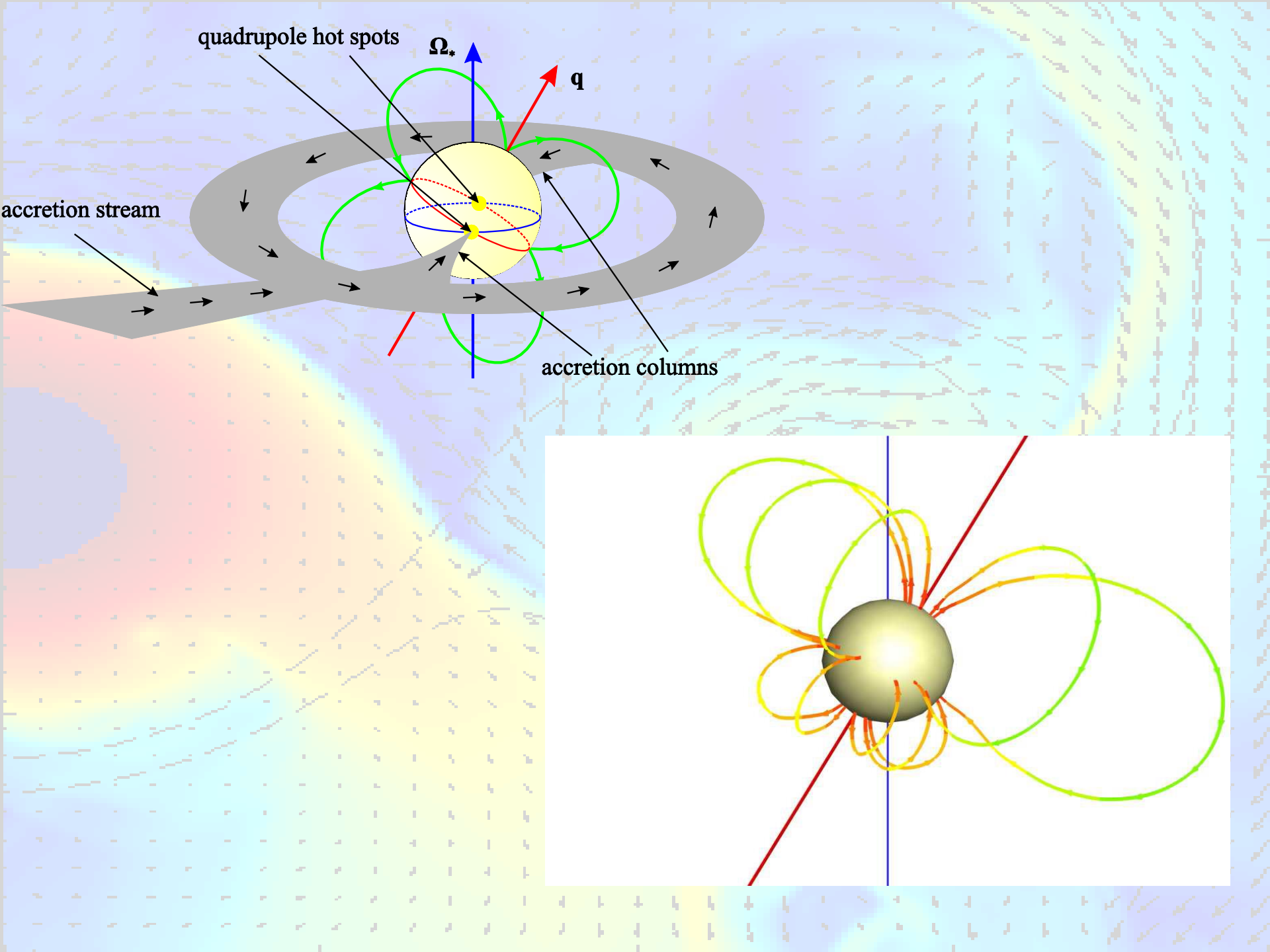
where η is the corresponding coefficient of magnetic viscosity and τ – a characteristic time scale. Taking $\tau = \omega_K^{-1}$ and taking η to be the Bohm diffusion coefficient $\eta_B = 1/16 ckT/(eB)$ we obtain

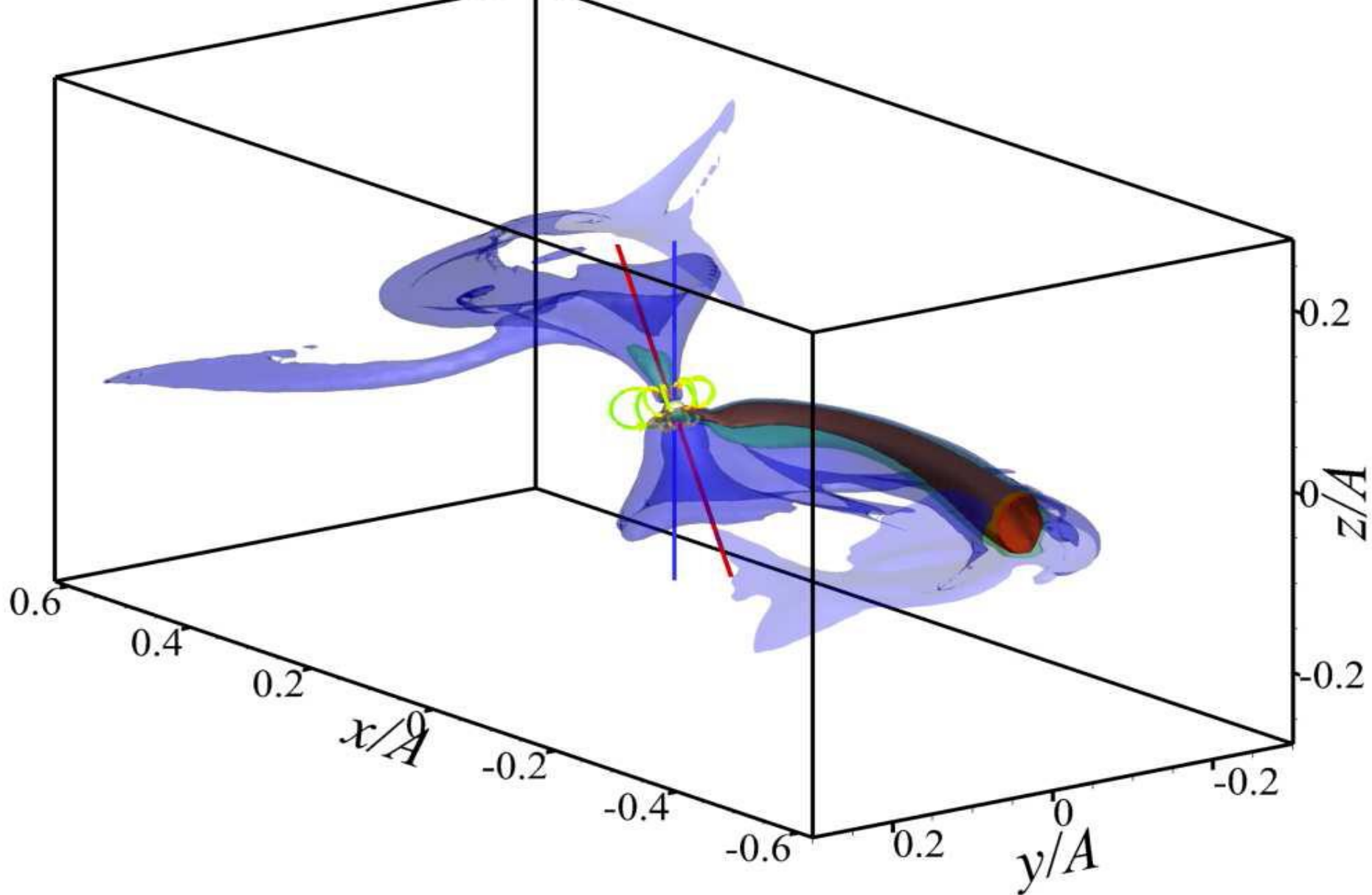
$$H_m \approx c_s / \omega_K \sqrt{\omega_K / \omega_c} \approx 2.5 \times 10^{-4} H_d.$$

Simple estimates show that the resulting values are in good agreement with the observational data.

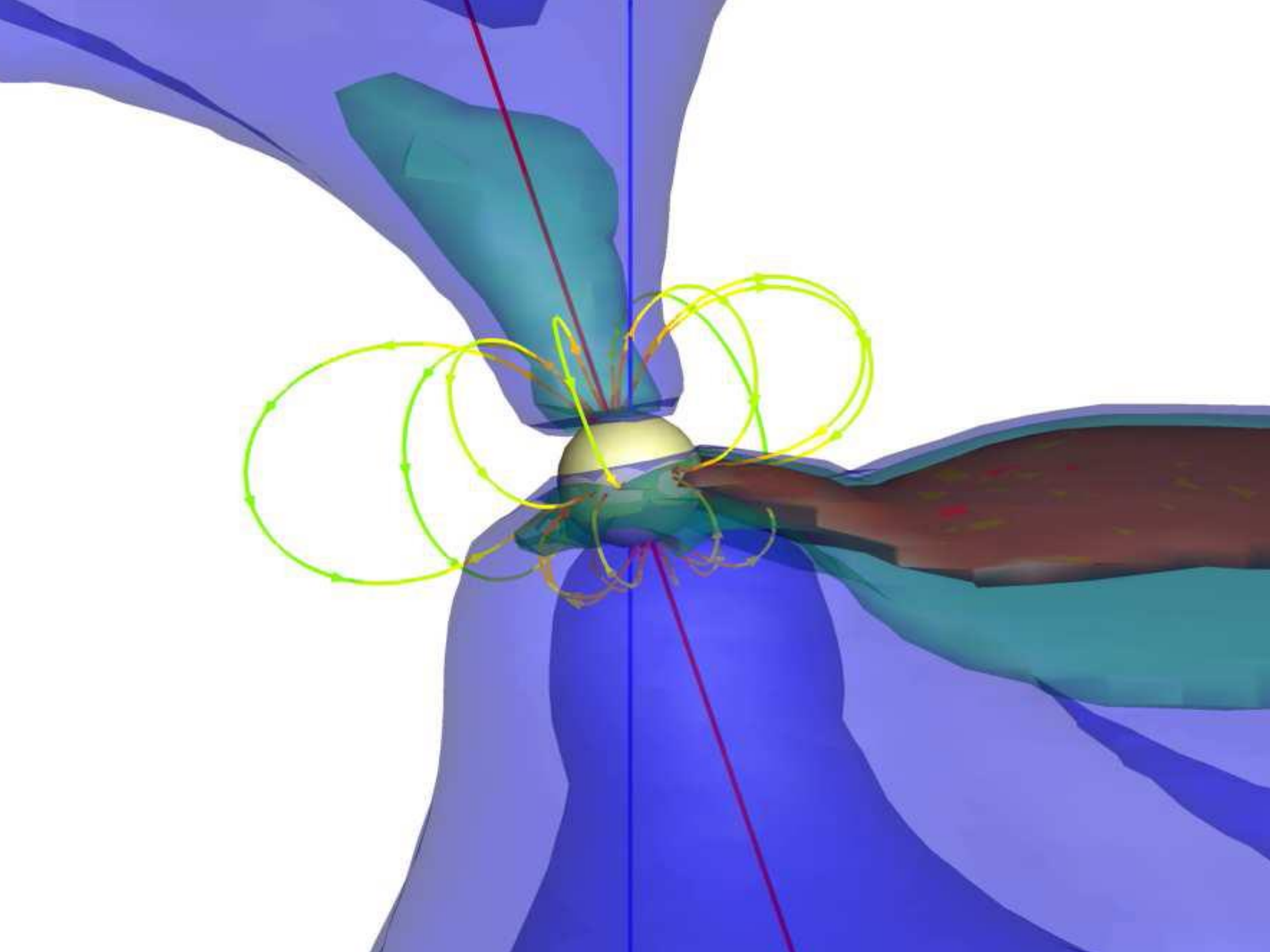


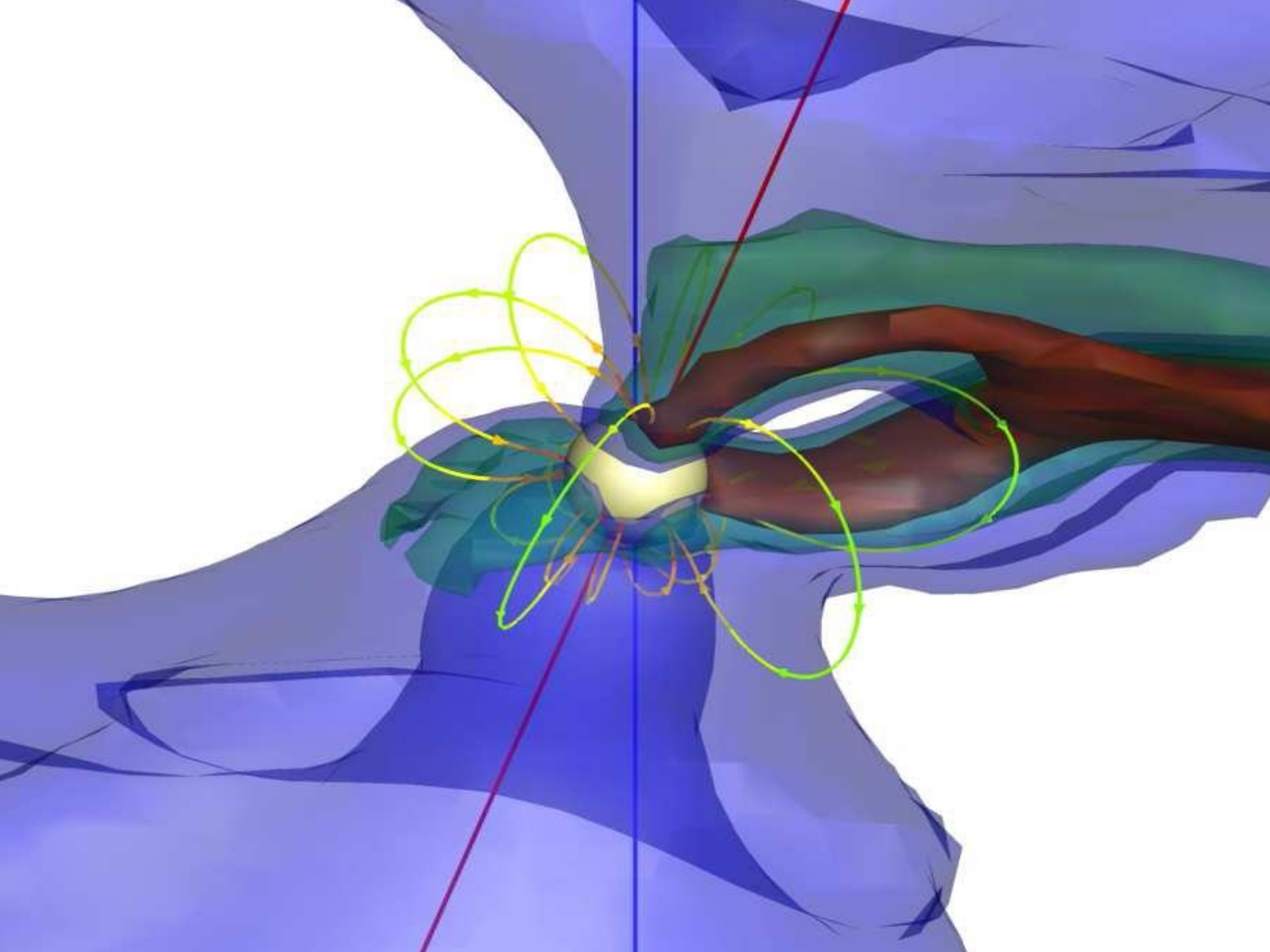
Polars with complex magnetic fields

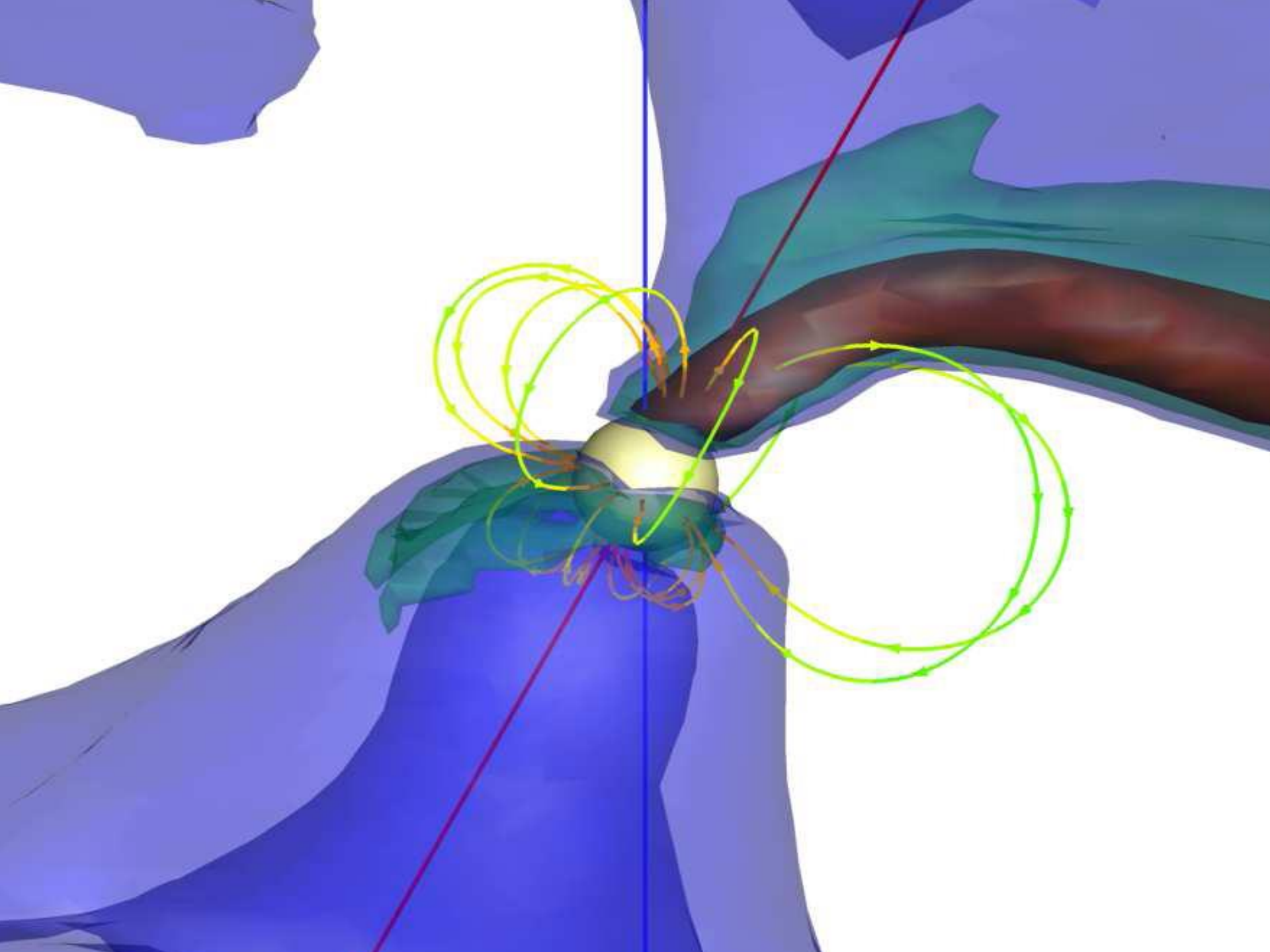


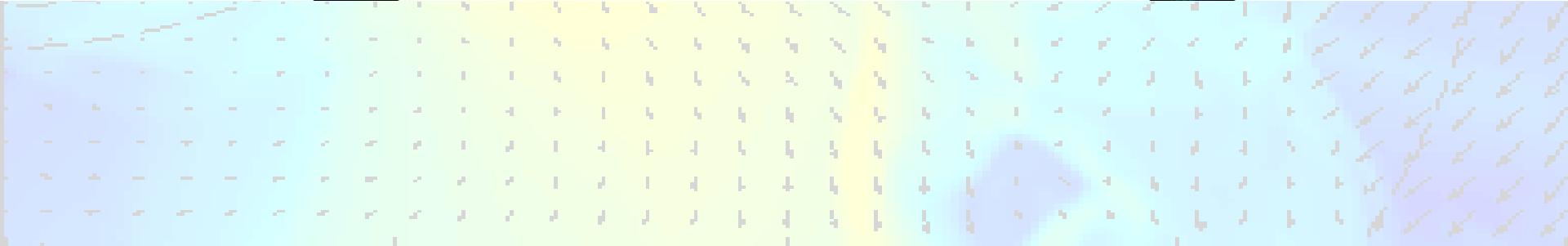
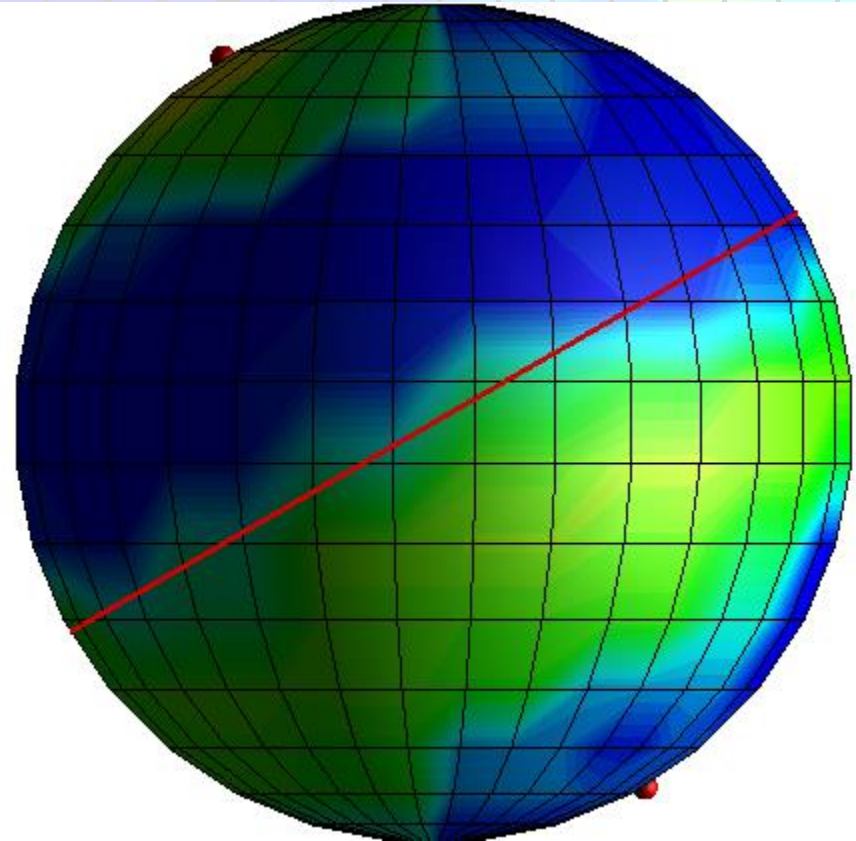
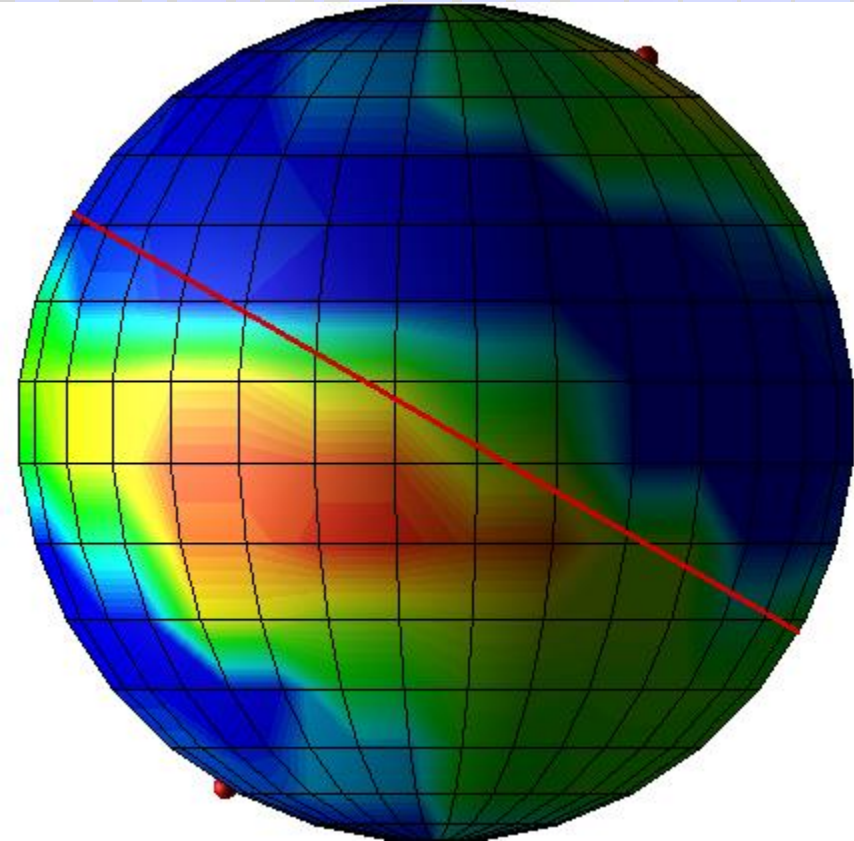


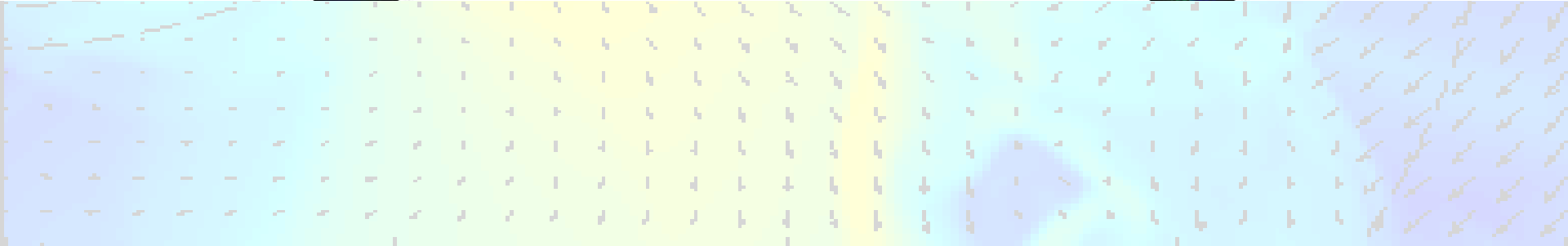
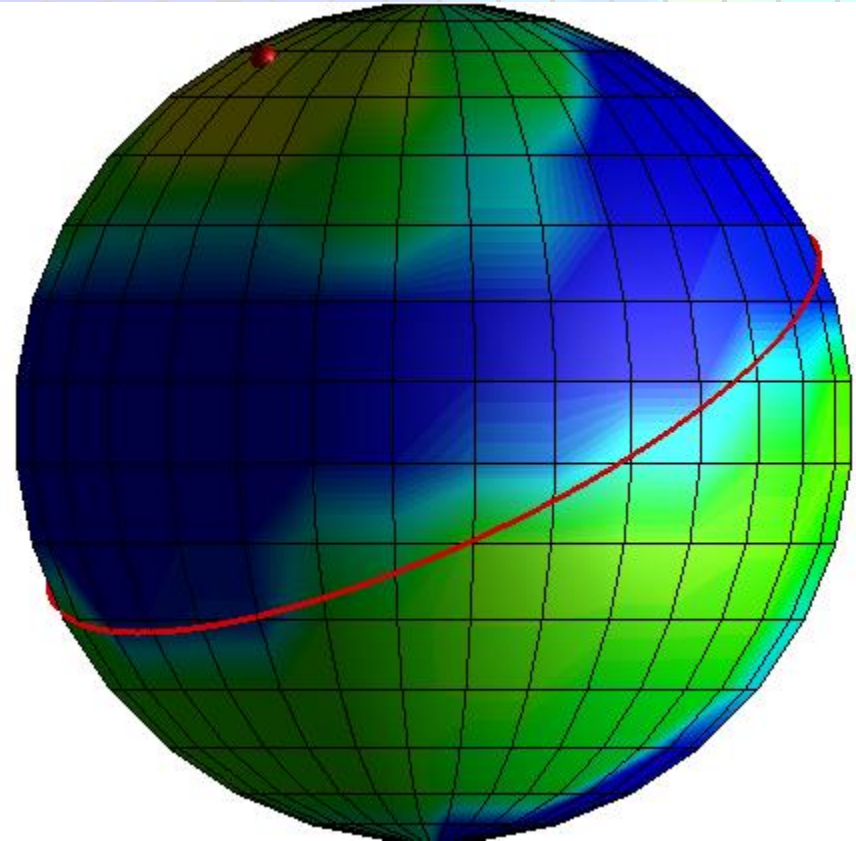
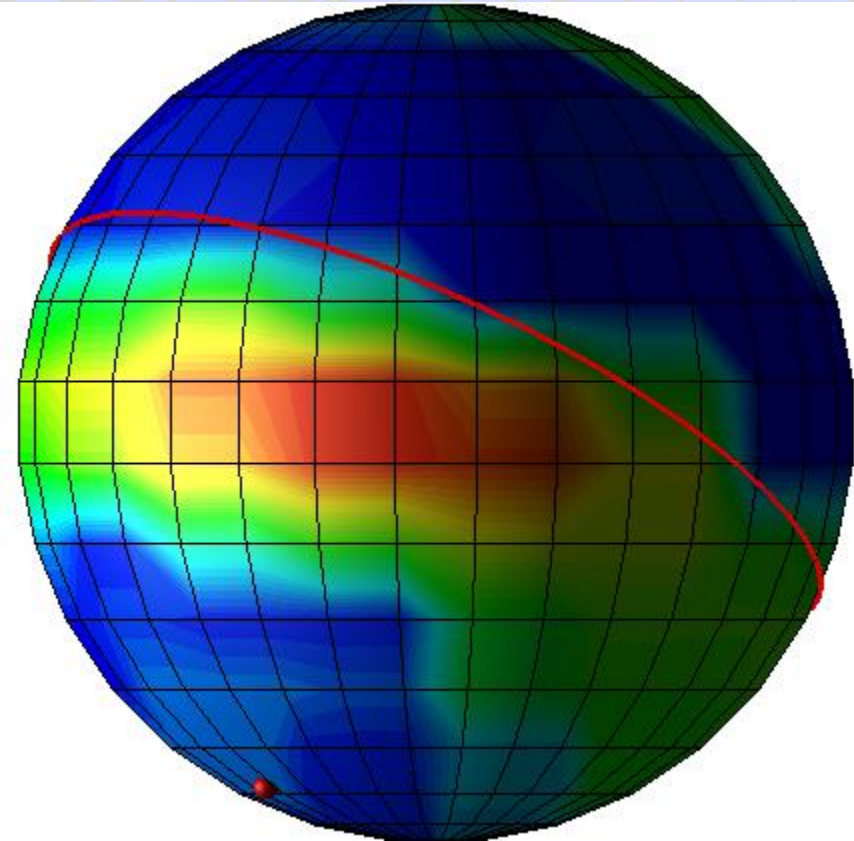
The isosurfaces of the $\lg \rho$ (in units of $\rho(L_1)$) for values -6 (blue), -5 (green) and -4 (red) and the magnetic field lines are shown.

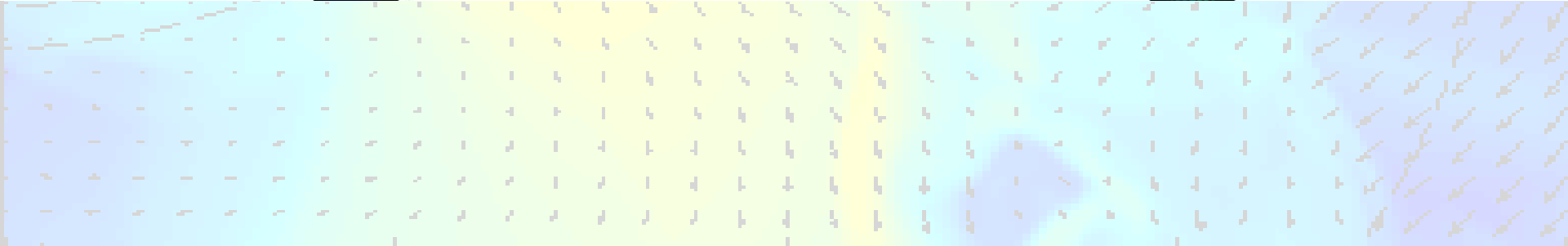
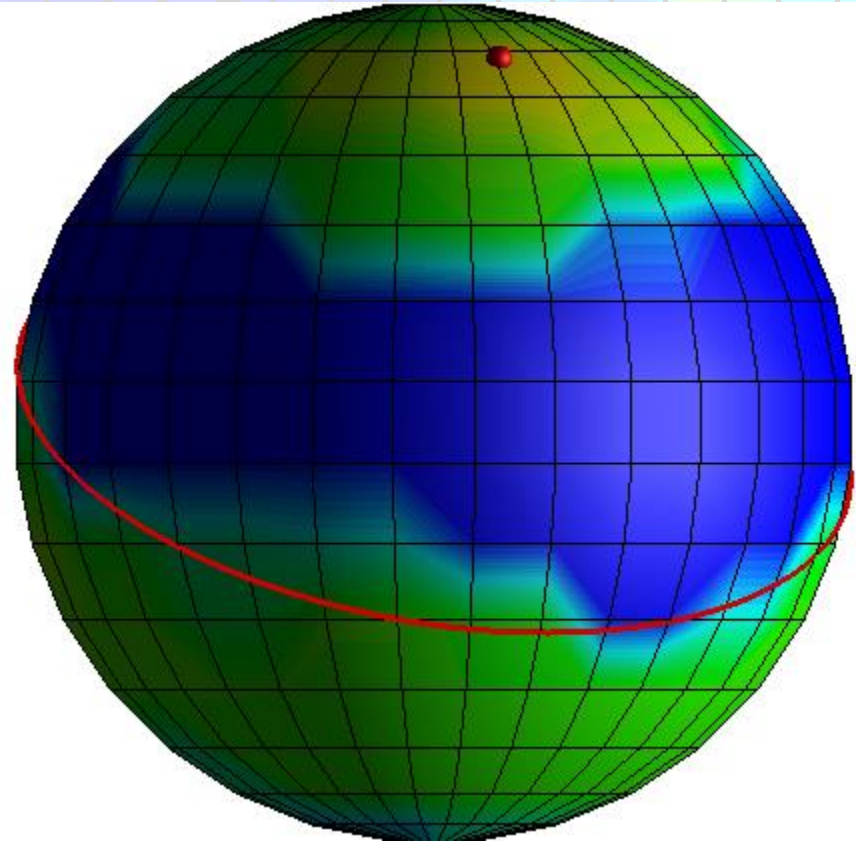
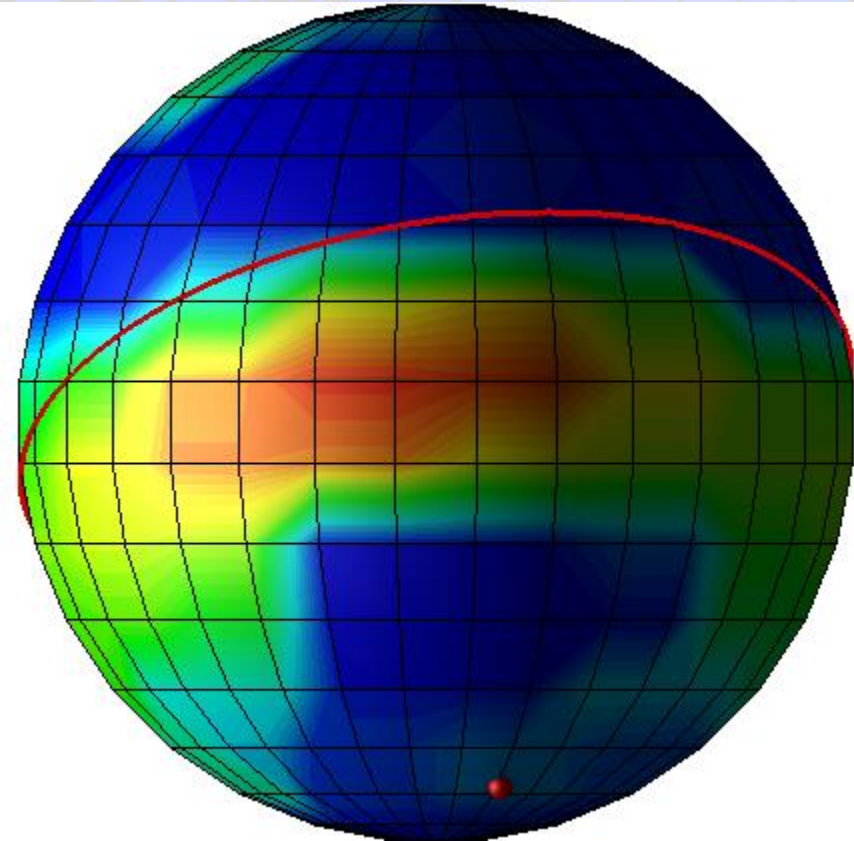
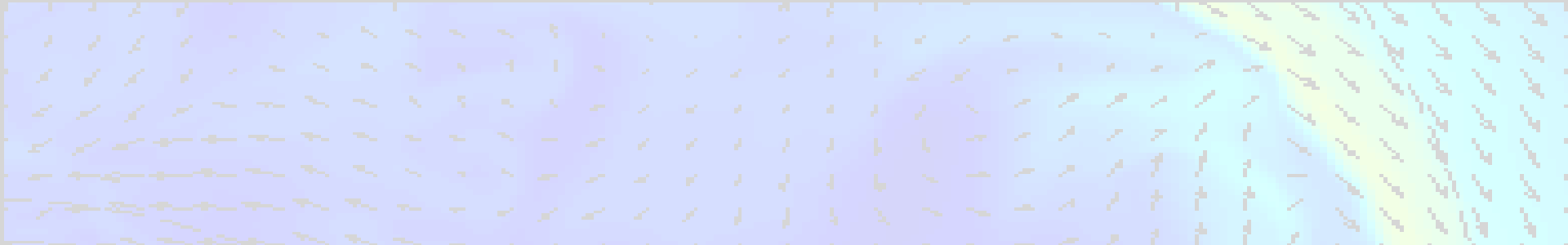


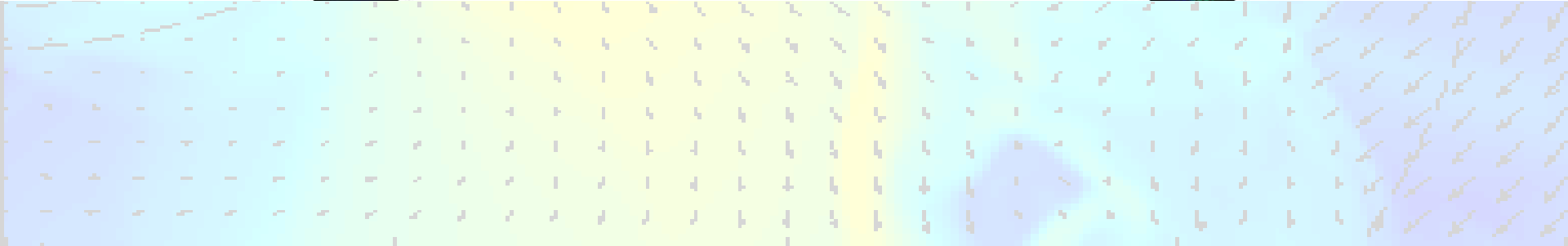
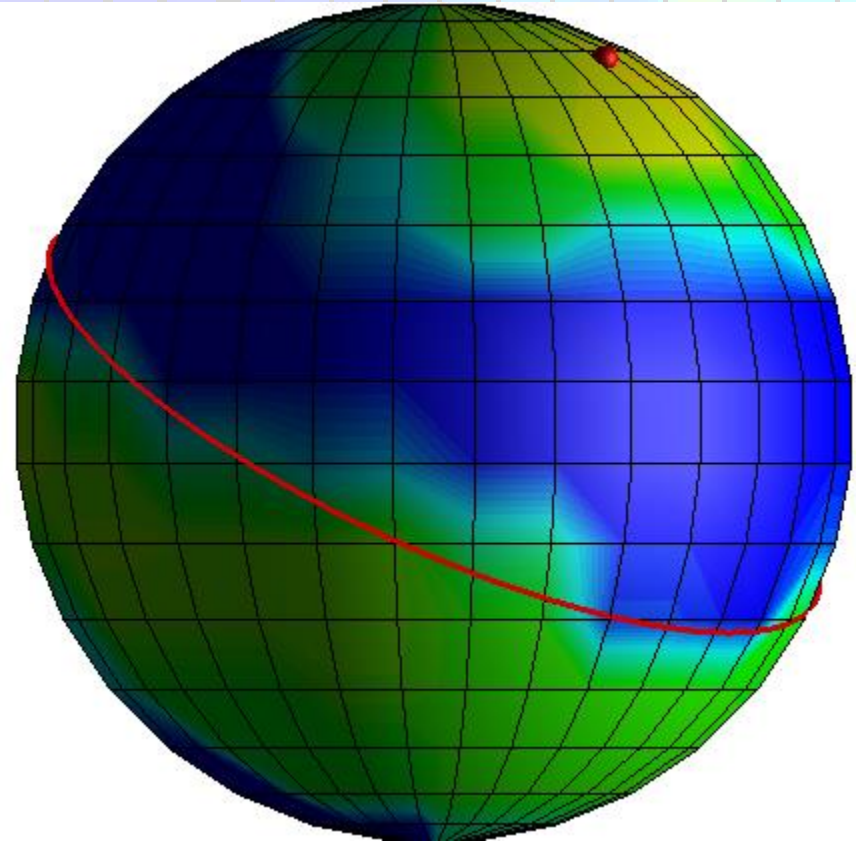
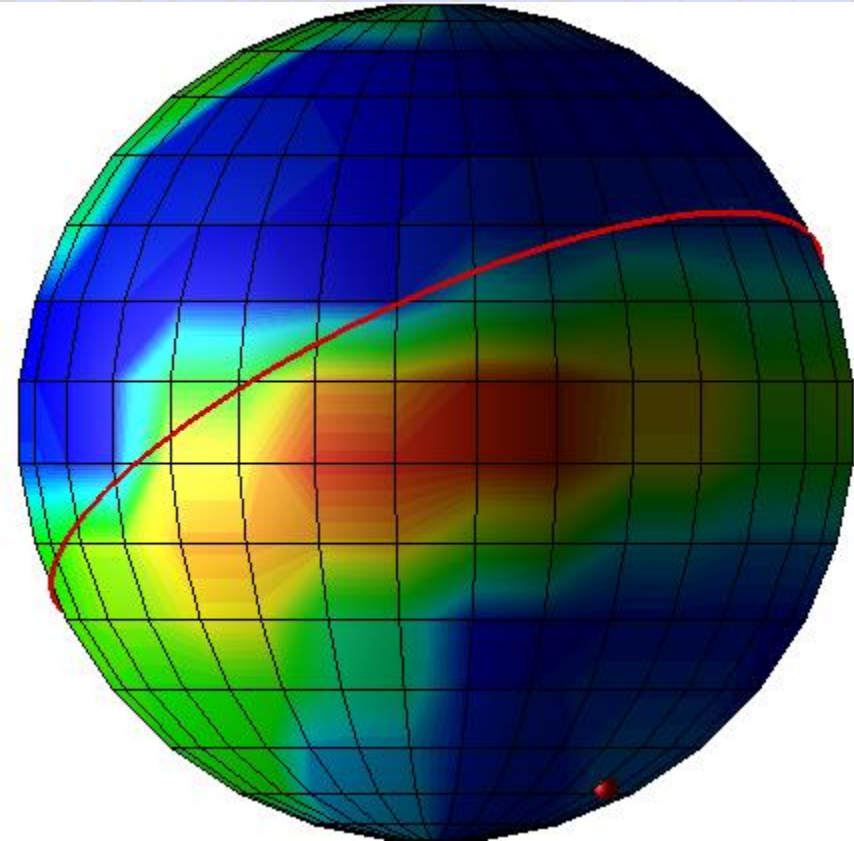


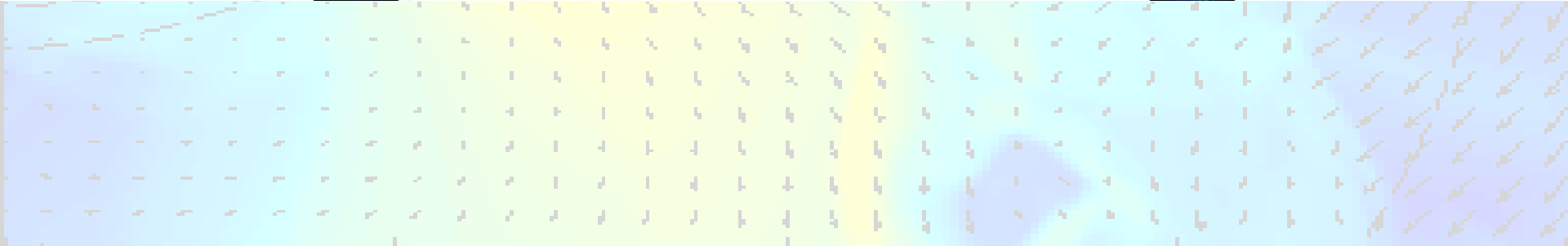
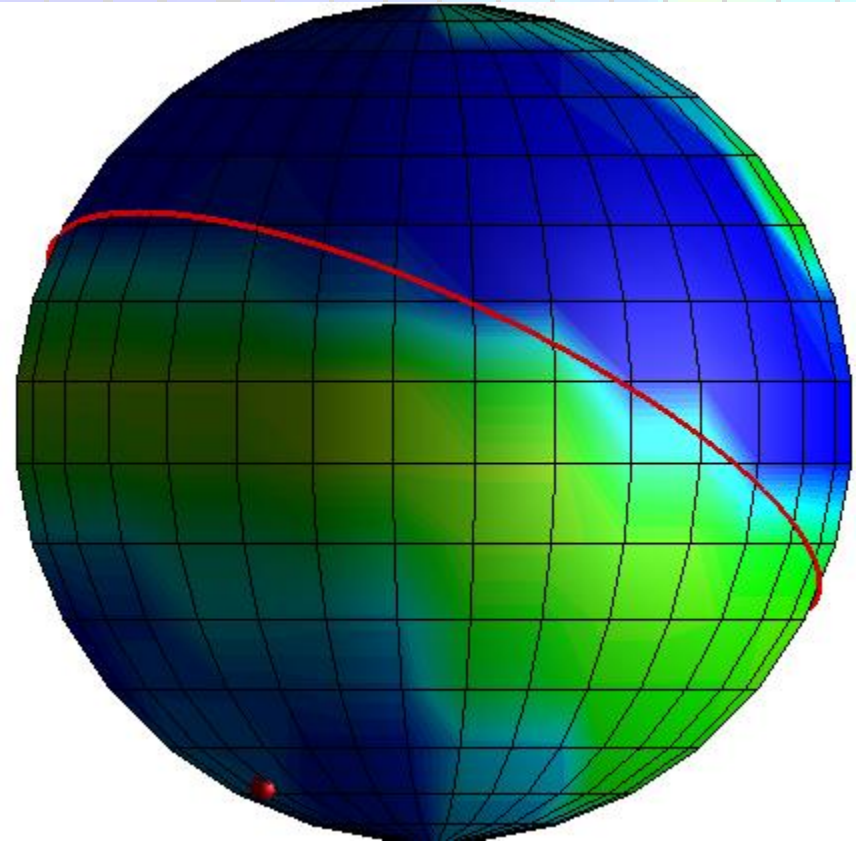
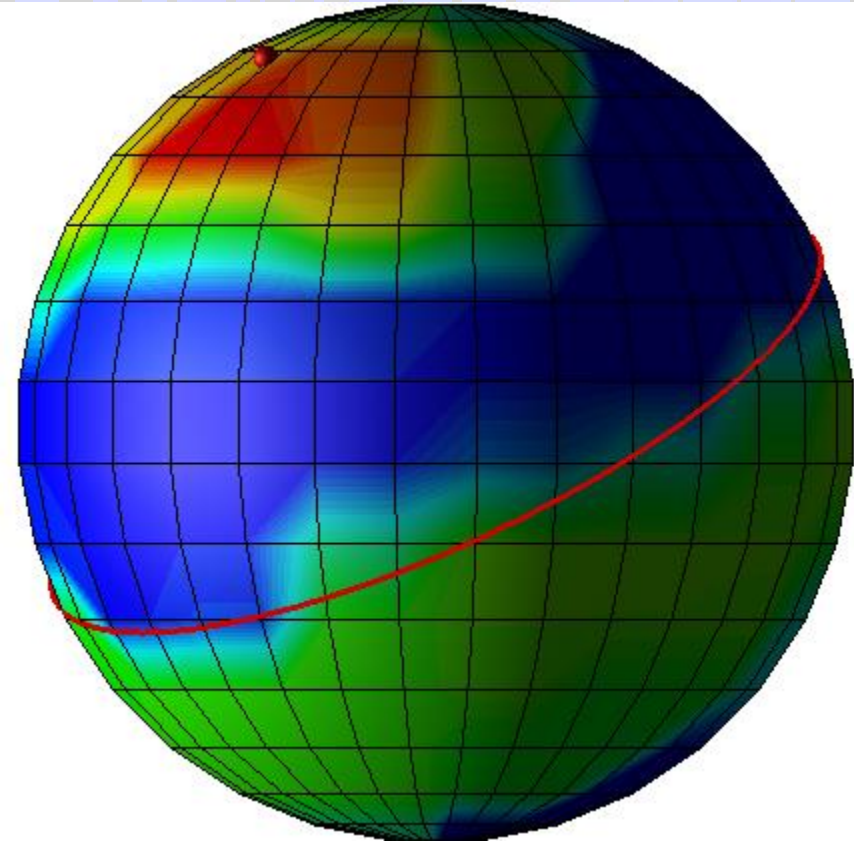


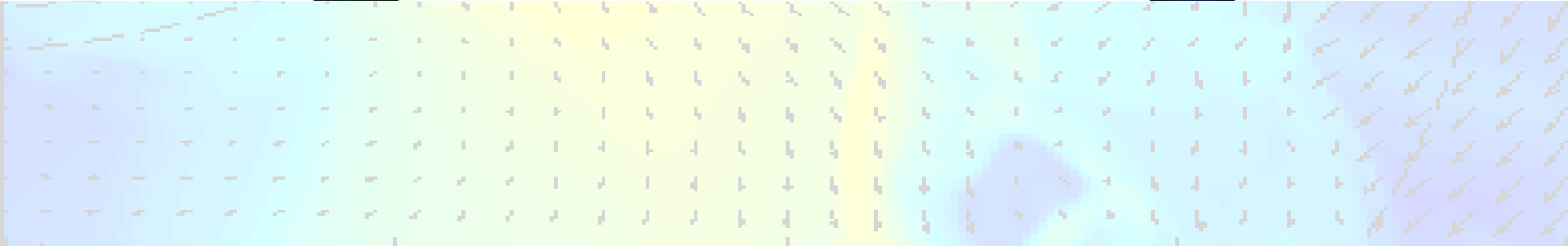
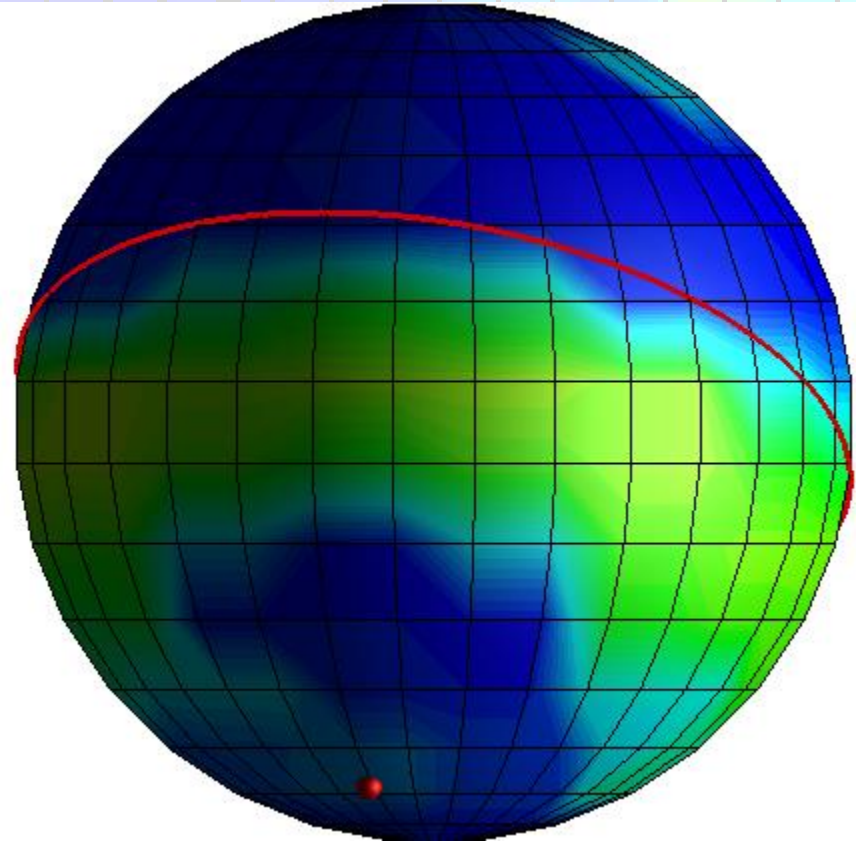
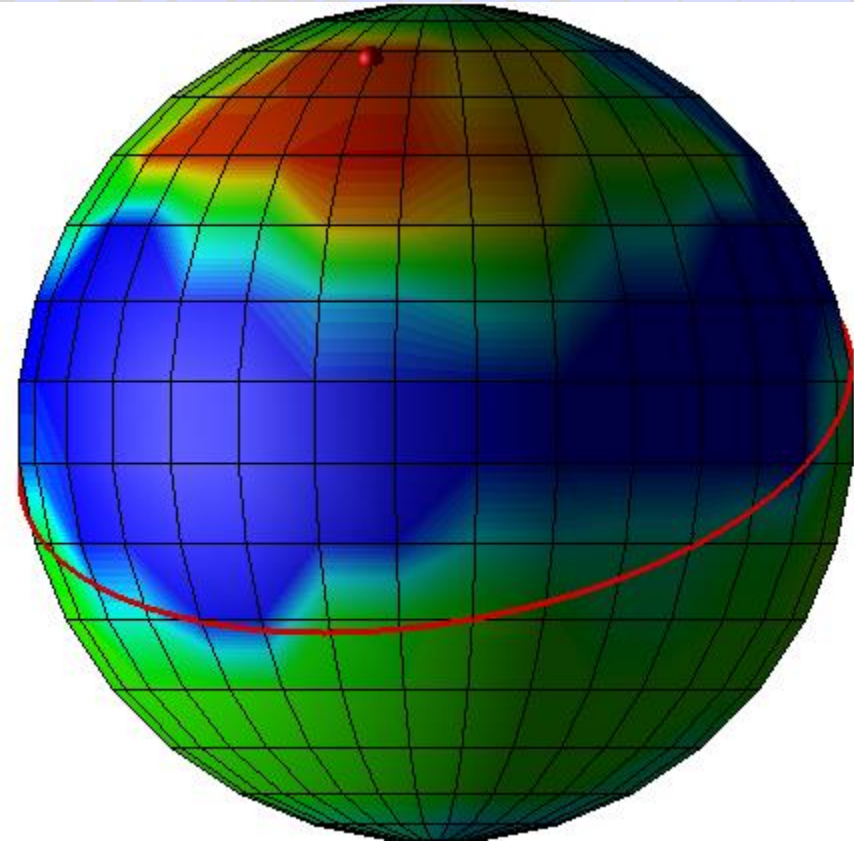


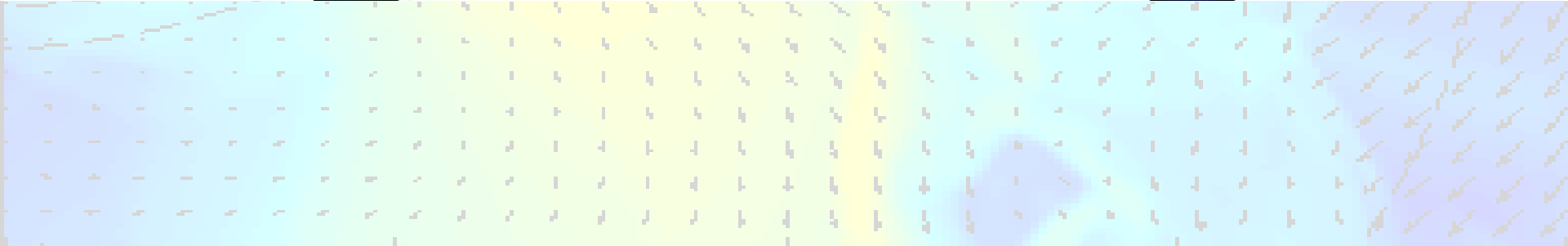
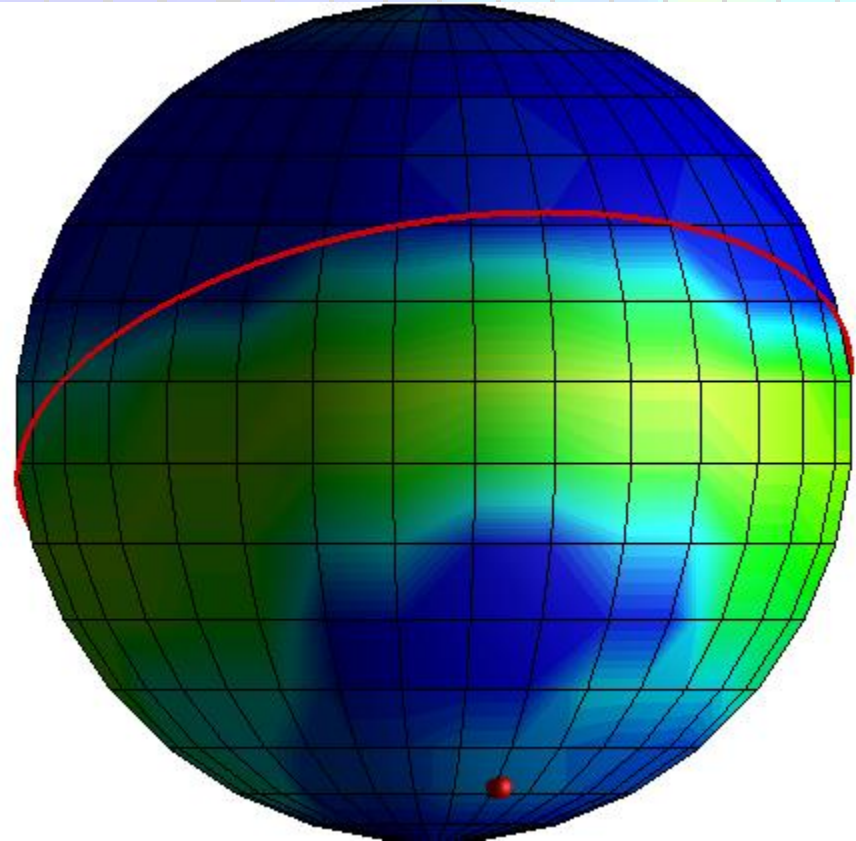
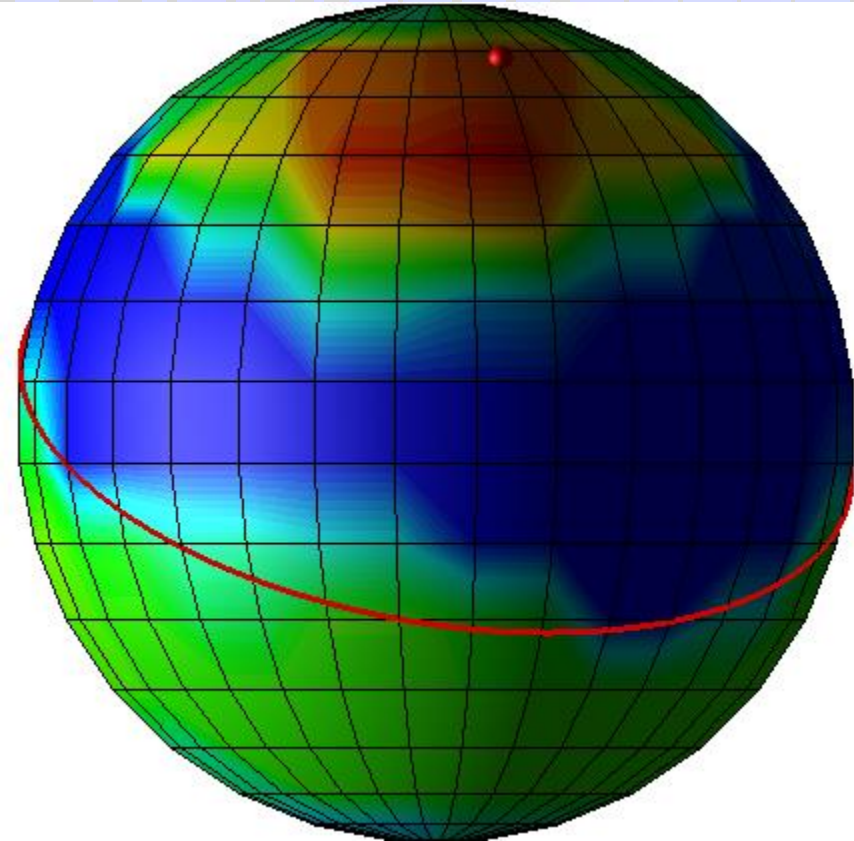
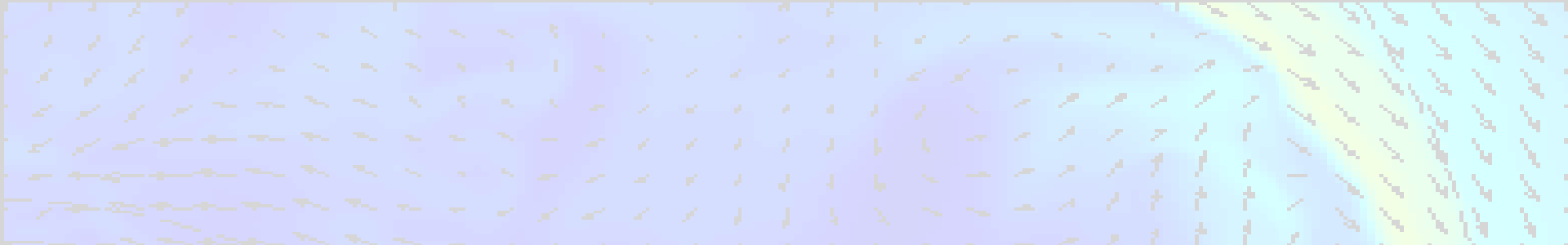


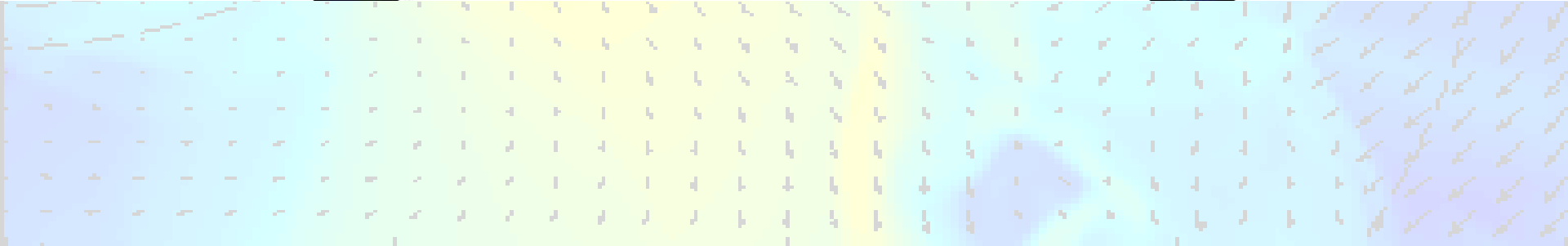
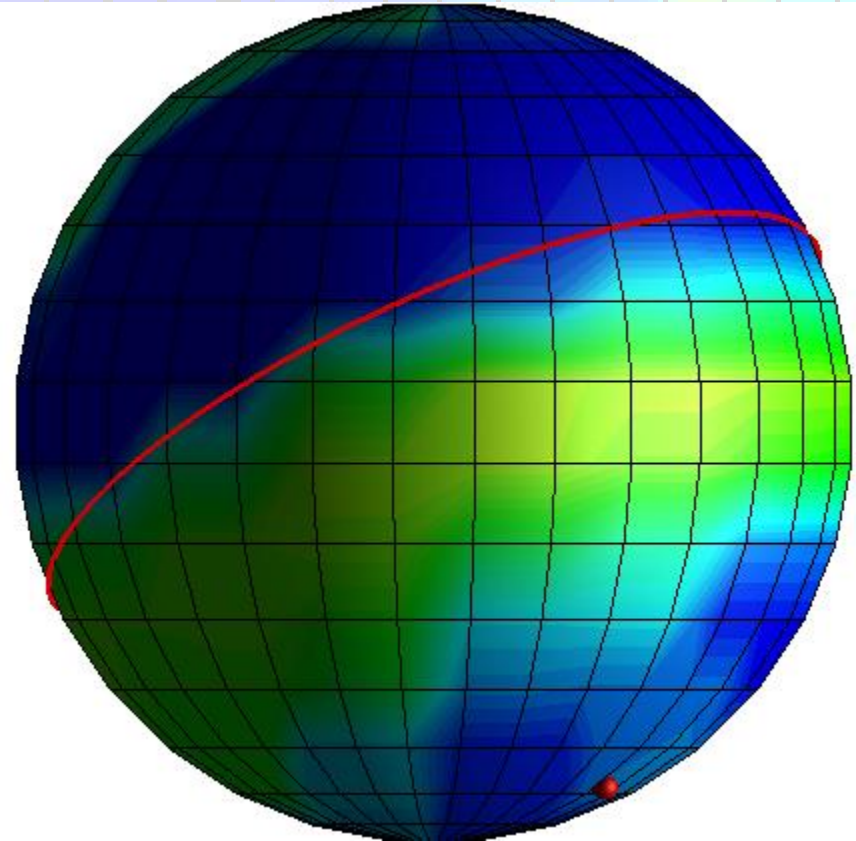
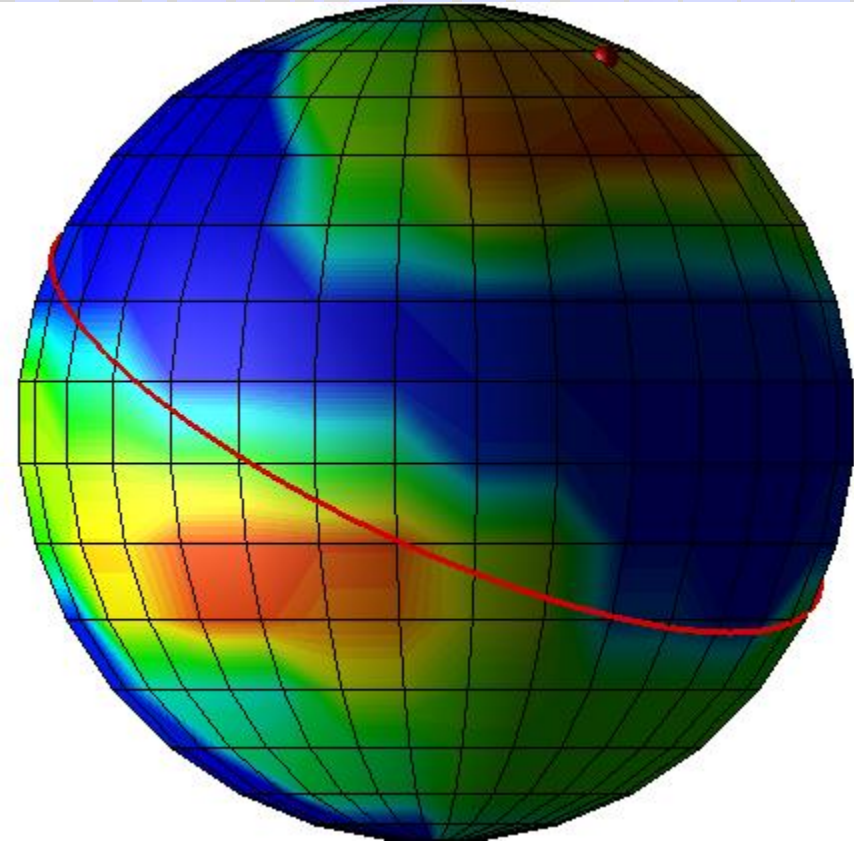
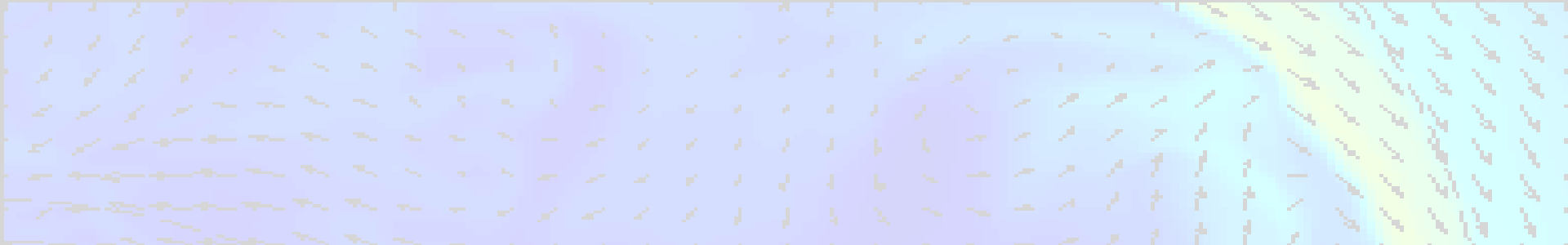












- *In mCVs the accretion columns have a **curtain-like** rather than tubular shape.*
- *The zones of energy release (**hot spots**) at the surface of the white dwarf that form in the vicinity of the magnetic poles as a result of the matter inflow **have the shape of arcs** or sections of an ellipse.*
- *According to observational constraints the spatial resolution in the model should be better than **10 km**.*
- *A **complex magnetic field** should be considered if there is an accretion zone near the white dwarf's spin equator (orbital plane) or if there are two or more accretion regions that cannot be fit by a dipole magnetic field.*

	Эксперимент	EX Hydrae		AM Herculis	
		$\perp \mathbf{B}$	$\parallel \mathbf{B}$	струи $\parallel \mathbf{B}$	струи $\perp \mathbf{B}$
x_0	$v_0 t_0$	R_m	$c_s / \Omega_K(R_m)$	R_m	c_s / Ω_{orb}
v_0	c_s	v_K	c_s	$v_{ff}(R_m)$	c_s
t_0	20 нс	$2\pi R_m / v_K$	x_0 / v_0	x_0 / v_0	x_0 / v_0
$\rho_0, \text{г/см}^3$	2×10^{-2}	3×10^{-10}	3×10^{-10}	1×10^{-11}	1×10^{-11}
$T_0, \text{К}$	2×10^6	1×10^4	1×10^4	1×10^4	1×10^4
$B_0, \text{Гс}$	1×10^5	8×10^1	8×10^1	3×10^1	3×10^1
$\text{Sh} = \frac{x_0}{v_0 t_0}$	1×10^0	2×10^{-1}	1×10^0	1×10^0	1×10^0
$\text{Eu} = \frac{P_0}{\rho_0 v_0^2}$	6×10^{-1}	9×10^{-6}	6×10^{-1}	3×10^{-4}	6×10^{-1}
$\text{Al} = \frac{B_0^2}{4\pi\rho_0 v_0^2}$	3×10^{-3}	2×10^{-5}	1×10^0	3×10^{-3}	4×10^0
$\text{Re}^{-1} = \frac{\nu_0}{x_0 v_0}$	5×10^{-3}	1×10^{-13}	6×10^{-9}	3×10^{-13}	8×10^{-10}
$\text{Rm}^{-1} = \frac{\eta_0}{x_0 v_0}$	1×10^{-5}	1×10^{-13}	9×10^{-9}	2×10^{-14}	6×10^{-11}
$\beta = \frac{2\text{Eu}}{\text{Al}}$	4×10^2	1×10^0	1×10^0	3×10^{-1}	3×10^{-1}
$\omega_B \tau_{fp}$	2×10^2	2×10^3	2×10^3	3×10^2	3×10^2



*The gaseous envelope of hot
Jupiter atmospheres*

HD 209458b – a typical representative of “hot Jupiters”. There are the most detailed observational data for this planet.

System parameters:

- $M_* = 1.1 M_{\text{sun}}$
- $R_* = 1.1 R_{\text{sun}}$
- $M_{\text{pl}} = 0.64 M_{\text{Jup}}$
- $R_{\text{pl}} = 1.32 R_{\text{Jup}}$
- $A = 0,045 \text{ a.u.}$
- $P = 3.5^{\text{d}}$

Atmosphere parameters :

$$\rho = \rho_0 \exp(-\mu GM(R-R_{\text{pl}})/kTRR_{\text{pl}})$$

$$\rho_0 = 3.2 \cdot 10^{-14} \text{ g/cm}^3$$

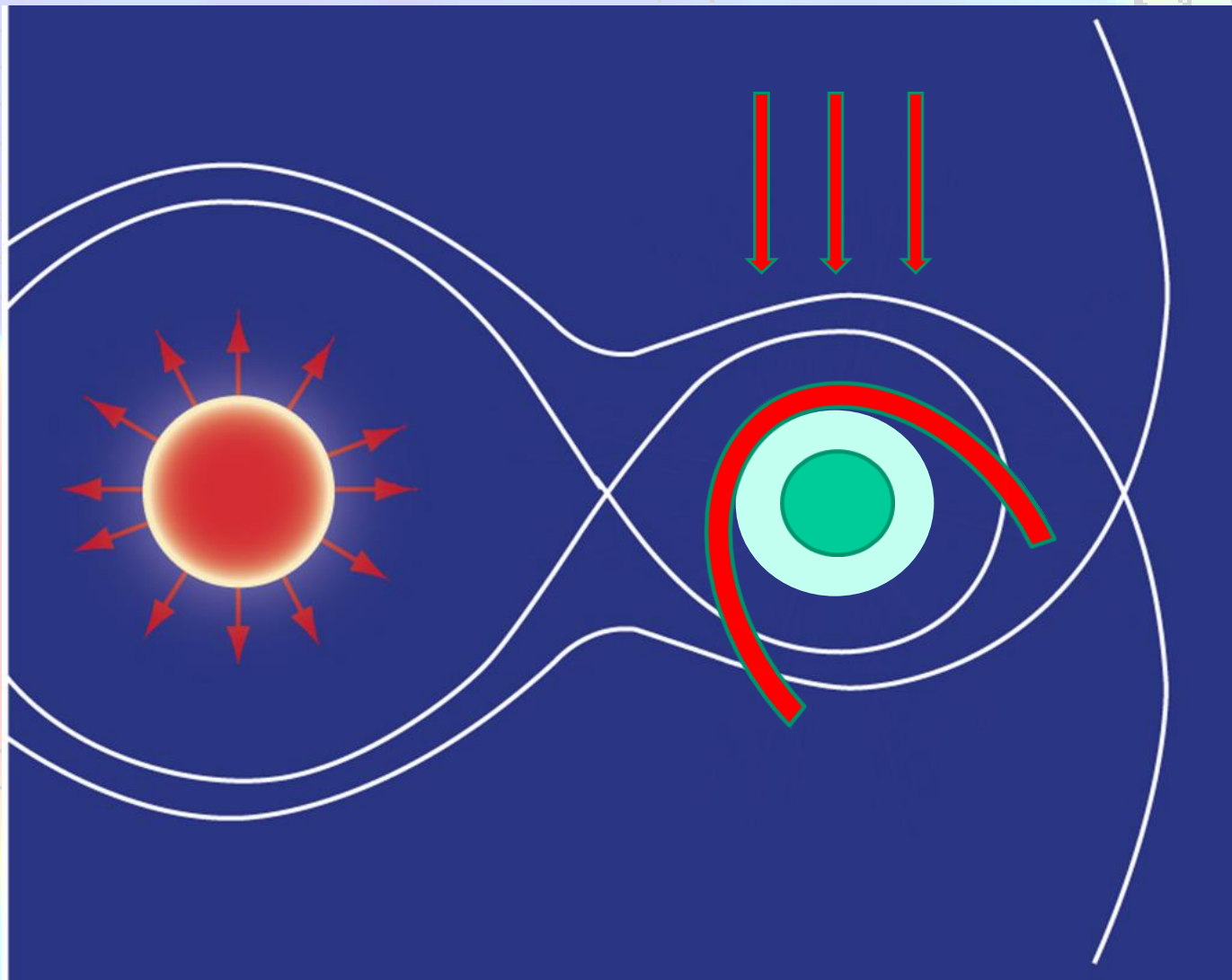
$$T = 5000 \div 10000 \text{ K}$$

Stellar wind parameters :

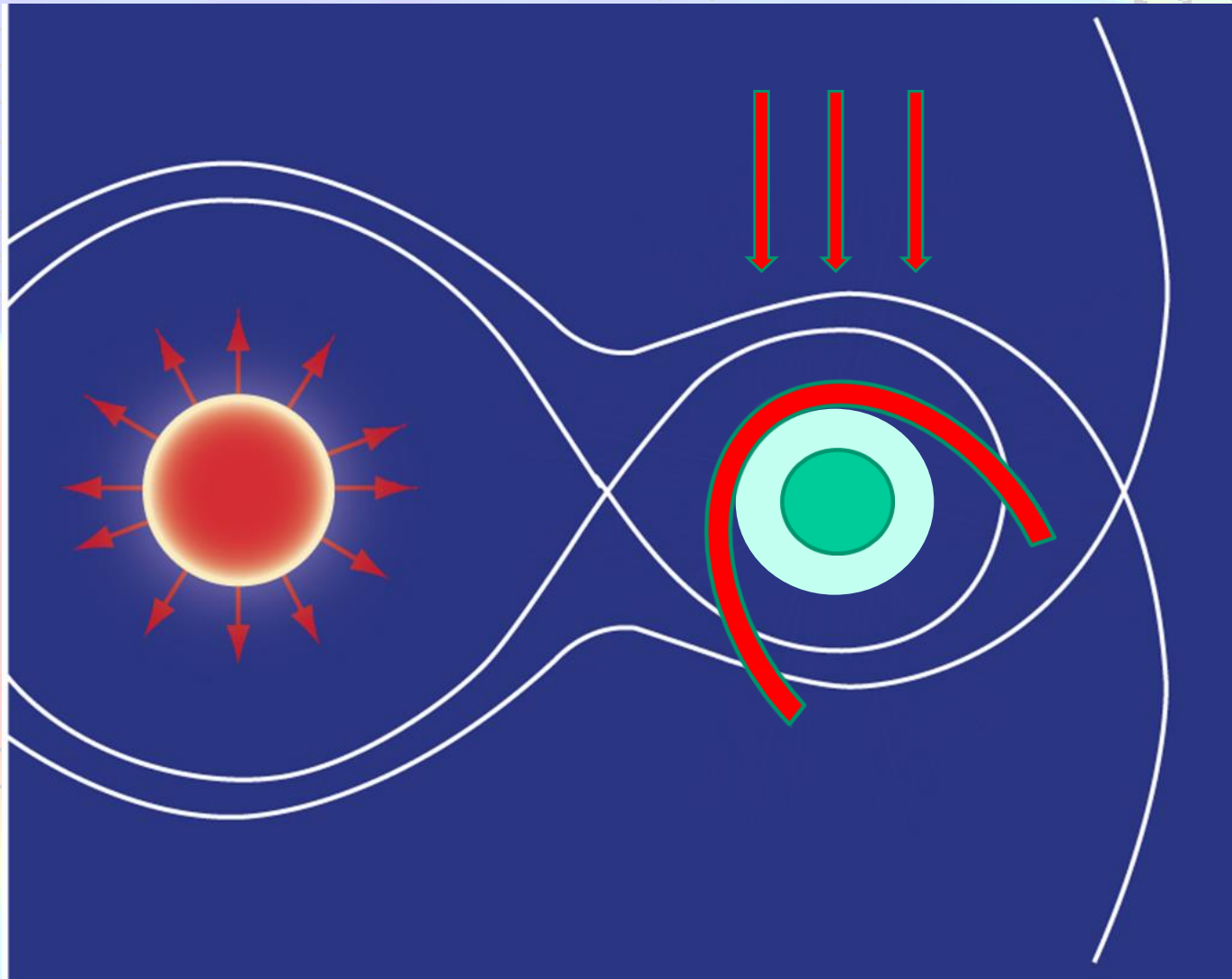
$$n = 1.4 \cdot 10^4 \text{ cm}^{-3}$$

$$T = 1 \cdot 10^5 \text{ K}$$

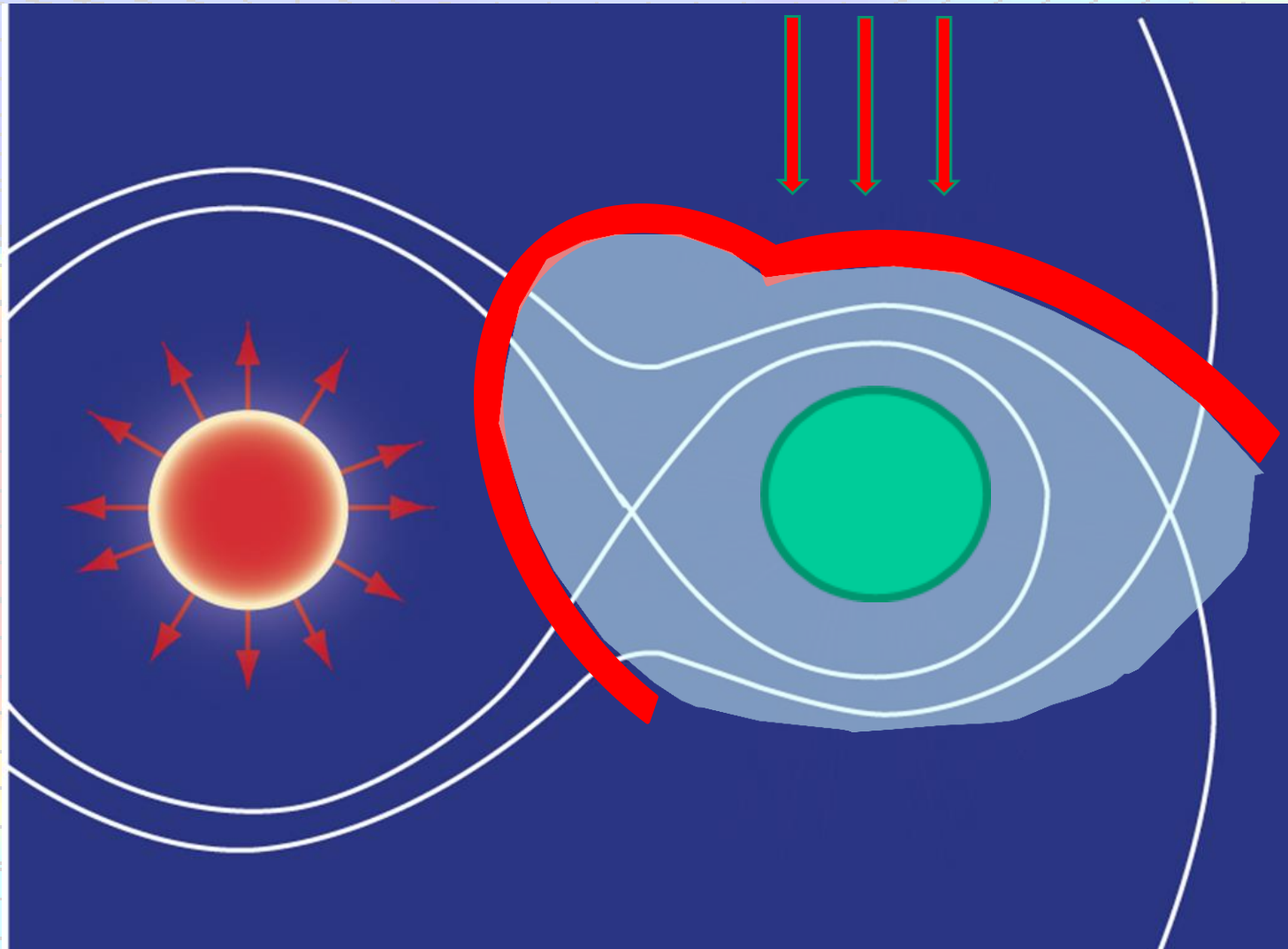
$$v = 100 \text{ km/s} (v_{\text{orb}} = 143 \text{ km/s})$$



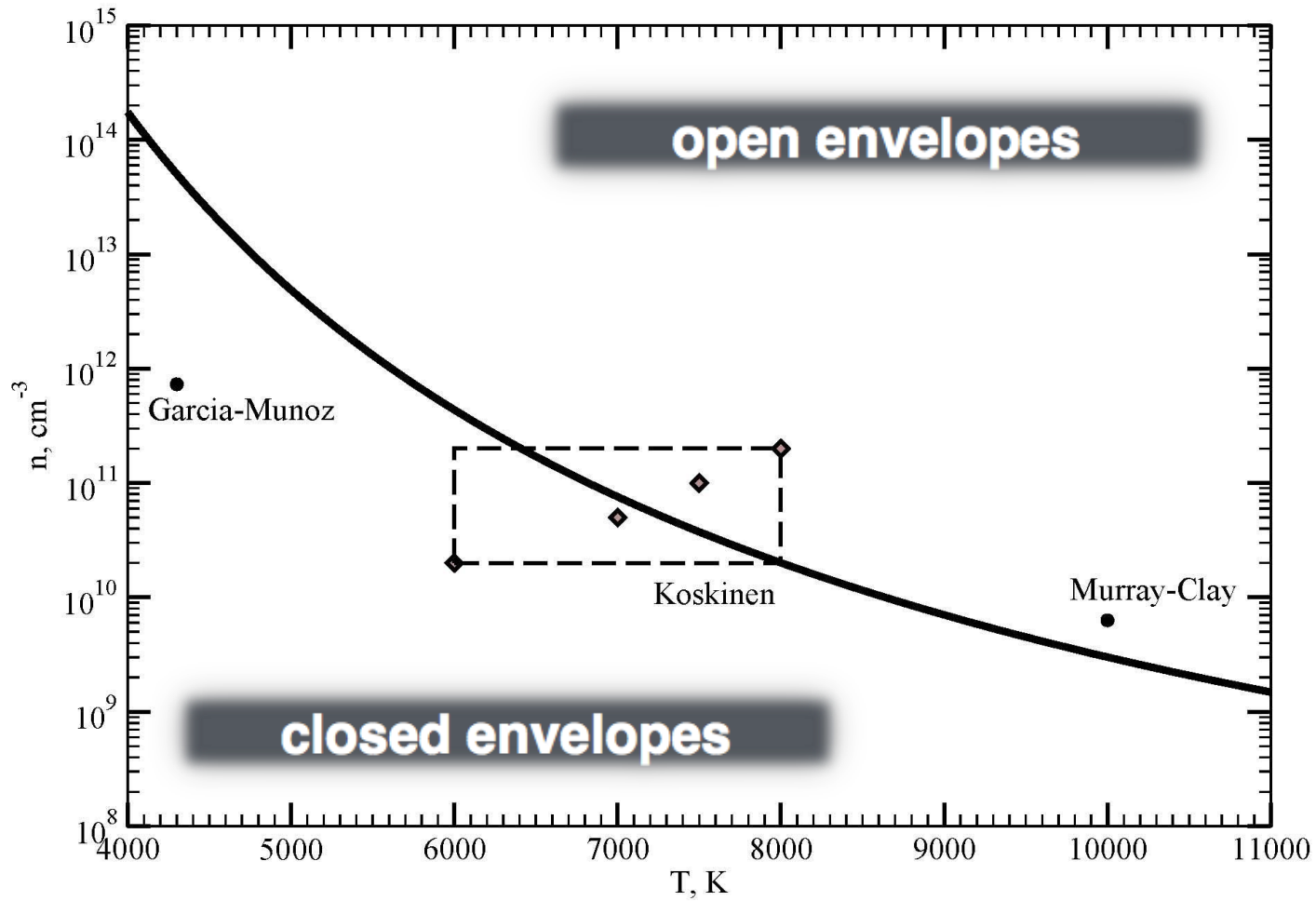
The distance of the center of the planet to the inner Lagrangian point is $\sim 4.5 R_{pl}$.

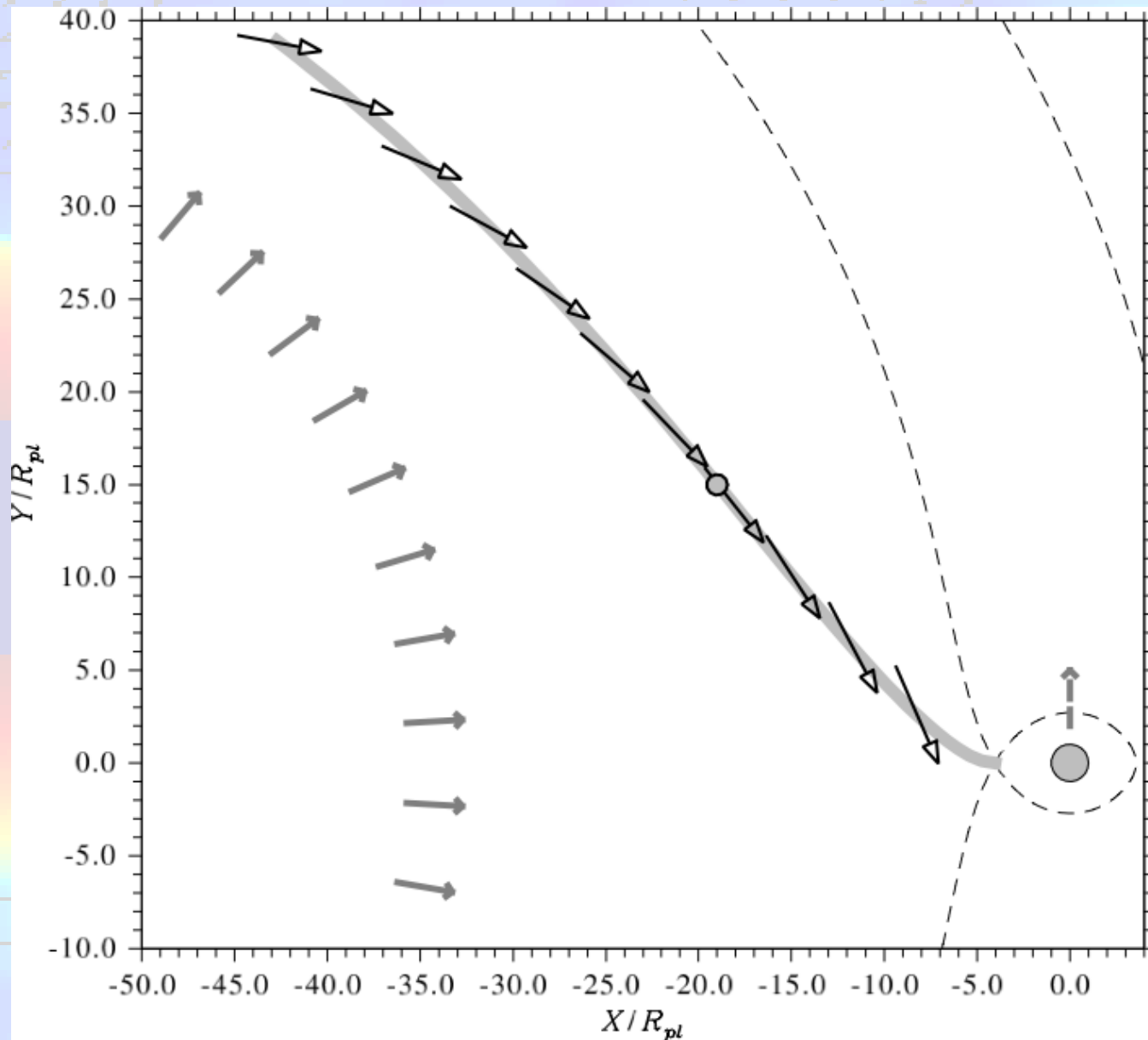


If the head-on collision point is located inside the Roche lobe we suppose that the atmosphere is closed while its shape could have some deviations from the spherical one.

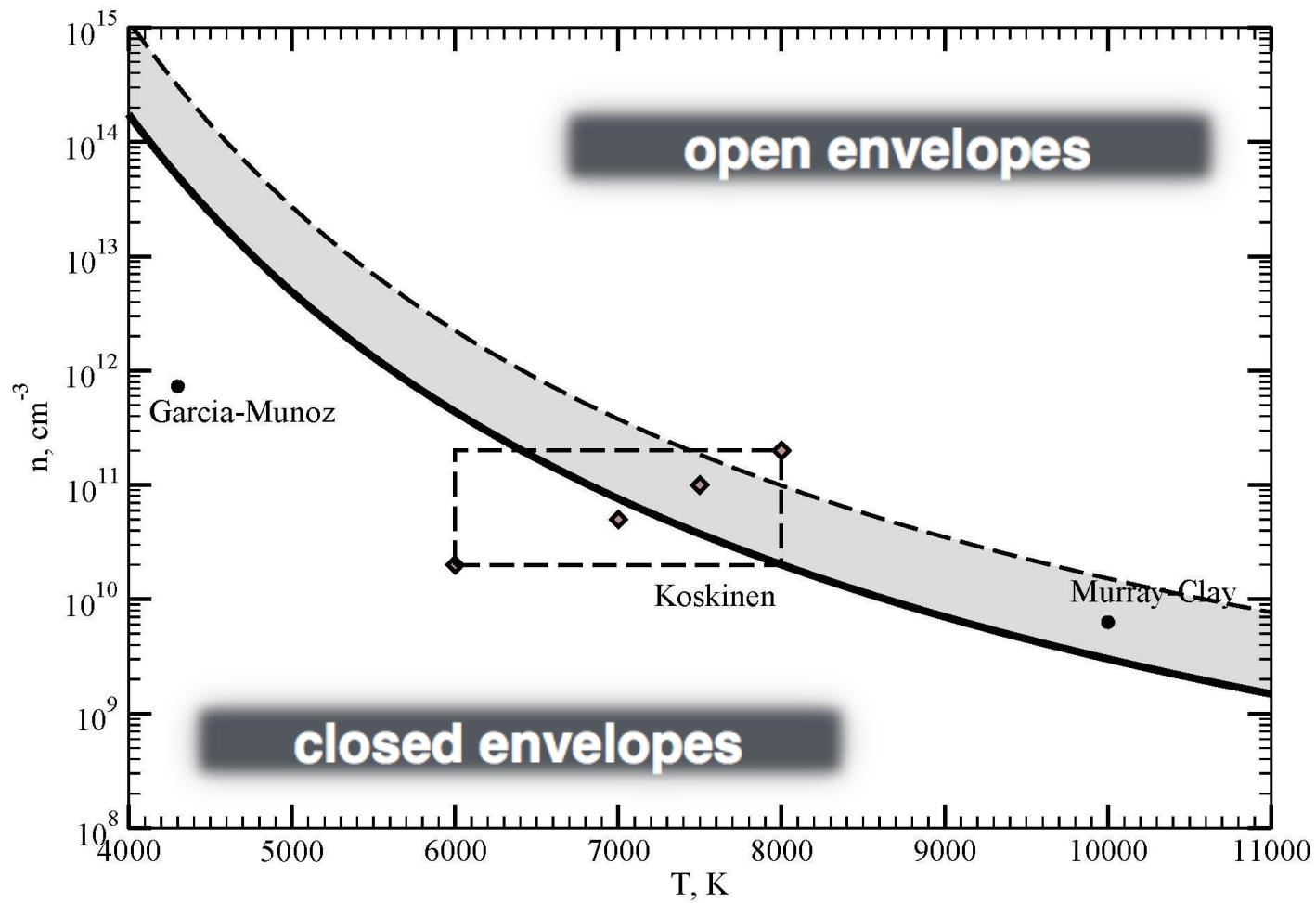


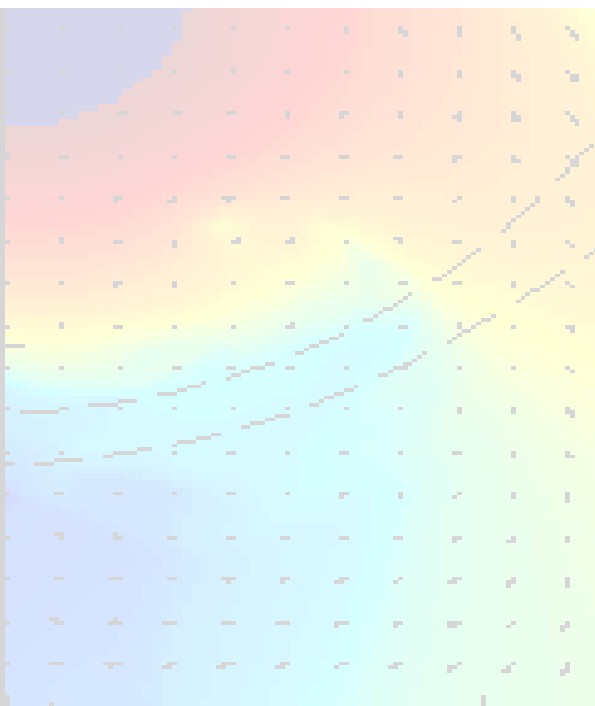
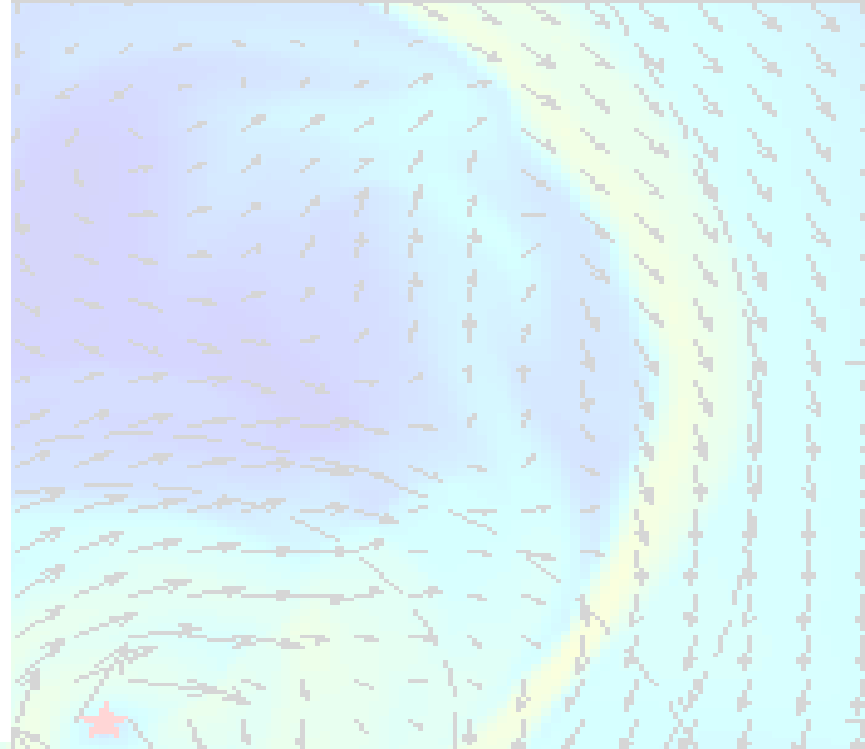
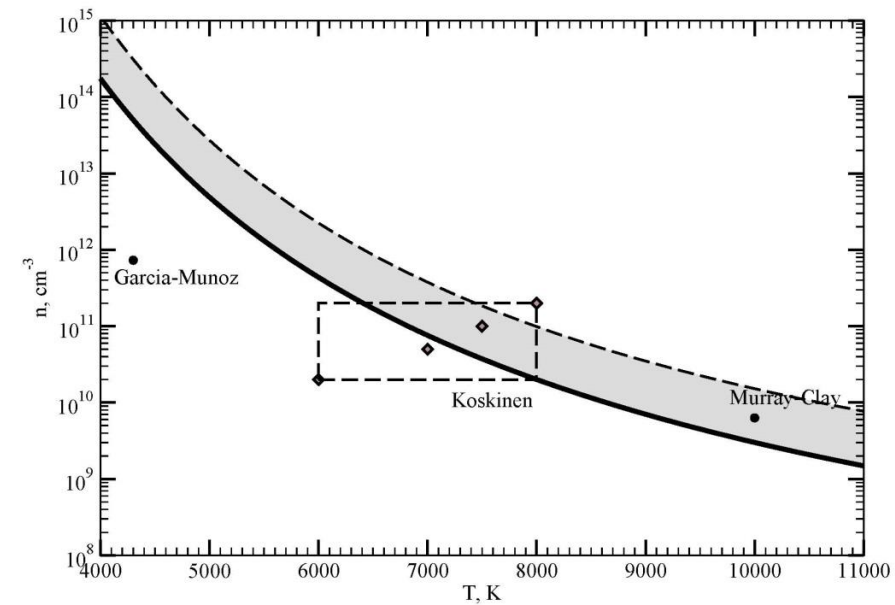
If the head-on collision point is located outside the Roche lobe we should see formation of the outflows.





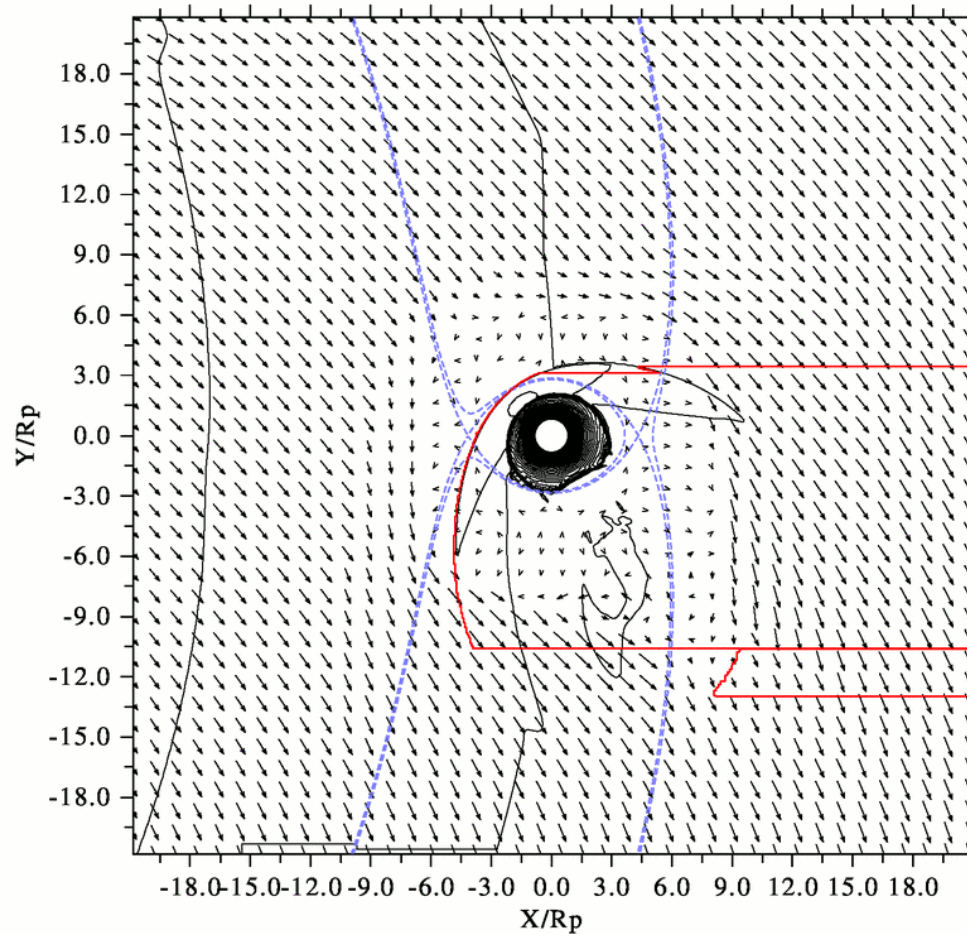
If the dynamic pressure of the stellar wind is high enough the stream from the inner Lagrangian point will stop at some distance from the planet and an asymmetric gaseous envelope around the planet will form.



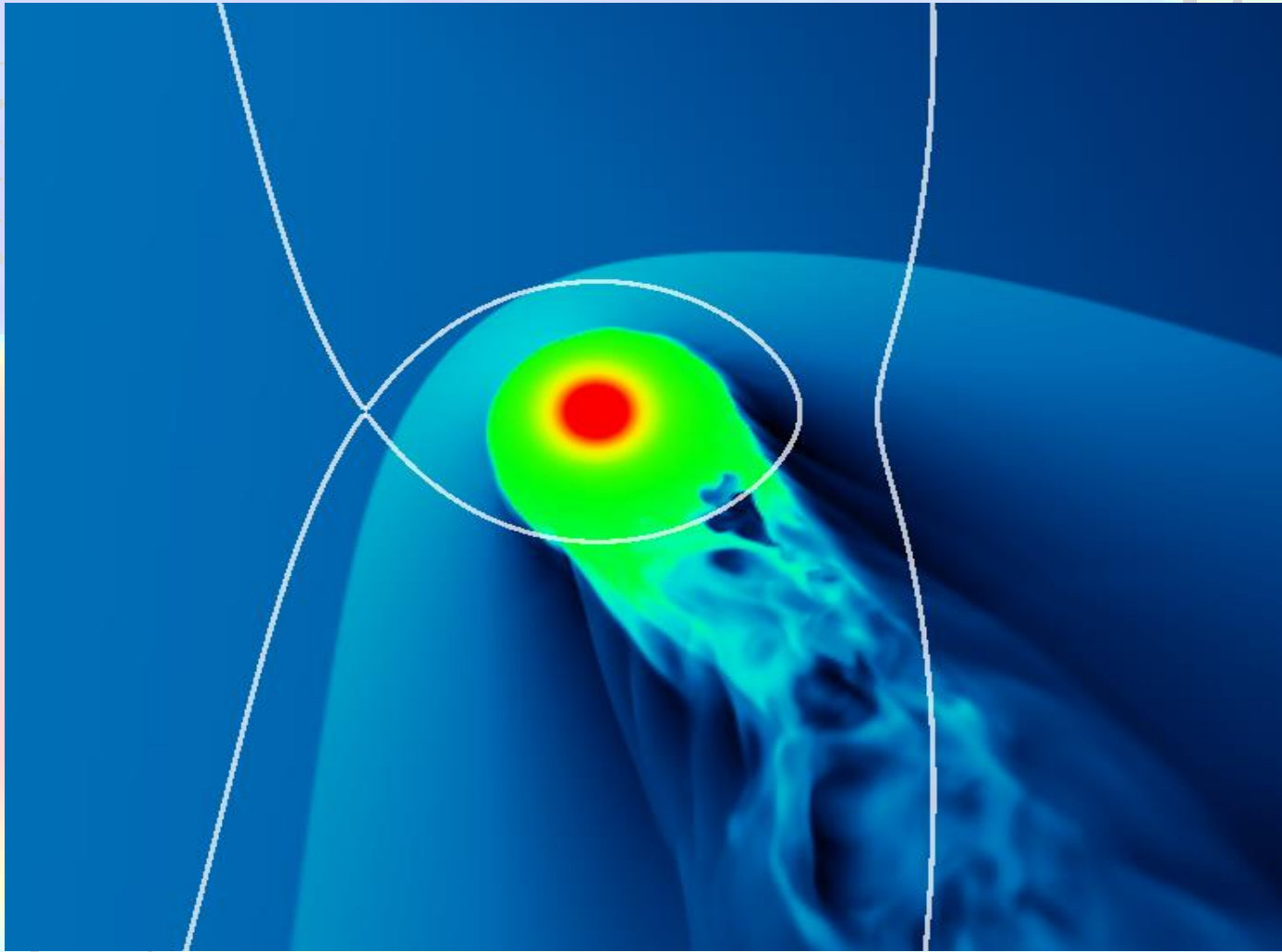


$N \text{ (cm}^{-3}\text{)}$	Temperature (K)
$2 \cdot 10^{10}$	6000
$5 \cdot 10^{10}$	7000
$10 \cdot 10^{10}$	7500
$20 \cdot 10^{10}$	8000

T = 6000 K

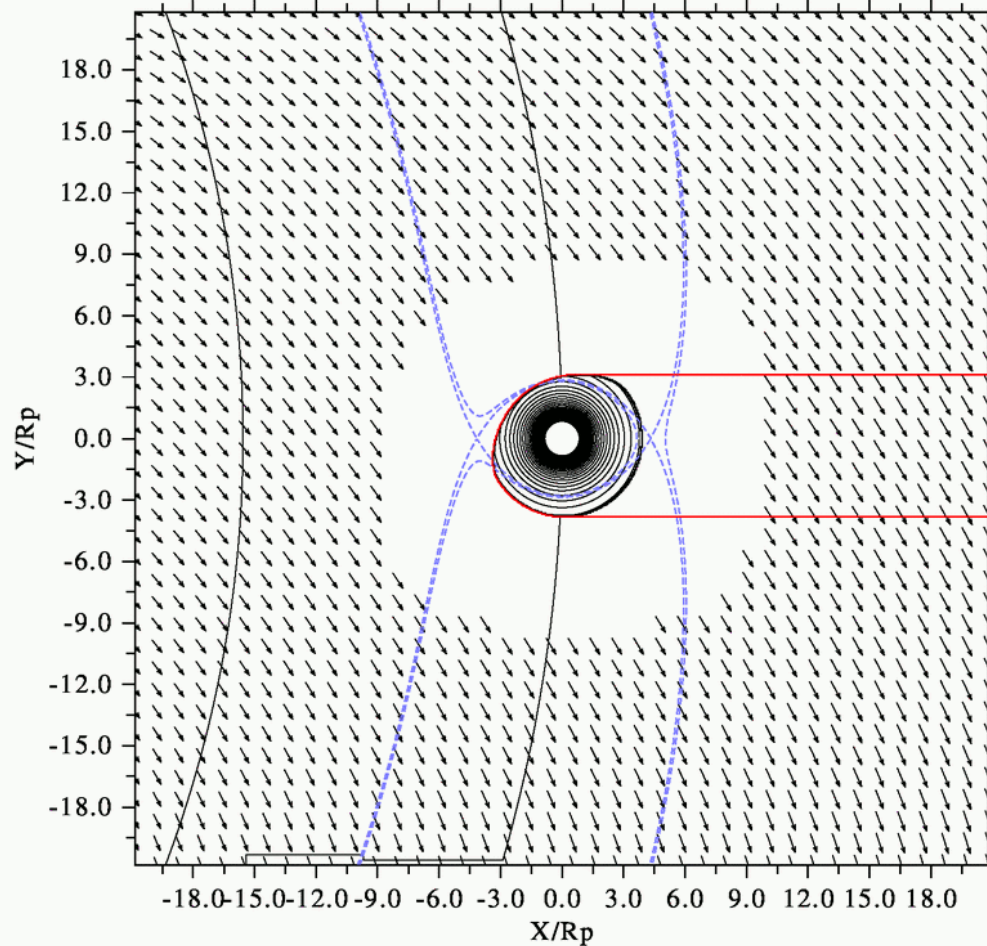


In Model 1 we have obtained a closed atmosphere flown around by the stellar wind. Here one can see the formation of a symmetrical bow-shock that is almost spherical near the HCP and tends to the Mach cone far from this point. As a whole, the planet's atmosphere very little differs from a sphere. The mass loss rate from the atmosphere is less than $1 \cdot 10^9$ g/sec.

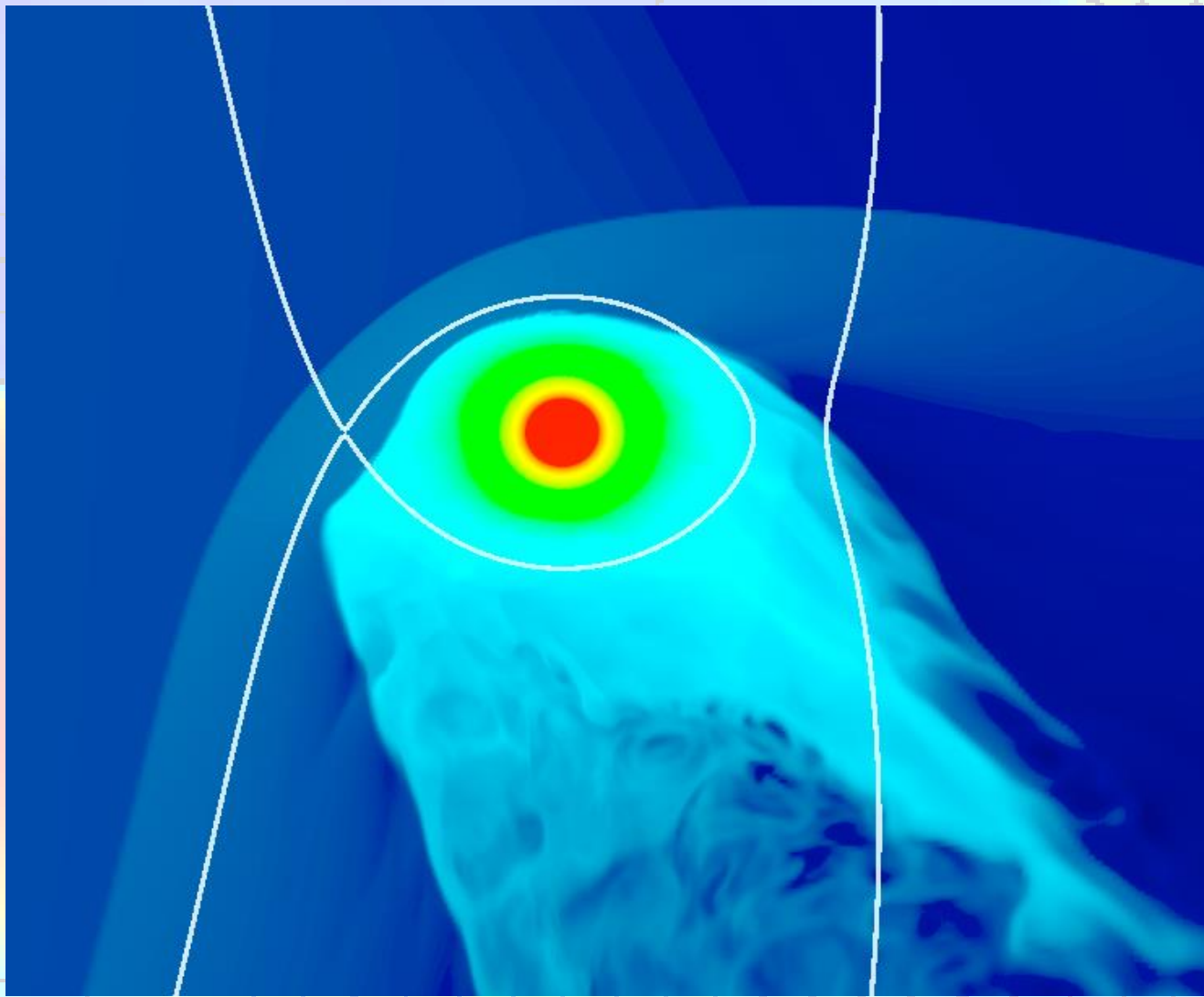


In Model 1 we have obtained a closed atmosphere flown around by the stellar wind. Here one can see the formation of a symmetrical bow-shock that is almost spherical near the HCP and tends to the Mach cone far from this point. As a whole, the planet's atmosphere very little differs from a sphere. The mass loss rate from the atmosphere is less than $1 \cdot 10^9$ g/sec.

$T = 7000 \text{ K}$

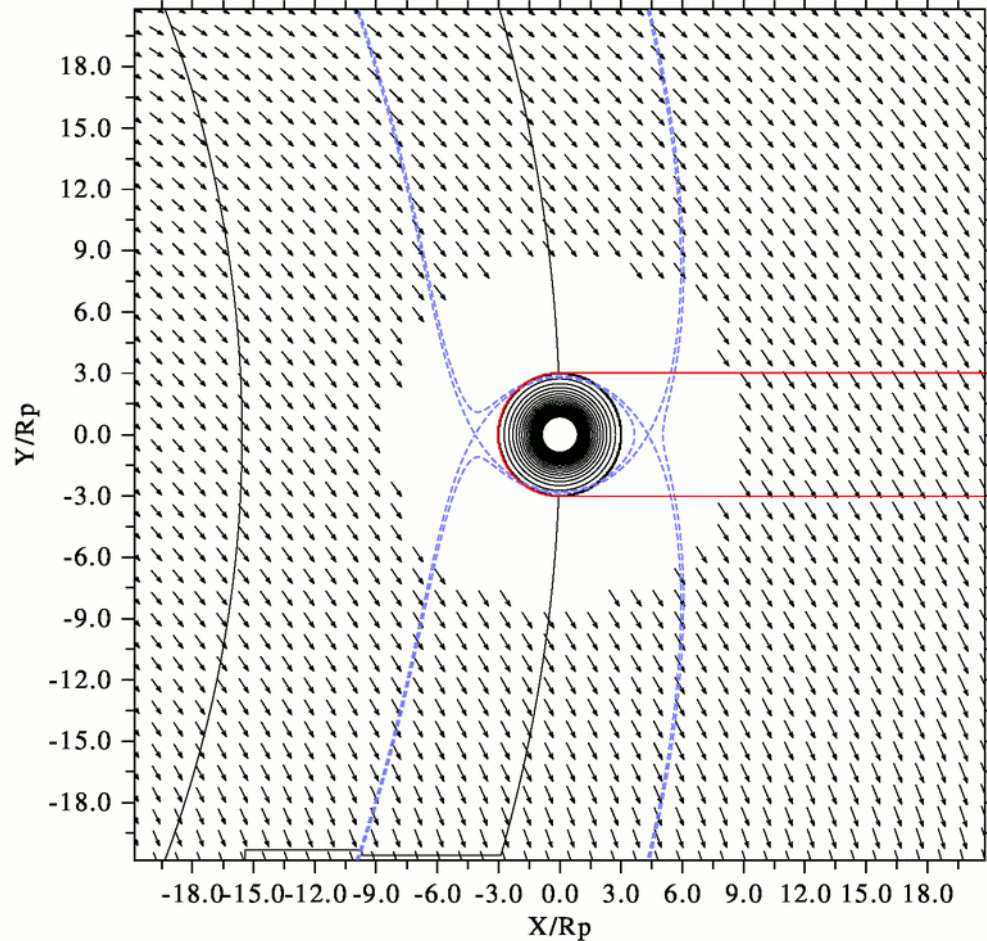


In Model 2 the shape of the atmosphere is non-spherical. In this case the HCP is shifted farther away from the planet, but it is still located within the Roche lobe of the planet. The trail behind the planet (a region edged by the bow-shock) is much broader than in Model 1. The total mass loss rate from the atmosphere in this Model is $2 \cdot 10^9 \text{ g/sec}$. Thus, the calculated envelope is partly open.

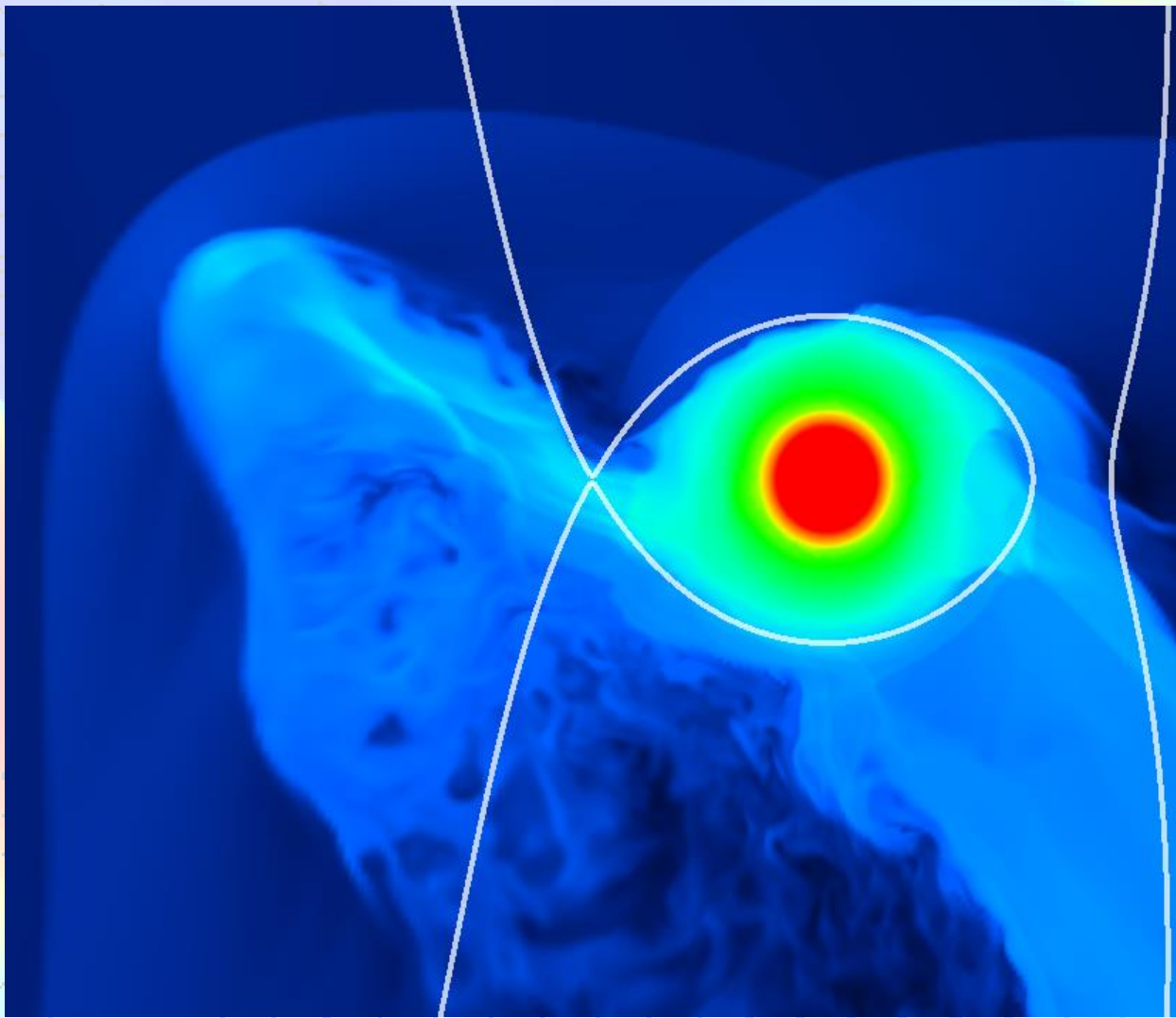


In Model 2 the shape of the atmosphere is non-spherical. In this case the HCP is shifted farther away from the planet, but it is still located within the Roche lobe of the planet. The trail behind the planet (a region edged by the bow-shock) is much broader than in Model 1. The total mass loss rate from the atmosphere in this Model is $2 \cdot 10^9$ g/sec. Thus, the calculated envelope is partly open.

T = 7500 K

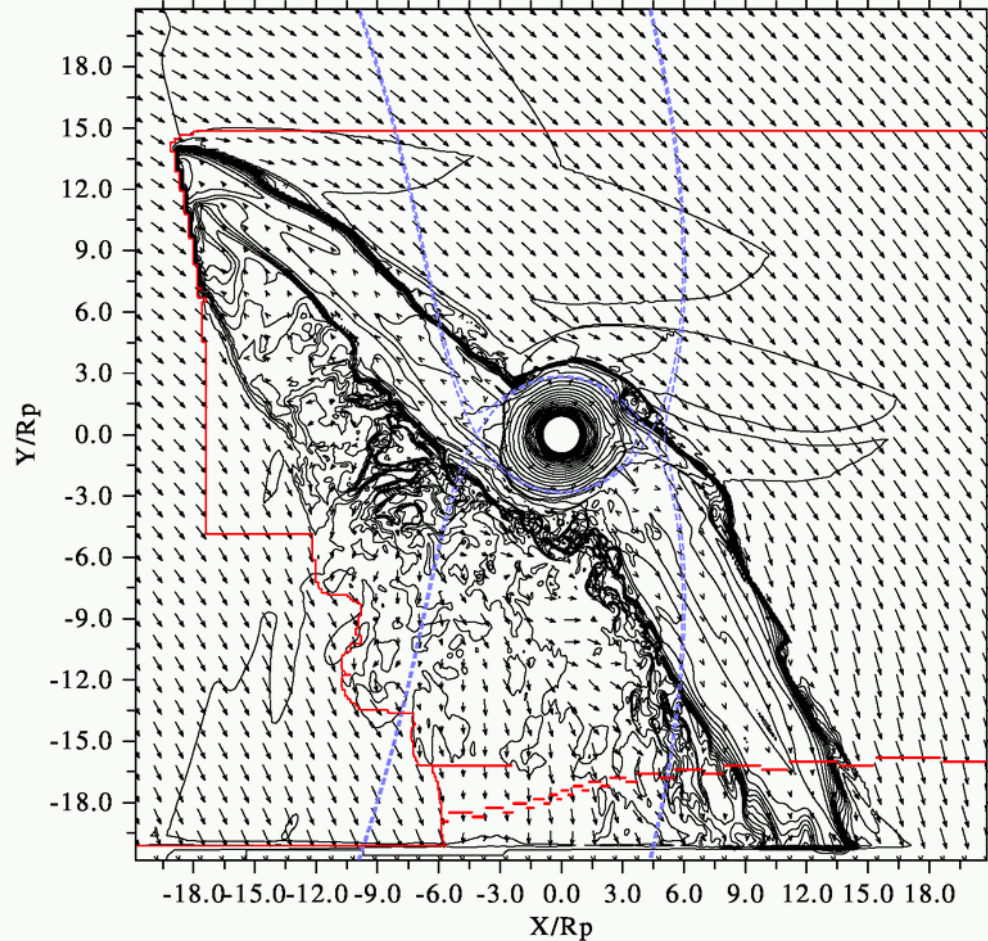


In Model 3 one can clearly see two streams, powerful from the L_1 point, directed to the star, and less powerful though noticeable, from L_2 . In Model 3 the atmosphere is quasi-closed, i.e. the streams are stopped by the stellar wind at certain distances. The weak outflow is observed along the discontinuity with a total mass loss rate of $3 \cdot 10^9$ g/sec.

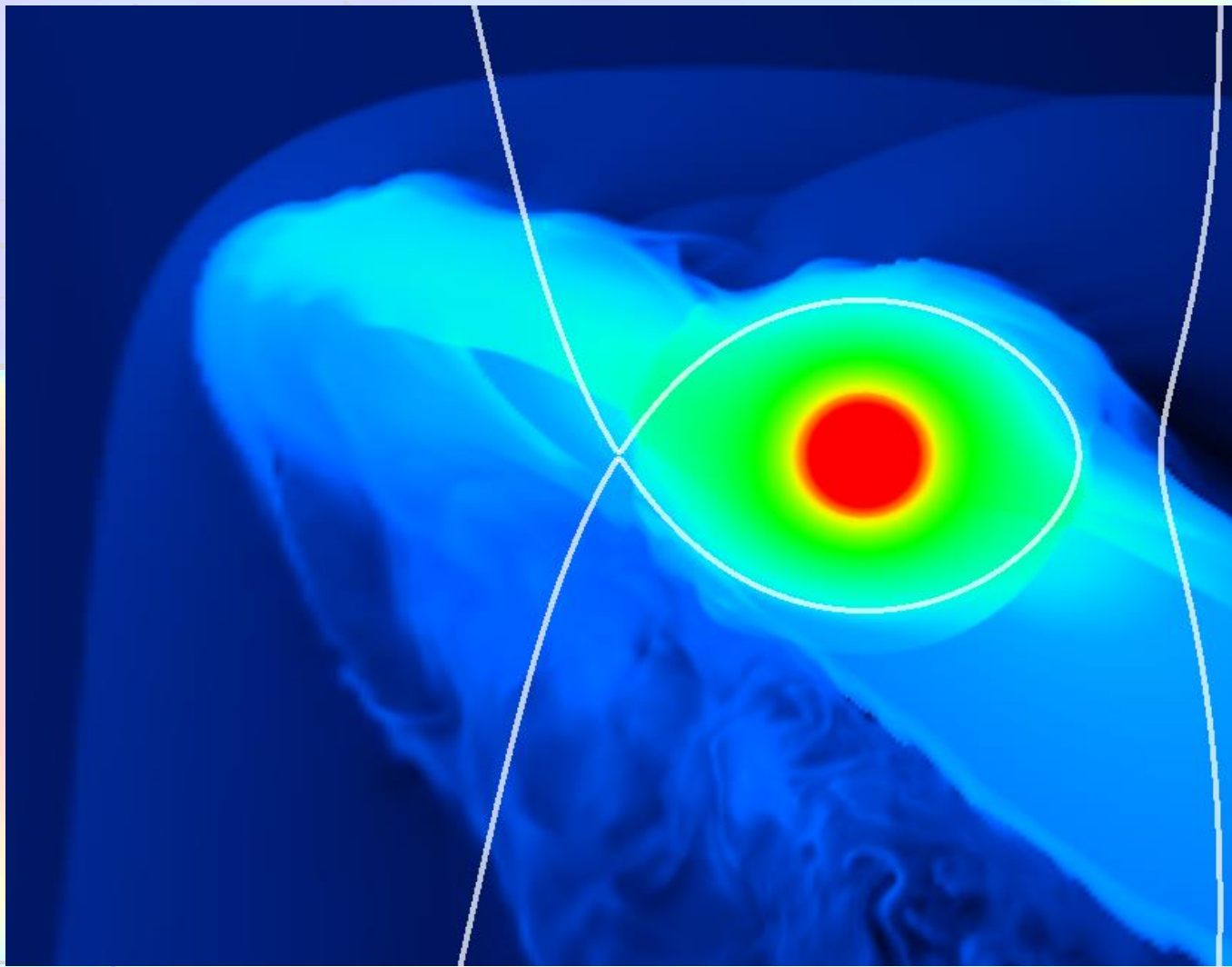


In Model 3 one can clearly see two streams, powerful from the L_1 point, directed to the star, and less powerful though noticeable, from L_2 . In Model 3 the atmosphere is quasi-closed, i.e. the streams are stopped by the stellar wind at certain distances. The weak outflow is observed along the discontinuity with a total mass loss rate of $3 \cdot 10^9$ g/sec.

T = 8000 K



In Model 4 the stream from the L_1 does not stop and keeps moving toward the star, i.e. the planet's atmosphere is open.



In the solution for Model 4 we have obtained a large mass loss rate of $3 \cdot 10^{10}$ g/sec. It is possible that, by analogy with close binary stars, in such systems accretion disks or tori of dense material may form.

•From the analytical consideration it is possible to define what type of the atmosphere the considered <hot Jupiter> will have. If the head-on collision point of the forming bow shock is inside the Roche lobe the **close quasi-spherical** atmosphere exists.

•If the head-on collision point is outside the planet's Roche lobe, the outflow from L_1 and L_2 occurs and the envelope becomes substantially asymmetric. The latter type may also be split into two sub-classes. If the stellar wind is not capable to stop the stream from L_1 an **open** envelope forms.

•If the dynamic pressure of the wind is sufficient to suppress the more powerful outflow through the inner Lagrangian point L_1 then a **non-spherical, stationary, quasi-closed envelope** forms in the system.

Conclusions

- *The most close to the laboratory experiment is the model of the "hot Jupiter": the parameter β in this case is only one and a half orders of magnitude smaller than in the experiment; the coincidence of AI can be achieved at a distance of the order of two radii of the planet from the L_1 poine.*
- *In order to reconcile the experimental data with the problems considered it is necessary to increase the value of the magnetic field (~ 20 times) or to reduce the plasma density ($\sim 2-3$ orders).*

	Эксперимент	EX Hydrae		AM Herculis		WASP-12b
		\perp В	\parallel В	струи \parallel В	струи \perp В	
x_0	$v_0 t_0$	R_m	$c_s / \Omega_K(R_m)$	R_m	c_s / Ω_{orb}	$3R_{pl}$
v_0	c_s	v_K	c_s	$v_{ff}(R_m)$	c_s	c_s
t_0	20 нс	$2\pi R_m / v_K$	x_0 / v_0	x_0 / v_0	x_0 / v_0	x_0 / v_0
$\rho_0, \text{г/см}^3$	2×10^{-2}	3×10^{-10}	3×10^{-10}	1×10^{-11}	1×10^{-11}	5×10^{-17}
$T_0, \text{К}$	2×10^6	1×10^4	1×10^4	1×10^4	1×10^4	8×10^3
$B_0, \text{Гс}$	1×10^5	8×10^1	8×10^1	3×10^1	3×10^1	9×10^{-2}
$\text{Sh} = \frac{x_0}{v_0 t_0}$	1×10^0	2×10^{-1}	1×10^0	1×10^0	1×10^0	1×10^0
$\text{Eu} = \frac{P_0}{\rho_0 v_0^2}$	6×10^{-1}	9×10^{-6}	6×10^{-1}	3×10^{-4}	6×10^{-1}	6×10^{-1}
$\text{Al} = \frac{B_0^2}{4\pi\rho_0 v_0^2}$	3×10^{-3}	2×10^{-5}	1×10^0	3×10^{-3}	4×10^0	2×10^{-1}
$\text{Re}^{-1} = \frac{\nu_0}{x_0 v_0}$	5×10^{-3}	1×10^{-13}	6×10^{-9}	3×10^{-13}	8×10^{-10}	4×10^{-6}
$\text{Rm}^{-1} = \frac{\eta_0}{x_0 v_0}$	1×10^{-5}	1×10^{-13}	9×10^{-9}	2×10^{-14}	6×10^{-11}	1×10^{-11}
$\beta = \frac{2\text{Eu}}{\text{Al}}$	4×10^2	1×10^0	1×10^0	3×10^{-1}	3×10^{-1}	7×10^0
$\omega_B \tau_{fp}$	2×10^2	2×10^3	2×10^3	3×10^2	3×10^2	1×10^4

Conclusions

- *The most close to the laboratory experiment is the model of the "hot Jupiter": the parameter β in this case is only one and a half orders of magnitude smaller than in the experiment; the coincidence of Al can be achieved at a distance of the order of two radii of the planet from the L_1 poine.*
- *In order to reconcile the experimental data with the problems considered it is necessary to increase the value of the magnetic field (~ 20 times) or to reduce the plasma density ($\sim 2-3$ orders).*

The background features a complex vector field visualization. It consists of a grid of small arrows, each representing a vector at that point. The color of the background transitions from purple and blue on the left to yellow and green on the right. The arrows are arranged in a pattern that suggests a flow or a field, with a prominent spiral-like structure in the center-right area. A small red star is located at the center of this spiral structure.

Thank you for your attention